Ministry of Higher Education and Scientific Research
University of Baghdad
Institute of Laser for Postgraduate Studies

Laser- Assisted Metal Micro- Nano Drilling Based on Nanoparticles

A Thesis Submitted to the Institute of Laser for Postgraduate Studies, University of Baghdad in Partial Fulfillment of the Requirements for the Degree of Master ofScience in Laser / Mechanical Engineering

By

Nibras Hamid Abed

B.Sc. Mechanical Engineering

Supervisor

Lecturer Dr. Mahmoad Shakir Mahmoad

2022AD **1443AH**

يَرْفَعِ اللَّهُ الَّذِينَ آمَنُوا مِنكُمْ

وَالَّذِينَ أُوتُوا الْعِلْمَ دَرَجَاتٍ

صدق الله العظيم

سورة المجادلة اية(

Dedication

To those who have lighted my way ……..

To the soul of My Mother……..

To my dear Father , dear sisters

To my abscent husband ……

And finally To my flowersdoughters……

Acknowledgments

First of all, praise is be for our Allah, most gracious, for enabling me to finish what I started and to present this work the way I would rather be thankful for.

Sincerely I fell with a great urge to present my deepest affection and gratitude to my supervisor **Dr. Mahmoad Shakir Mahmoad**, for his unending support, scientific guidance, encouragement, enlightenment, and his creative and enthusiastic approach to research which had made my graduation work a rewarding experience without his this study could not have been presented in the fashion hereunder.

I would like to express my sincere appreciation to every single staff and colleague in the Institute of Laser for postgraduate Studies for their efforts and cooperation.

I would also like to thank to **Dr. Tahrir S. Mansour**, Head of the engineering and industrial application department for her kind support and generous assistance. My thanks to **Dr. Hanan Jaafar Taher** for her support and useful Advice.

I would like to express a great Thank to **Dr.Zainab Fadhel**, for her kind support since the beginning in my project, and a special word of thank to **Dr. Rawaa Faris**, for facilitating my work in their laboratory.

ABSTRACT

In this work, nano and microholes have been obtained when the Q-switched Nd:YAG laser (1064 nm) interplay with different materials utilizing nanoparticles. Different laser pulse energies (600, 700, 800) mJ, two repetition rates (5Hz and 10Hz) and different nanoparticle concentrations (90%, 50% and 5%) were used.

Three types of materials has been used in this work. These materials are aluminium alloy (8009), titanium, and copper. Also, two types of nano particles were used, these nanoparticles are silica carbide (SiC) and tungsten carbide(WC) nanoparticles.

The effects of the laser pulse energy, pulse repetition rate, concentration ratio of nanoparticles and exposure time on shape and size of holes have been analysed.

The different concentration ratios effect for both nanoparticles were studied on different materials. The high concentrations of the nanofluid (50% and 90%) caused drawback of drilling process in materials such as cracks generation, and aggregations.

The micro and nano holes were detected for each material through the use of (5%) nanoparticle concentration. For aluminium alloy (AA8009), the perfect holes were appeared when the laser energy is 600mJ, repetition rate is 5Hz, light concentration of silica carbide nanoparticles (5%) and exposure time is 5sec. In titanium material, the regular holes were also investigated in the same parameters of laser and the same concentration of two types nanoparticles with exposure time of 5sec for silica carbide nanoparticles, and 30sec for tungsten carbide naoparticles. In copper material, the fine holes were appeared at the same parameters of laser with (5%) concentration of silica carbibe nanoparticles and exposure time is 5sec.

TABLE OF CONTENTS

List of Abbreviations

Symbols	Meaning
MRR	Material removal rate
EDM	Electrical discharge micro machine
HAZ	Heat affected zone
LBM	Laser beam machine
DTM	Difficult to machine
LBMM	Laser beam micro machine
PLD	Pulsed laser deposition
NMs	Nano materials
NPs	Nano particles
TAA	Thermal activation analysis
LSM	Laser surface melting
LA	Laser ablation
MEMS	Micro electro mechanical system
PLA	Pulsed laser ablation
WC	Tungsten carbide
SiC	Silicon carbide

List of Symbols

Symbol	Meaning
ps	Pico second
ns	Nano second
fs	Femto second
k	Scherer constant
	Full width at half maximum(FWHM)
λ	Wavelenght of X-ray
θ	Bragg diffraction angle
α	The absorptivity
t	Laser pulse irradiation time
I_o	Laser intensity
ρ	Density
c	Speed of light
z	Depth of absorption
K	Thermal conductivity
d_p	Diameter of particle
σ_{abs}^{λ}	Particle absorption cross section
U(σ)	Activation energy
K_B	Boltzman constant

Chapter One

Introduction and Basic Concepts

1.1 Introduction

The drilling process has a significant impact in manufacturing and production. Drilling is one of the most prevalent machining processes in the manufacturing industry [1]. Laser drilling is an excellent selection in order to produce holes with a minimum hole taper. Laser drilling process removes materials by thermal energy. It is a contactless drilling process with no tool wear and not restricted to only conductive materials. Drilling by laser uses a thermal heating source to melt and vaporize the workpiece [2]. It is an important industrial process to produce various sizes of holes for critical applications, such as cooling holes in turbine, components guide vanes, casings, aerospace, biomedical, communication, electronics and automotive industries. In microhole drilling via laser ablation, it is important to control material removal rate (MRR), ablation depth, and aspect ratio [3]. This process can be used by femtosecond laser micromachining with very high peak powers which provide a minimal thermal damage to surroundings and high aspect ratios (the ratio of hole length to its diameter). Femtosecond laser drilling is capable of economically drilling of number of closely located holes on micro-scale [4]. The development of femtosecond laser sources provide a precise and versatile method for micro-scale and even nano-scale fabrication techniques [5]. Micro drilling process has a great use for manufacturing of sophisticated items [6]. This process can also be used for advanced electronics and precision machine components, additionally used in aerospace, biomedical, communication, electronics, automotive industries, microelectronics, turbine blades, blind holes in surgical needle and other higher-precision applications [7,8]. The low cost of such miniaturized products with their best-of-class quality makes them suitable for extensive use of micro-machining processes. The micro-machining processes include microturning, micromilling, microdrilling, microgrinding, micropunching, and microcutting [9]. The effects of laser parameters, including

the wavelength, energy, pulse repetition rate and beam polarization on the drilling dimensions, when using the highest laser energy and the shortest laser wavelength, leads to the smaller the hole diameters in micro drilling process. Thus, other parameters related to the laser wavelength, such as the material absorptivity, have a significant impact on the hole diameter [6, 10]. The walls of a micro drilled hole are among the smoothest surfaces produced by un conventional processes [11].

1.2. Unconventional processes

Classification of Unconventional processes is carried out depending on the nature of energy used for material removal. The broad classification is given as follows:

1.2.1 Mechanical Processes

- Abrasive Jet Machining (AJM)
- Ultrasonic Machining (USM)
- Water Jet Machining (WJM)

1.2.2 Electrochemical Processes

- Electrochemical Machining (ECM)
- Electro Chemical Grinding (ECG)
- Electro Jet Drilling (EJD)

1.2.3 Electro-Thermal Processes

- Electro-discharge machining (EDM)
- Laser Jet Machining (LJM)
- Electron Beam Machining (EBM)

1.2.4 Chemical Processes

- Chemical Milling (CHM)

- Photochemical Milling (PCM)

The laser-beam machining process is stress less allowing very fragile materials to be laser cut without any support, very hard and abrasive material can be machine, sticky materials are also can be machine by this process, it is a cost effective and flexible process, high accuracy parts can be machined, no cutting lubricants required, no tool wear and narrow heat effected zone [12].

1.3 Laser interaction with material

The interaction of a laser beam with a material can cause permanent changes in the substance's characteristics. Laser irradiation alters the local chemistry, crystal structure, and morphology, all of which have an impact on how the material behaves in a specific application [13]. The laser has established as an important technology in variety fields of materials processing and mainly material removal, referred to as laser ablation [14].

Lasers are unique energy sources with great intensity without using tools. When laser interacts with matter, it can be reflected, scattered, absorbed or transmitted based on the material characteristics such as (composition, physical, chemical and optical properties), and laser parameters such as laser energy, wavelength, spatial and temporal coherence, exposure time and pulse duration [15].

Laser-induced damage threshold (LIDT) is defined as the highest quantity of laser radiation incident upon the optical component or material. LIDT is the maximum fluence laser, intensity and wavelength at which a material will be damaged. LDT values are relevant to both transmissive and reflective optical elements and in applications where the laser induced modification or destruction

of a material is the intended outcome. When the irradiated materials begin to melt, the temperature rise may alter physical and optical properties of materials, so the laser energy irradiated material by damage threshold (LIDT) is directly proportional to laser pulse time $\sqrt{t}$ as shown in Eq. (1.4) [16]:

$$LIDT = \frac{2\alpha I_{\circ}\sqrt{t}}{\sqrt{\pi k \rho c}} \qquad (1.4)$$

Where, $LIDT$ is Laser-induced damage threshold in J / cm^2 t is the exposure time, α is the absorptivity, I_o is the spatial distribution of laser intensity, K is thermal conductivity, ρ is the density of irradiated materials and c is the specific heat of material. Materials can absorb the energy of the incident laser, a part of which will be converted into heat. Non-uniform temperature distribution will appear because of the uneven heat diffusion. Consequently, expansion and contraction will lead to laser-induced thermal stress [16]. In metals, there is a large number of free electrons available. The laser energy excites these electrons to various energies [17]. Once inside the material, absorption causes the intensity of laser to decay with depth at a rate determined by the material's absorption coefficient (as shown in Figure (1.4)).

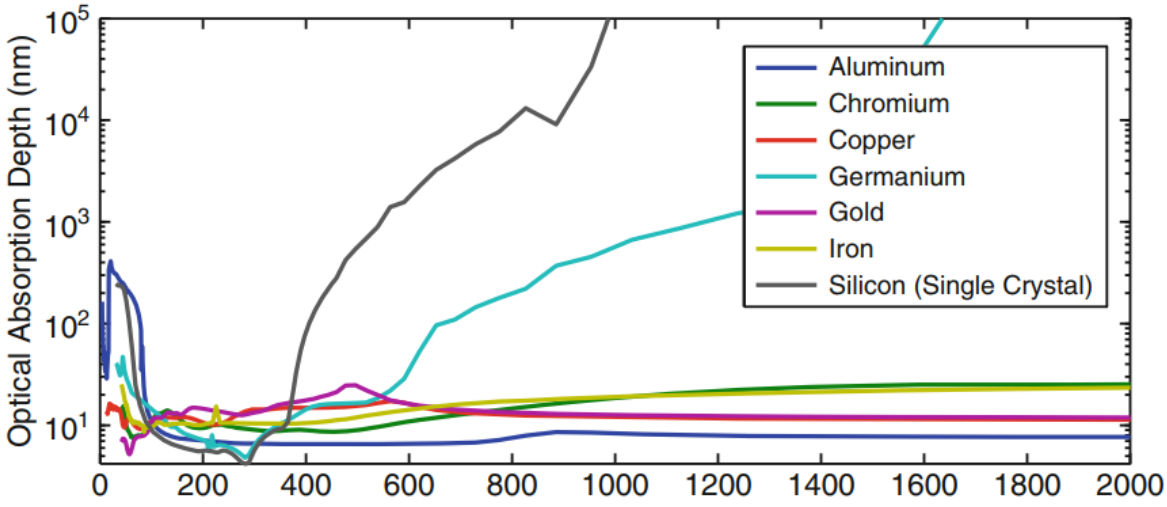

Fig.(1.4): Optical absorption depths for several materials over a range of wavelengths[18]

The absorption coefficient, determines the absorption of laser as a function of depth. However, the specific mechanisms by which the absorption take place will relied on the type of material. In general, photons will couple into the available electronic or vibrational states in the material depending on the photon energy[19].

1.3.1 Classification of metals

The engineering materials can broadly be classified as:

a) Ferrous Metals and alloys (irons, carbon steels, alloy steels, stainless steels, tool and die steels).

b) Non-ferrous Metals and alloys (aluminum, magnesium, copper, nickel, titanium).

c) Plastics (thermoplastics, thermosets).

d) Ceramics and Diamond.

e) Composite Materials.

f) Nano-materials.

The engineering materials are often primarily selected based on their mechanical, physical, chemical and manufacturing properties. Mostly, pure metals are not of any use to the engineers. The desired properties for engineering purposes are often found in alloys. Typical examples of metallic materials are iron, aluminium, copper, zinc, etc. and their alloys[20].

1.3.1.1 Aluminum and Aluminum Alloy

Aluminium is the third most abundant element in the Earth´s crust . It is the chemical element of the 3rd group in the periodic table of the elements [21]. It has a low melting and boiling point. Aluminum alloys have been developed for the aerospace industry to reduce the weight of aircraft and therefore improve performance of the aircraft. Aluminium alloys are advanced materials because of their low density, high specific modulus, excellent fatigue and cryogenic toughness properties [22].

Alloy occurs when two or more pure metals are melted together to form a new metal whose properties are quite different from those of original metals. The alloy identification system employs different nomenclatures for wrought and cast alloys, but divides alloys families for simplification into:

• 1xxx: Controlled unalloyed (pure) composition, used primarily in the electrical and chemical industries

• 2xxx: Alloys in which copper is the principal alloying element, although other elements, notably magnesium, may be specified. 2xxxseries alloys are widely used in aircraft where their high strength is valued.

• 3xxx: Alloys in which manganese is the principal alloying element, used as general-purpose alloys for architectural applications and various products

• 4xxx: Alloys in which silicon is the principal alloying element, used in welding rods and brazing sheet

• 5xxx: Alloys in which magnesium is the principal alloying element used in boat hulls, gangplanks, and other products exposed to marine environments.

• 6xxx: Alloys in which magnesium and silicon are the principal alloying elements, commonly used for architectural extrusions and automotive components

• 7xxx: Alloys in which zinc is the principal alloying element (although other elements, such as copper, magnesium, chromium, and zirconium used in aircraft structural components and other high-strength applications. The 7xxx series are the strongest aluminium alloys [23].

• 8xxx: Alloys characterizing miscellaneous compositions. The 8xxx series alloys contain amounts of tin, lithium, and iron .The aluminium alloy (AA8009) is important in industry because it can be used in manufacturing a new supersonic aircraft, missile fins (it is the bases in which a 30- 40 % of weight saving may be expected), the helicopters transmission shafts, and many other different applications [24,25].

1.3.1.2 Titanium and Titanium Alloy

Titanium as a chemical element is known for more than 220 years, and as a concentration in the earth's crust, it is on the fourth place among the metals after aluminium, iron and magnesium. Most authors do refer it to black, refractory metals (its temperature melting is 1668°C). In pure state titanium is rarely used, but in recent years the use of titanium alloys have increased significantly due to the development of methods involved in their production and further processing [26]. Titanium material is one of the nonferrous metals, normally used in the industries and construction sites. Given its advantages titanium it is evidently desirable in several military, civilian, and medical uses . Similar to other metals, titanium can crystallize in various crystal structures at a wide range of temperatures. Transformation that is complete from one into another crystal structure is called allotropic transformation, while the respective transformation temperature is transition temperature. Pure titanium and most of

the titanium alloys, crystallize at low temperatures and room temperature (25℃) in an ideally modified hexagonal close packed structure (HCP), called α titanium or alpha crystal structure. At high temperatures, however, the body-centred cubic structure (BCC) is characteristically stable and is referred to β titanium (beta crystal structure). The β transition temperature for pure titanium is noted as 882±2℃ . Both crystal structures, which are different, and the corresponding allotropic transformation temperatures are vital since they constitute the basis for the multiple properties achieved by titanium alloys. Both plastic deformation and diffusion rate are very much attached with the respective crystal structure. Furthermore, the hexagonal crystal lattice causes a distinctive anisotropy of mechanical behaviour for α-titanium [27]. Titanium material has high strength, difficult to machine, high hardness and heat resistant materials possess challenge during machining by conventional machining processes. It is widely used in construction, manufacturing, civilian, and medical applications, and it is clearly desired by numerous military branches. This is due to their high strength and low thermal conductivity [28].

1.3.1.3 Copper and coper alloy

Copper is the oldest metal used by man. It is malleable, ductile, and a good conductor of electricity and heat. The physical properties of melting point, density, young's modulus, and thermal expansion coefficient of pure copper and copper alloys are quite similar[29]. Copper and copper alloys are some of the most versatile engineering materials available. The combination of physical properties such as strength, conductivity, corrosion resistance, machinability and ductility make copper suitable for a wide range of applications [30].

1.3.2 Industrial lasers

The most important industrial lasers used in operation and manufacturing **processes:**

1- Fiber Laser, it has efficiency robust design, beam quality, and easy delivery and maneuverability with fiber optic beam delivery system, fiber laser is fast becoming a workhorse for many industrial applications**.**

2- CO2 Laser Continuous Wave (CW) lasers, which generate continuous light, and pulsed. The CW are not suitable for laser ablation, because light intensity is typically below threshold levels for surface ablation until subsurface temperatures decompose the substrate material[31].

3- Diode Laser These lasers are semiconductor diodes that create laser light directly from electricity. They are the most efficient in converting electrical input power to laser output power, but they are either CW or long pulse so they have coating removal characteristics similar to flash lamps.

4- Neodymium-doped: Yttrium Aluminum Garnet (Nd:YAG) Laser An Nd: YAG is a solid state laser and is the most frequently used for laser ablation.

5- The flash lamp pumped, Q-switched Nd: YAG laser provides the shortest pulses (10 ns). These short pulses make for efficient stripping[32].

1.3.3 Underwater-laser drilling of material

The laser–material coupling greatly depends on the type of medium where ablation takes place (air, vacuum, gases, liquids, gels) and affects the quality and the properties of the pulsed-laser micro-machined structures. It is well known that heat accumulation around the laser pulse-affected zone is a significant problem in the laser micro-fabrication of materials. By adding a water layer onto the target surface, the formation of the melted flow and the re-deposition of ablated material may be avoided. Due to its high heat capacity and thermal conductivity. The rapid temperature increase due to the laser pulse induces the formation of vapor bubbles and of two shock waves (one expands

into the water and the other into the target) which play an important role in underwater-laser drilling [33].

1.4 Surface Melting

Laser surface melting (LSM), is a suitable technique which amount of heat is penetrating to repair damaged surfaces by meltting the surface locally and rapid solidification to get fine homogeneous structures (recrystallize) [34]. The fluencies above the threshold of melting of material can lead to the formation of transient pools of molten material on the surface. The molten material will support much higher atomic mobilities and solubilities than in the solid phase, resulting in rapid material homogenization. At temperatures far above the melting temperature, hydrodynamic motion can reshape and redistribute material. The temperature gradients can develop in melt pools, causing convective flows to circulate material. For most materials, the liquid's surface tension decreases with increasing temperature and the liquid is pulled from the hotter to the cooler regions [35].

Some laser processes (like surface annealing), do not require high density of laser beam energy. However, surface melting, glazing, cladding and welding that involve melting require high laser power density to induce the change in state and phase transformation in large volume and area. Additionally, processes like cutting, drilling and similar machining operations that remove material as vapour, need high power density within a short pulse or continuous wave according to selected material and its application [36]. Applications of laser technology in metal surface modification are important technique due to change and enhance the surface characteristics of materials. Laser processing, as shown in Fig.(1.5) has more advantages over the conventional methods which include

local heating of the surface without changing the substrate material properties, precision and high speed of operation with low cost. [37, 38].

1.4.1 Heating and melting

At high laser beam intensity values (in the range $1x10^5$ W/cm^2 for metals), the material being heated will change state. Most materials will melt due to the different physical mechanisms, and in the molten state, the absorption of laser light increases. The absorption coefficient rises to about 90% for common metals subject to infra-red laser light.

Melting progresses by conduction on an approximately hemi-spherical front through the material. Convective heat transfer, as well as conduction, becomes important and this can be driven by changes in surface tension of the molten pool arising from temperature gradients. These latter factors will distort the melt shape away from being spherical [39].

1.4.2 Vaporization and (Laser Ablation)

Laser ablation (LA) is a process in which a laser beam is focused on a surface of material to remove material from the irradiated zone [40]. Laser ablation mechanism focuses a laser beam on a substrate for the removal of any surface material. The removed mass relies on the material itself, pulse length, intensity power and laser wavelength [41]. laser ablation (LA) is describing the laser-material interaction and refers to the removal of material from a solid with the utilizing of a pulsed laser beam with vapour transport to an analytical excitation source for analysis as shown in Figure (1.6). It has been considered and used for many technical applications, including the production of nano materials, deposition of thin metallic, fabrication of superconducting materials, routine welding bonding of metal parts and micromachining of micro electro mechanical systems (MEMS) structures [42].

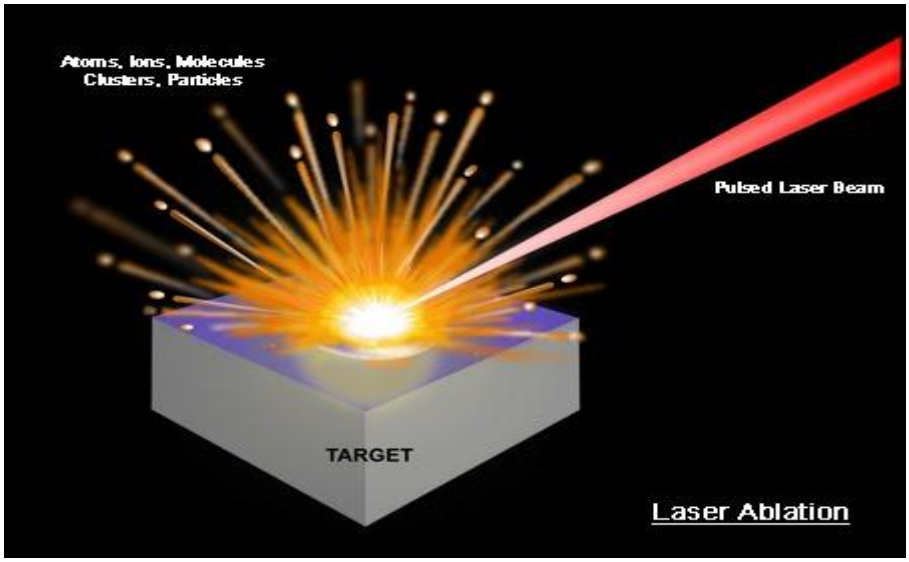

Fig.(1.6): Laser ablation[42]

Laser ablation process can be done by removing material from a substrate by absorbing laser energy directly. This methods are mainly depending on mechanical, acoustic, and optical principals [43]. The ablation occurs above a threshold fluency, which will depend on the absorption mechanism, particular material properties, microstructure, morphology and on laser parameters such as wavelength and pulse duration. During laser ablation, a number of material removal methods may be engaged on the particular material system and laser processing parameters. photothermal processes operate at high fluencies, for ablation include material evaporation and sublimation. With higher fluency, heterogeneous nucleation of boiling this will leads to vapour bubbles [44]. If material heating is sufficiently rapid to approach its thermodynamic critical temperature, rapid homogenous nucleation and expansion of vapour bubbles

lead to explosive boiling (phase explosion) carrying off solid and liquid material fragments. So according to the response of material to incident laser, the responses can be divided into two groups: thermal and mechanical effects. Thermal effects refer to melting, vaporization, boiling, and phase explosion while mechanical response involves deformation and resultant stress in materials. Different thermal processes will induce different mechanical responses [45]. Pulsed laser ablation (PLA) is a useful technique for surface machining. Although micro cracks and heat-affected zone (HAZ) are formed as a result of thermal stresses and heat conduction into the bulk medium (as shown in Figure (1.7)), this process provides an advantage of minimizing the heat affected zone (HAZ) under certain circumstances.

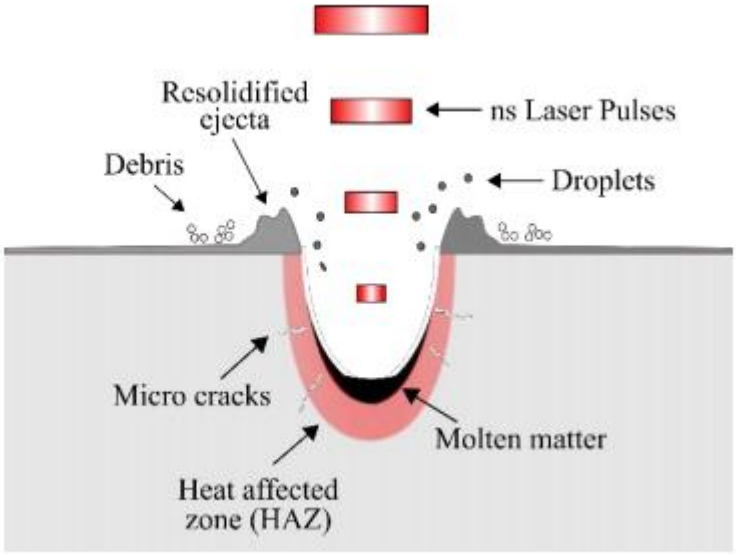

Fig.(1.7): Illustration of nanosecond pulsed-laser ablation[46]

In the case of nanosecond laser pulses, the heat affected zone will be minimal if the ablation depth per pulse (Δh) is comparable to the values of $\boldsymbol{L_t}$ and $\boldsymbol{L_\alpha}$ that have been calculated by the following equations [46]:

$$\boldsymbol{L_t = 2\sqrt{D\tau_1}} \qquad (1.8)$$

$$\boldsymbol{L_\alpha = \alpha^{-1}} \qquad (1.9)$$

$$\boldsymbol{\Delta h = \max (L_t, L_\alpha)} \qquad (1.10)$$

Where, L_t is the thermal penetration depth in (mm), D is the thermal diffusivity of the material in (mm^2/s), τ_1 is the laser pulse duration in (ns), L_α is the optical penetration depth in(mm), α is the optical absorption coefficient of the material in cm^{-1} and Δh is the ablation depth per pulse in (μm/pulse).

In case of ablation with ultrashort laser pulses, HAZ is nearly absent or is negligible due to non-thermal mechanisms governing the ablation [46].

Nanosecond laser is suitable for removing materials or ablation. Short pulse duration (picosecond laser) and ultra-short pulse duration (femtosecond laser) yield better results, suited to the production of high-precision micro- and nanomachining [47].

The laser ablation mechanisms are different for short pulse as (nanosecond), and ultrashort pulse (pico and femtosecond) laser in which the difference in laser coupling with matter at different timescales has been involved [48].

The quality of ablated holes induced by femtosecond laser pulse is much better than those produced by nanosecond or even more large pulses. The key feature of femtosecond laser ablation of metals is the quick development of plasma phase and the absence of a heat effect zone (HAZ) surrounding the holes [49].

Short pulse, which is nanosecond pulse ablation, can be distinguished by thermal, non-thermal and combination of both mechanisms. These are also referred to as photo-thermal, photo-chemical and photo-physical mechanisms. Figure (1.8) illustrates the laser ablation process through thermal, non-thermal and photo-physical processes. The physical mechanics of nanosecond pulsed laser ablation are based on vaporization, which is the primary material removal mechanism, and the theoretical vaporization rate depending on the target temperature [46,50].

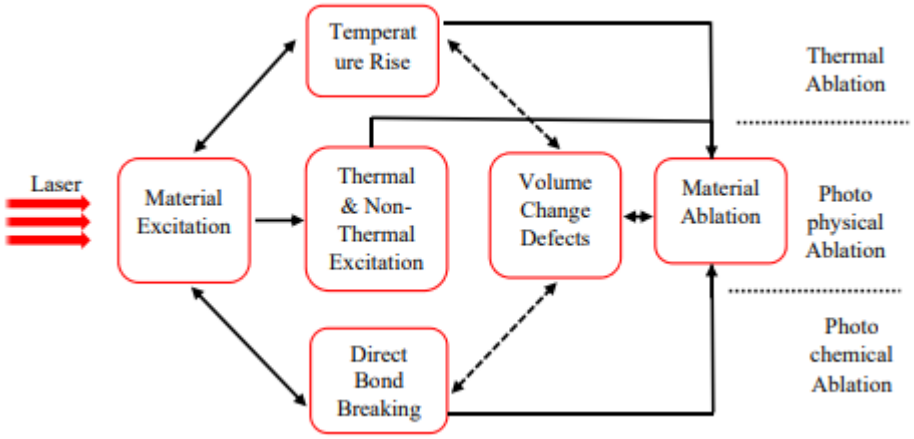

Fig.(1.8): Graphical illustration of mechanisms leading to pulsed laser ablation[46]

1.5 Laser Beam Machining

Laser beam machining (LBM) is a machining process that can be used to machine almost any known material ranging from soft materials to difficult to machine(DTM) materials [51]. Laser drilling is a machining operation by

melting and evaporation of the workpiece using a high power laser beam. Metals, alloys, polymers and ceramics may be drilled by laser assisted drilling [52]. Laser beam machining (LBM) process has a very high material removal rate (MRR) compared to other non-conventional machining processes such as electrical discharge micro machine (EDM) [51, 52]. The Laser beam machining process (LBM) can be considered as one of non-conventional machining process because of their precision of operation, low cost, localized processing, wide range of material processing flexibility and high speed of operation [53]. In laser micromachining, tool wear is not needed; it produces minimal heat-affected zone (HAZ) and repeatability of the process, and its precisions are high. In order to minimize thermal degradation of the material outside the production zone, limited heat transport is required which is achieved by using nanosecond, picoseconds, or femtosecond pulse widths [54]. During laser beam machining process, the laser beam interact with workpiece, and the beam energy is partially absorbed by the workpiece material. This will first heats up the surface to boiling point, followed by melting or sublimation, evaporation, plasma formation and ablation [55].

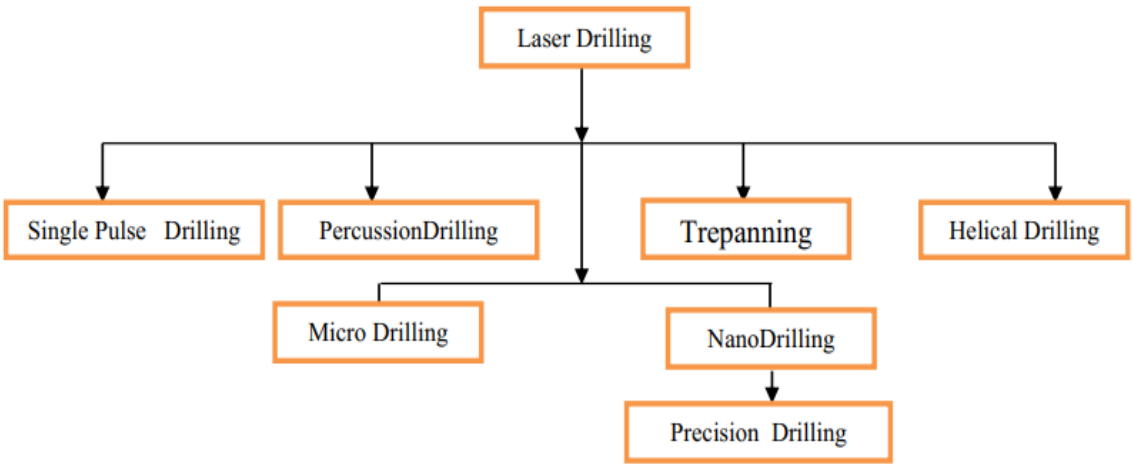

Fig.(1.1): Classification of laser beam drilling process [56]

The laser drilling can be classified according to process mechanism, as shown in Figure(1.1), into single pulse drilling referred to drilling of blind and

through holes by pulse duration of few microseconds. Percussion drilling delivers a successive number of pulses to the same spot on the workpiece to produce a hole. The drawbacks of percussion drilling are recast layer formation, spatter deposition, tapered hole, and micro crack [56]. Trepan drilling is used to remove material from the work piece surface in the form of a circular disc. The Helical drilling process is similar to Trepan drilling process, but very large and deep high quality holes can be produced easily in the helical drilling process as shown in Fig. (1.2)[57].

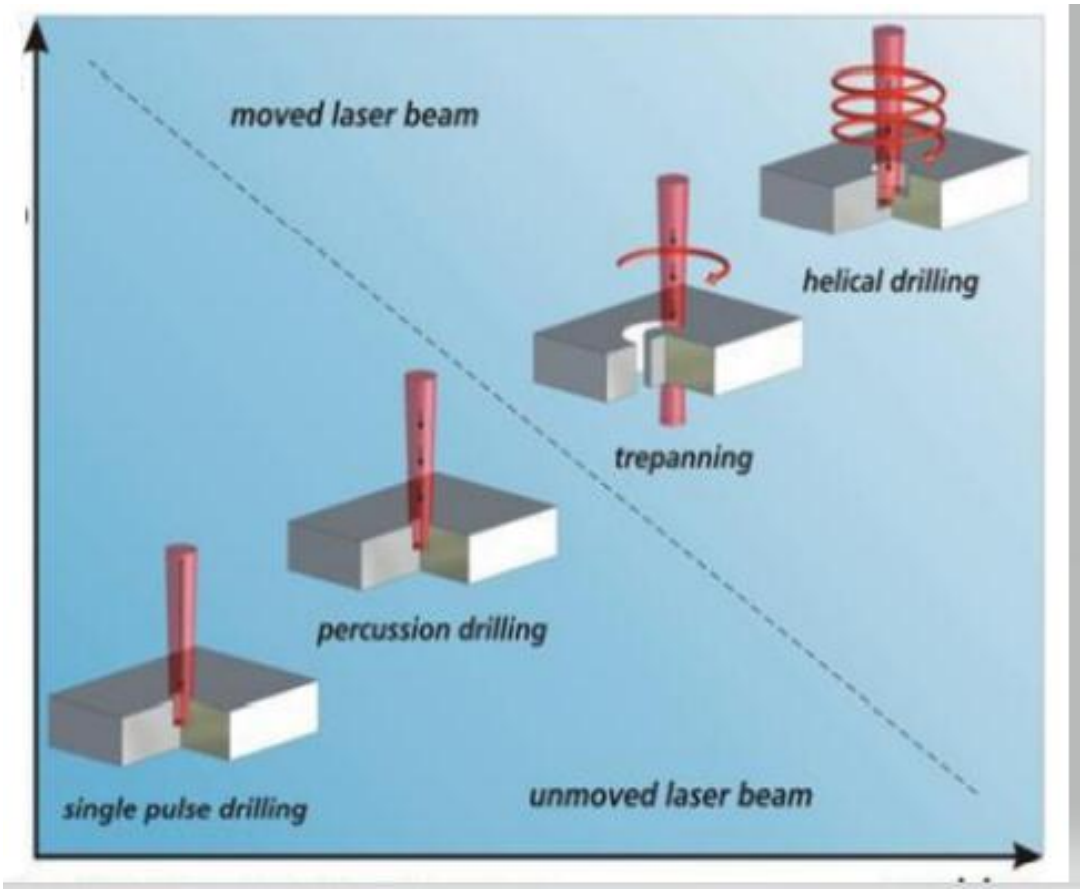

Fig. (1.2): Clarification of drilling process[58]

The laser drilling process can also be classified into other types like nanodrilling, micro drilling and precision drilling according to the hole size. Nanodrilling usually performed with short and ultra-short laser pulses. Laser with pulse duration in nanosecond is known as short pulse laser, and for pulse

duration less than 1 ps are referred to ultra-short pulse laser [58]. The laser is also used to perform turning as well as milling operations but important application of laser beam is mainly in cutting and drilling of metallic and non-metallic sheets. Nd:YAG lasers have high peak powers enable it to machine even thicker materials. Also, shorter pulse duration suits for machining of thinner materials. Due to shorter wavelength it can be absorbed by high reflective materials which are difficult to machine by longer wavelength lasers [59].

1.5.1 Laser Beam Microdrilling

Microdrilling is the future technology and industry. Conventional mechanical drilling has to face increasing physical limitation when hole diameter is decreased. Below some critical dimension, friction surpasses the mechanical strength of the tool and machining is possible only by choosing specially designed tools made of high modulus materials (such as diamond). In any case, it means that the cost of the process can be prohibitively increased. In this context, laser microdrilling offers an attracting alternative to mechanical machining and is already widely used in numerous applications [60]. The ability to machine very small features such as holes into a metal, ceramic, semiconductor or polymer by laser ablation with an unmatched precision, accuracy and speed has opened a very useful scope with respect to the process variables such as focusing optics, laser power, wavelength and repetition rate [61]. Pulsed lasers are fundamental tools for industrial micromachining applications. Nanosecond pulsed lasers are cost effective solutions being widely employed in marking, cutting, drilling and texturing operations. Ultra-fast pulsed lasers operating at pico second (ps) to femtosecond (fs) pulse durations provide superior machining quality and have become much more reliable and affordable in the last few years [62]. Micromachining refers to machining of workpieces or features having dimensions below 1 mm. Lasers are being used

for micromachining operations with short pulses (pulse duration varies from microsecond to femtosecond) and very high frequencies (in kHz range). Pulsed Nd:YAG, is most commonly used for laser beam machine LBM applications [63]. Laser beam micro machining (LBMM) has revolutionized many industries by providing innovative solutions in numerous industrial micro-engineering applications. High-intensity short or ultrashort laser pulses are powerful thermal energy source for creating micro-drilling in wide range of materials. These lasers can precisely ablate various types of materials with little or no collateral damage. LBMM associated with beam laser radiation on a sub-micrometer scale. [64].]. Laser micro machining can often be a more cost effective alternative to other techniques such as electrical discharge micro machine (EDM) which involves material removal through the generation of sparks between the tool and workpiece gap in the presence of dielectric fluid [65]. Pulsed lasers (specially Nd:YAG laser) micro drilling on different materials have been carried out to study the effect of process parameter such as pulse energy, pulse frequency, pulse width and focal length which effect on material removal rate (MRR), formation of holes and heat affected zone (HAZ) width [66]. The use of laser microdrilling or micromachining in manufacturing industry can be attributed duo to its flexibility and ability to process variable quantities and qualities of materials in a very short time with very high surface finish, accuracy, and minimum amount of wastage. Laser drilling process can be used with materials including of super alloys and special materials [67]. Some materiaĺs properties like higher toughness, high strength and wear resistance make them used in several applications, including cutting, drilling materials and highly competitive against other conventional materials so these properties enhanced the properties of holes [68]. When the machining dimension (hole diameter) is less than 1 mm, then it is termed as micro drilling. Precision drilling refers to drilling of small and highly accurate holes which is a common

requirement of the industries [69]. The heat affected zone(HAZ) width and hole taper of the drilled micro hole has been calculated by[70]:

$$\textbf{HAZ width (mm)} = \frac{HAZ_{dia.top} - Hol_{dia.top.}}{2} \quad (1.1)$$

$$\textbf{Hole taper (rad)} = \frac{Hole_{dia.top} - Hole_{dia.Bot}}{2 * Thickness} \quad (1.2)$$

Where, $HAZ_{dia.top}$ is the outer diameter of heat affected zone on top surface of material in (mm), *Hole taper* is the mean diameter of hole in (rad), $Hol_{dia.top}$ is the outer diameter of hole taper on top surface in (mm), $Hol_{dia.Bot.}$ is the inner diameter of hole taper on bottom of material in (mm) and the thickness of used material is in (mm).

Pulsed Nd:YAG lasers have expanded high beam quality for laser machining to micron scale precision. The high peak powers obtained by these lasers enable material removal through thermal ablation [70].

In micro-hole drilling (by laser ablation), it is important to control material removal rate (MRR), ablation depth, and aspect ratio [71]. Hole and heat affected zone (HAZ) width are considered as process responses. The important reasons for holes creation and improvement of the measurement them are ejected the irregular molten material and erosion of the hole walls as the laser power reduction as the beam propagated to the hole [72].

1.5.2 Laser beam nanodrilling

Ultrashort pulsed laser radiation with pulse durations of less than 10 picoseconds has outstanding properties due to their light-material interaction, especially in view of continuously growing accuracy requirements. Due to short interaction times between laser and material, which are below the electron

lattice interaction time for metals, a processing can be realized that stands out by a negligible thermal load of the workpiece. Hence, the resulting ablation process is free of melt and avoid the thermal damage of the surrounding material. In most applications for precision laser structuring a picosecond laser sources with limited average power range of about 1 to 50 W is applied to generate the desired workpiece in a single beam process. Here, the average power of the laser system is limited by the maximum pulse energy which can efficiently applied within the process. The multibeam approach is promising, as the quality of a single beam laser ablation process can be maintained while multiple structure can be generated in parallel. Therefore, higher pulse energies can be applied as the pulse energy is distributed across multiple beamlet [73]. Surface engineering in micro/nanoscales plays a major role in a material's performance improvement. For example, the material's photoelectrical properties can be modified by changing its surface morphology and chemical energy states[74].

1.6 Plasma formation

Plasma is widely considered to be the fourth state of matter due to its unique properties. So, plasma is a gas in which the atoms are ionized, meaning there are free negatively charged electrons and positively charged ions. This collection of charged particles can be controlled by electromagnetic fields and this allows plasmas to be used as a controllable reactive gas [75]. During the last decades, lasers and plasmas have both become important components of current industrial technology and surface engineering [76]. Plasma ignition process includes bond breaking and plasma shielding during the laser pulse interaction with the material surface [77].

Plasma has three main regions as shown in figure(1.3). The "core" is the first region. It is the hottest and densest part of the plasma, is located near the target surface. The material in this region is mostly found in the ionized state because of high temperatures. In the mid-region of plasma, ions and neutral (atoms + molecules) coexist due to the continues processes and in the third region is the cold plasma, non-thermal plasma, or non-equilibrium plasma. It is a plasma which is not in thermodynamic equilibrium. As only electrons are thermalized, their velocity distribution is very different from the ions velocity distribution. So the temperature of electrons is much hotter than the temperature of (ions and neutrals atoms) [78].

Nanosecond lasers have been used for laser-machined through-holes. Laser drilling typically involves dealing with a deep narrow hole with high aspect ratio. Ablation from a deep, narrow hole has a few unique characteristics [79]:

(a) The absorption of an incoming laser beam in a plasma plume alters the propagation and absorption of incident radiation in the hole, preventing incident radiation from reaching the hole bottom but transforming it into plasma energy.

(b) The plasma stream travelling from the hole outwards provides a new source of energy that acts on the side walls in a different way than the laser beam's direct absorption by the walls. This novel heating source has additional spatial and temporal properties and has the potential to significantly enhance the amount of energy emitted across the side walls.

The generated plasma plume interacts with the surface, resulting in largely negative repercussions. Using pulse duration of laser radiation interaction with metals, higher accuracy and quality of drilling processes were obtained [75,80]. The combination of laser irradiation with plasmas, which may be generated at low or atmospheric pressure, has shown to be a powerful combination for a variety of applications. Plasma-assisted pulsed laser offer the possibility of

increasing the total efficiency by a reduction of the laser ablation threshold of some target materials [46,76].

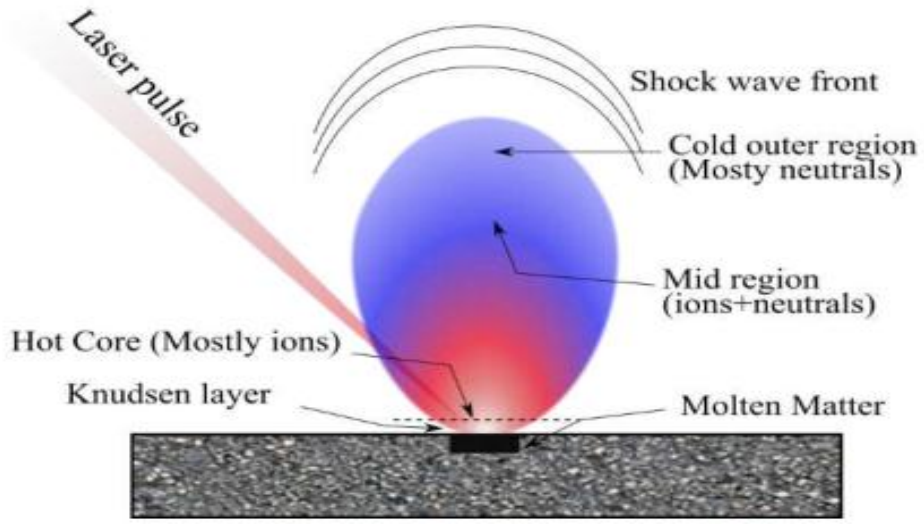

Fig.(1.3): Schematic illustration of laser-induced plasma[46].

1.7 Nanoparticles

Nanoparticles are zero-dimensional nanomaterials, as opposed to one- and two-dimensional nanomaterials, which have one or two dimensions greater than the nanoscale. They differ from their bulk counterparts in size, chemical reactivity, movement, and energy absorption [81].

Nanomaterials (NMs) have risen to prominence in technological breakthroughs due to their tunable physical, chemical, and biological characteristics, as well as their superior performance over bulk equivalents. Nanomaterials are classified based on their size, composition, form, and source [82].

Nanotechnology is referred to as a particle with lengths larger than 1 nm and less than 100 nm in two or three dimensions [83]. It exhibits a size-related intensive property, the high surface area to volume ratio of nanomaterials means

that a significant portion of the atoms of a nanomaterial are on the surface and this leads to high chemical reactivity in nanomaterials. Nanoparticles (NPs) can be classified based on their properties such as shape, size, activity, and type of the materials they are made of. The role of size, shape, and other characteristics nanoparticles (NPs) can be obtained by manipulating of the synthesis conditions [84]. Nanoparticles have unique optical, electrical, magnetic, and thermal properties. The selection of an appropriate synthesis technique is crucial for synthesizing application-oriented NPs. There are numerous methods to rely on bottom up and top down techniques that have been created over time, with each providing a certain degree of success [85].

The nanomaterials are generally classified according to the dimensions, according to the shape, according to the composition[86]. The composite nanoparticles constituted by two or more components of nanoscale with special physical and chemical properties and the last part is carbon nanoparticles which contains completely of carbon [86].

Also, nanoparticles (NPs) can be also classified into different types according to the size, morphology, physical and chemical properties. Some of them are carbon-based nanoparticles, ceramic nanoparticles, metal nanoparticles, semiconductor nanoparticles, polymeric nanoparticles [87]. Laser-machined nanostructures offer a wide range of uses in photonics, surface plasma resonance, optoelectronics, biochemical sensing and nano fluid [88].

1.7.1 Tungsten carbide nanoparticles (WC)

Tungsten carbide nanoparticles (WC) is a very desirable material due to its attractive mechanical, physical and chemical properties such as high hardness, high melting point, good electrical, good thermal conductivity, and high corrosion resistance [89]. Tungsten carbide nanoparticles (WC) is an interstitial compound of C atoms filling into W crystal, which has high strength and rigidity as covalent compound. [90]. Tungsten carbide nanoparticles have wide applications in chemical industries, electronic industries and mechanical tools.

1.7.2 Silicon carbide nanoparticles (SiC)

Silicon carbide (SiC) is a non-metal semiconductor, which has been used for different applications owing to its inherent chemical inertness, high thermal, mechanical, chemical stability and also their unique photoelectrical properties [91].

These nanoparticles have wide spectrum of physical, chemical and mechanical properties which utilize according to extensive application. The silica carbide nanoparticles (SiC) properties depend on the crystallite size, the specific properties and structure of these component [92]. Silicon carbide (SiC) nanoparticles have been widely used for thermal and structural applications due to low bulk density, low thermal expansion and tuneable bandgap [93, 94]. It is widely used in high-temperature, high power, and high-frequency electronic applications [95].

The nanofluids made by combining nanoparticles with a base fluid, such as water, have a high thermal conductivity and, as a result, a high rate of heat transfer. The thermal conductivity is the quantity of heat that passes in unit time, through unit thickness, and under unit degree of specified temperature. Heat transfer rates are faster in materials with higher thermal conductivity than in materials with lower thermal conductivity. As a result, greater thermal conductivity materials are employed for heat absorption, the quantity of nanoparticles to the base fluid always enhances its thermal properties, so the nanofluid characteristics has a principal role in its industrial applicability [96].

The nanoparticles can increase the stability of based nano fluid by having a large free energy of adsorption and by having high thermal conductivities that can dissipate heat efficiently. When the nanoparticles are dispersed in the base fluid, this will lead to increase the friction between layers of the fluid, which results to increase in viscosity of nano fluid and can create the homogeneous solid–fluid at light concentrations of small nanoparticles [97].

1.7.1 Laser interaction with nanoparticles

Laser beam interaction with the particle's electrons such as absorption and scattering of the incident laser's photons [98].

With metallic nanoparticles, this interaction involves the collective motion of all conductive electrons in a particle. If the energy of the electrons can be rapidly transferred to the crystal lattice due to good heat transfer between the electrons and the phonons, the particle heats rapidly. If enough energy is absorbed, the particle can melt and finally evaporate. The amount of energy that a particle absorbs from the pulse laser beam, is calculated by [99]:

$$E_{abs} = J\sigma_{aьs}^{\lambda} \qquad (1.12)$$

Where J= $\frac{E_o}{A_o}$

J is laser fluencies, E_o is pulse energy, A_o is spot size area and σ_{abs}^{λ} is the particles absorption cross section, which strongly depends on the laser wavelength, so the amount of energy of the particle´s absorption is equal to [99]:

$$E_{abs} = \frac{E_o}{A_o}\sigma_{abs}^{\lambda} \qquad (1.13)$$

The absorption efficiency for a spherical nanoparticles can be calculated as follows [99] :

$$Q_{aьs}^{\lambda} = \frac{4\sigma_{aьs}^{\lambda}}{\pi d_p^2} \qquad (1.14)$$

Where d_p is the diameter of nanoparticle, Q is the absorption efficiency (unit less) and both Q and σ also strongly depend on laser wavelength, particle size and shape [99]. When the laser beam interacts with a material in vacuum, air or liquid medium, the incident light can either be reflected or absorbed. The laser absorbed energy can react with materials in either a thermal or chemical reaction. Generally, the mechanisms that can possibly occur as a result of the laser- matter as photochemical, photothermal and photophysical [100]. For the particles, the amount of energy absorbed by a particle (the equation(1.14)) of any size from the laser pulse can be calculated. According to the equation (1.14), this energy is spent for the particle heating–melting–evaporation process. If the amount of absorbed energy is rather small, only particle heating can be expected. And with more absorbed energy, melting occurs[99,100].

1.8 Literature Review

This review describes and shows some of results and researches of laser micro and nano drilling with material .

L. Li, et. al. (2006), investigated into a sequential laser and EDM micro-drilling technique for the manufacture of next generation fuel injection nozzles. A laser-drilled pilot hole is rimmed out by EDM drilling. It was found that this hybrid process has eliminated the problems of recast and heat affected zones typically associated with the laser drilling proc Nd:YAG laser (1064 nm wavelength) with 10-40 μs pulse length at a repetition rate of up 2000 Hz with 15 mJ/pulse and a Spectra Physics Powergator diode pumped solid state (DPSS) laser (1064 nm wavelength) with 15 ns pulse length at a repetition rate up to 10 kHzess on plastic material. [101].

In 2011, C. A. Biffi, et. Al, studied the effects of the main process parameters (pulse energy and pulse frequency) on the quality features of the machined

through holes, i.e., diameters, taper, circularity, and area of top spatter. Adequate regressive models are developed to define the functional relationship between the hole quality and the main process parameters [102].

I. J. Mahmood, et. al. (2015), found that the wavelength and the duration of the laser pulse play an important role in laser drilling process where considered very short pulses (picoseconds) is the best in the drilling process. It has been used Nd:YAG laser (with minimum pulse duration of 0.5 ms) on the drilling process with Stainless steel304 and Single crystal silicon) [103].

L. N. Meng, et. al. (2015), constructed blind micro-hole array templates by laser drilling using fiber laser on a Ti6Al4V substrate.The influence of laser parameters on the morphology of the blind holes was investigated and the blind micro-hole array templates were fabricated by the optimized laser parameters [104].

J. Tu, et. al. (2016), investigated rapid, high aspect ratio microhole drilling using a CW Single-Mode Fiber Laser based on the single pulse drilling technique, samples of stainless steel, aluminum . However, the peak power values of subsequent pulses decrease with higher repetition rates. Another contributing factor of the synergistic effect is related to the melt ejection efficiency. As the hole deepens, the melt ejection becomes less effective to eject the melt completely out of the hole, resulting in a partially blocked [105].

F. Courvoisier, et. al. (2016), studied the benefits and applications of nondiffracting beams for laser micro- and nano-processing in the general context of materials processing with ultrashort pulses in the filamentation regime and mentioned the applications on ultra-high aspect ratio nano-drilling and direct laser processing [106].

K. L. Dhaker, et. al. (2017), investigated the effect of laser process parameters like, gas pressure, pulse laser energy, pulse width, frequency, stand of distance,

and cutting speed on the drilled hole diameter in the laser trepan drilling of Inconel718 sheet. Also, made the small hole of desired size in the aerospace components which was a challenging task for the manufactures [107].

G. D. Gautam, et. al. (2018), emphasized the use of pulsed Nd:YAG laser drilling of different materials in order to enhance productivity of this process without adverse effects on the drilled holes quality characteristics. Additionally, they studied the possible scope in the area of pulsed Nd:YAG laser drilling[108].

A. Stephen, et. al. (2018). studied the possibility of drilling titanium sheets using the laser processes of single pulse and percussion drilling [109].

G. G. Dongre,et. al. (2019), carried out micro-hole drilling using alloy, super alloys and composite materials, analyzed the effect of pulse duration and beam energy on materials to achieve quality holes. Holes are analysed for size and shap. It also investigated effect of laser drilling techniques like percussion, trepanning and helical on accuracy of holes. [110].

D. Pramanik, et. al. (2021), confirmed the use of unique parameter of sawing angle and constant focal point distance strongly influence on hole diameter and circularity in laser trepan drilling and investigated the laser trepan drilling by multi diode pulsed fiber laser beam machining [111].

V. Chengal Reddy, et. al. (2021), optimized the surface roughness (Ra) and HAZ in fbre laser drilling of AISI 303 material. Surface roughness and heat-afected zone (HAZ) are the important features which infuence the performance of the laser-drilled products[112].

S. Chatterjee, et. al. (2021), used pulsed millisecond Nd:YAG laser for micro drilling of titanium alloy and stainless steel under identical machining

conditions by varying the process parameters such as current, pulse width, pulse frequency, and gas pressure on accuracy of holes [113].

X. Jia, et. al. (2022), achieved the high-quality and high-efficiency micro-hole drilling through controlling the laser–matter interaction, compared the characteristics of different laser drilling method (LDM) with systematically the morphology, diameter, circularity, taper angle, cross-section, heat affect zone, recast layer, cracks, roughness, micro–nano structure, photothermal effect and photochemical reaction of the drilling. The material is ceramic and it is drilled hole by (1064 nm wavelength, 4 J pulse energy, 20 Hz repetition rate, 0.5 ms pulse duration) with different pulse numbers [114].

T., Barthels, et. al. (2019, September). They developed technology high-precision ultrashort pulsed laser drilling of micro and nano holes using multibeam processing, femtosecond laser source with stainless steel [115].

1.9 Aim of the work

In this work, the aim is to study the effect of interaction of Q-switched Nd:YAG laser with different nanoparticles types on different materials (metals) and try to obtain microholes and nanoholes according to this effect. Also, studying the effect of laser parameters (laser pulse energy, laser repetition rate) and different concentrations of nanoparticles on the accuracy and size of holes.

Chapter Two

The experimental Details

2.1 Introduction

This chapter deals with the experimental setup, and the technique, which has been used in this work. In addition preparation of nanofluid will be introduced. The mixing of the nanoparticles with water to make the nanofluid at an appropriate concentration are explained in detail. The importance and key points of selection for both nanoparticles and different materials are discussed. As both of nanoparticles rely on the interaction with the laser beam and the amount of energy absorption from it to reach the melting point for each of them, the operation principles of both nanoparticles are similar except of the physical properties that are different. The selection of different materials depend on their characteristics that are discussed in this chapter. This system is constituted by an auxiliary part that interacts with the laser beam and deals with different materials with the technique that is mentioned in detail. The necessary instruments and devices used in this experiments are listed and discussed in details in terms of performance and specifications, and this chapter expresses the certification standard for obtaining micro and nano holes.

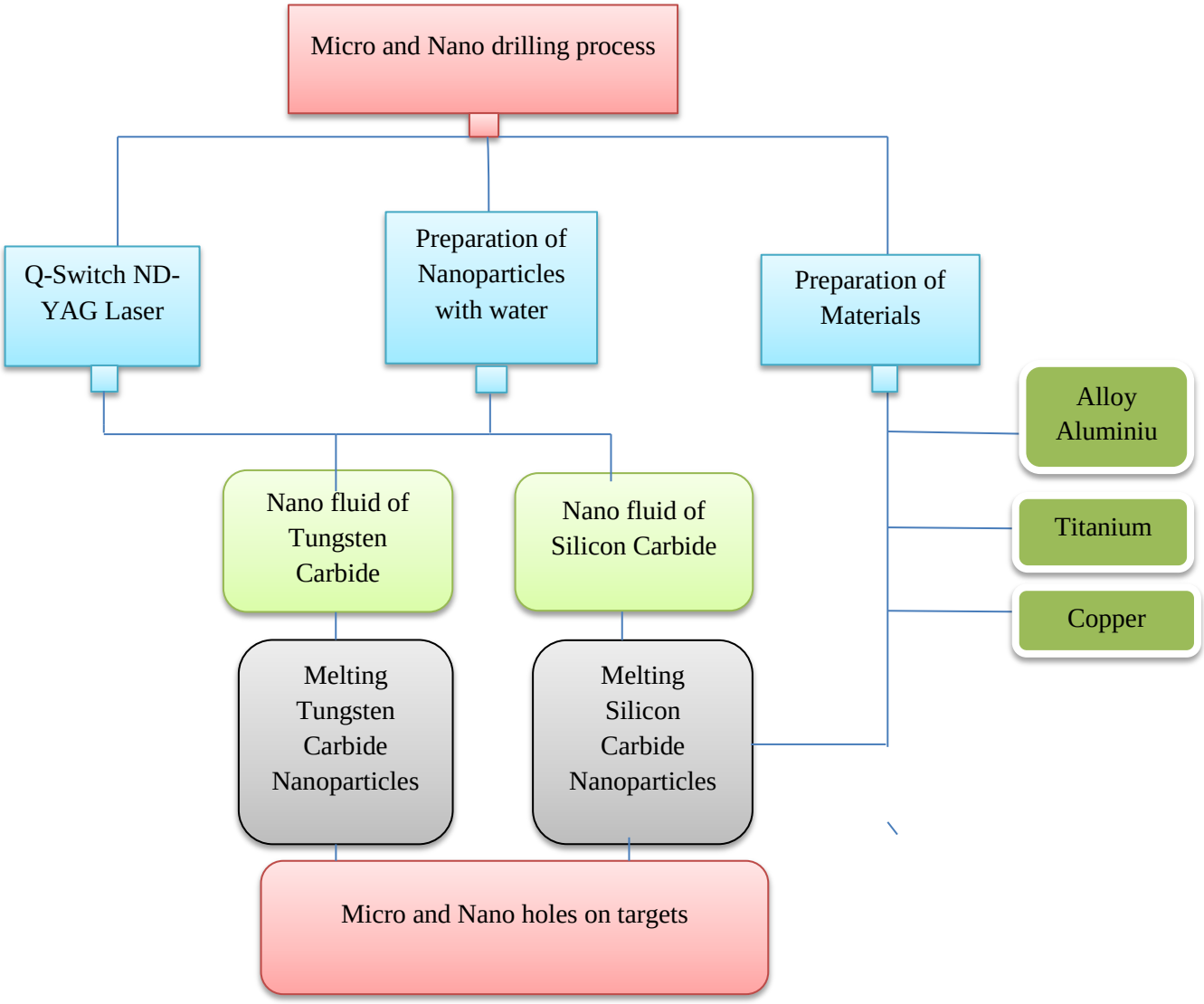

Figure (2.1): Diagram showing the setup of the work

2.2 The experimental setup

The experimental setup that has been used in this work is shown in Figure (2.2).

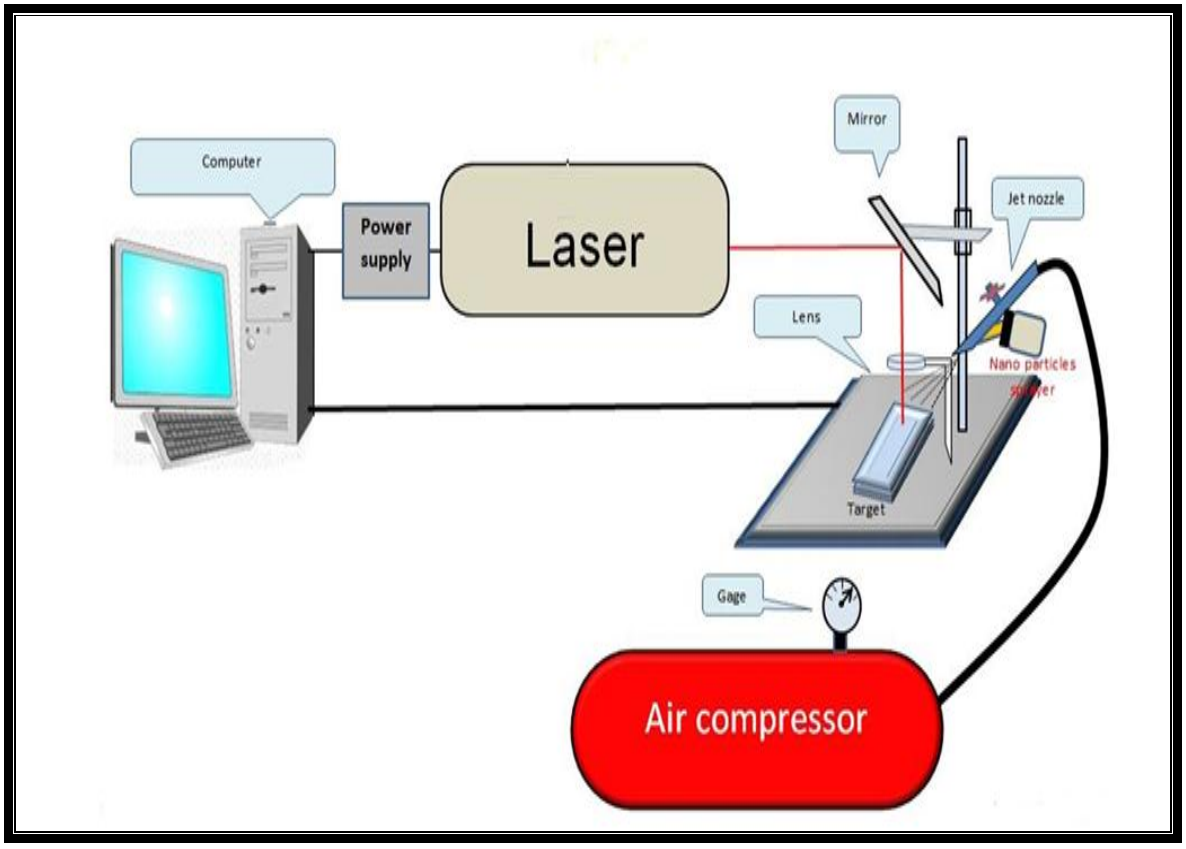

Fig.(2.2): Schematic diagram of the experimental setup for laser microdrilling

The study employed a Q-switched Nd:YAG laser system of 1064nm wavelength, 10ns pulses width, a range of pulse repetition rate of 1-20 Hz, and maximum pulse energy of 900mJ. An air compressor pumps air through a jet nozzle. Convex lens of 100mm focal length is used to focus the laser beam. Three types of metals of 0.1mm thickness were utilized as target namely aluminium alloy AA8009, pure titanium (Ti) and pure copper (Cu). Two types of nanoparticles were used in this work, tungsten carbide (WC)of 55nm grain size and silicon carbide (SiC) of 50 nm grain size. In this setup, different ratios of nanoparticles were mixed with distul water to make the nanofluid. So, the first type of nanoparticles SiC is mixed with distul water at room temperature using the mixing capsule magnetic stirrer bar. This solution is placed on a magnetic stirrer device for 30 minute at a temperature of 50°C to obtain a

homogeneous suspended solution. The nanofluid is injected into a jet nozzle that is coupled to an air compressor with a work pressure of 150-200 psi. The laser beam is focused on the nanofluid spray above the surface of the target, this technique is also used with tungsten carbide nanoparticles using the same procedures.

2.2.1 Q-switched Nd:YAG Laser source

The pulsed Q-switched Nd:YAG laser is utilized in this work as a source of energy to interact with different materials and nanoparticles. It plays important role in drilling process. This device was of model is LF117, manufactured by SOL instruments with equimpped cooling system and power supply, as shown in Figure (2.3), and the specifications of laser source are listed in Table (2.1). A Bi-convex spherical lens (type 1187-C-ML) manufactured by Thor Labs was also utilized in this setup with focal length is 100mm.

Figure(2.3): (a) Pulsed Nd:YAG laser LF117, (b) Laser power supply and (c) cooling system

The specifications of the laser source show in Table (2.1).

Table(2.1) parameters of laser source

Specification	
Type	Solid laser
Active medium	Nd:YAG
Wavelength	Near infra –red(1064 nm)
Output	Pulsed (Q-switched)
Max- Pulse energy	900 mJ
Pulse width	10 ns
Pulse Repetition Rate	1-20 Hz
Beam Divergence	<0.7>mrad
Beam diameter	~7.5 mm
Operating Mode	Pulse
Radius of spot size after focusing	0.758mm

2.2.4 Air compressor

An Air compressor model Abollo50, fiac was used in this setup. The compressor gives a pressure of range 0-230 psi (0-16 bar) with running power 1.5HP, as shown in Figure (2.4).

A Jet nozzel (model: KMOON, Single Action 0.8mm Airbrush) with nozzle diameter 0.8mm (0.031in) was connected to air pressure and utilized to spray the nanofluid on the material's surface, as shown in Figure (2.5).

Figure(2.4): Air compressor

Figure(2.5): Jet nozzle

2.2.5 Magnetic stirrer device

A magnetic stirrer device with model MAGNETIC STIRRE HOTPLATE, manufactured by L.I.P.EQUIPMENT&SERVICES LTD GTURT SCIENTIFIC CO. LTD**.**, was used for mixing and blending the nanoparticles powder with water, as shown in Figure (2.6a). A magnetic stirrer or magnetic mixer is a laboratory device that employs a rotating magnetic field to cause a stir bar immersed in a liquid to spin very quickly, thus stirring it [116]. The magnetic stirrer bar (or mixing capsule) was also employed in this work to stir, mix and homogenize the nanofluid in a small container. The standard laboratory magnetic stirrer bar has diameter of Φ5mm diameter and length of 20mm, as shown in Figures (2.6b).

(a). **(b)**

Figure (2.6a): Magnetic stirrer device **Figure (2.6b): magnetic stirrer bar**

2.2.6 Ultra- Sonic Cleaner

The ultra- sonic device is used to clean and sterilize the small container and the mixing capsule that has been used in this work. The ultra- sonic device was of model is 010, INSP No.: Qc 11, IN PUT from US and Engineered to Last company, as shown in Figures (2.7).

Figure (2.7): Ultra-Sonic Cleaner .

2.3 Materials

The materials that have been used in this work was as follows that aluminium alloy (AA8009), pure titanium(Ti), pure copper(Cu), and two types of nanoparticles include tungsten carbibe nanoparticles (WC) and silicon carbide nanoparticles (SiC). The diamentions of each samble are (20*20*0.1)mm.

2.3.1 Aluminium alloy (AA8009)

This alloy has good thermal stability, high temperature strength, high wear resistance and good thermally properties[117]. This material produced by Zhogke Yanno company, North District of Xinyan, Science and Technolgy Park, Beijing. The chemical components using X ray fluorescence test, as shown in Table(2.2) of this alloy are aluminium, manganese, titanium, iron, silicon, zinc and vanadium etc. [118].

Table(2.2): The chemical composition of aluminium alloy(AA8009)

Symbol	Mg	Al	Si	P	S	Ti	V	Cr	Mn	Fe	Co	Ni	Cu
Concentration %	0.015	88.3	0.66	0.003	0.002	0,26	0.00085	0.0142	0.299	3.797	0.154	0.1074	1.530
Symbol	Zr	Nb	Mo	Ag	Cd	Sn	Sb	W	Zn	Pb			
Concentration %	0.0076	0.0012	0.504	0.0073	0.0105	0.00024	0.015	0.07	1.514	0.622			

Sum of concentration is 99.00%

2.3.2 Titanium material

Titanium material has high strength, difficult to machine, high hardness and heat resistant. It represents a challenge during machining by conventional machining processes. This is due to their high strength and low thermal

conductivity [119]. This material produced by Zhogke Yanno company, North District of Xinyan, Science and Technolgy Park, Beijing. The chemical composition of this material using X ray fluorescence test, as shown in Table(2.3).

Table(2.3): The chemical composition of pure Titanium

Symbol	Mg	Al	Si	P	S	Ti	V	Cr	Mn	Fe
Concentration %	0.022	0.0048	0.0016	0.0033	0.002	98.3	0.034	0.00035	0.0472	0.1836
Symbol	Cu	Zr	Nb	Mo	Ag	Cd	Sn	Sb	W	Zn
Concentration %	0.0613	0.016	0.0061	0.161	0.0248	0.0063	0.001	0.0199	0.0018	0.0693
Symbol	Co	Ni	Pb							
Concentration %	0.0091	0.0145	0.00076							

Sum of concentration is 99.00%

2.3.3 Copper material

Copper has several advantageous characteristics, including strong electrical conductivity, thermal conductivity, corrosion resistance, ease of alloying, ease of joining, toughness, and non-magnetic qualities [120]. This material produced by Zhogke Yanno company, North District of Xinyan, Science and Technolgy Park, Beijing. The chemical composition of this material using X ray fluorescence test, as shown in Table(2.4).

Table(2.4): The chemical composition of pure Copper

Symbol	Mg	Al	Si	P	S	Ti	V	Cr	Mn	Fe	Co
Concentration %	0.024	0.0377	0.0017	0.0012	0.002	0.0125	0.0015	0.06	0.0468	0.0514	0.0312
Symbol	Ni	Cu	Zn	As	Zr	Nb	Mo	Ag	Cd	Sn	Sb
Concentration %	0.0896	98.57	0.0049	0.00032	0.01	0.0037	0.088	0.0027	0.007	0.001	0.0085
Symbol	W	Pb									
Concentration %	0.0087	0.0015									

Sum of concentration is 99.00%

The properties of the materials used in experimental work were listed in Table(2.5).

Table(2.5): The properties of the materials.

Material	**Aluminium**	**Titanium**	**Copper**
Symbol	Al	Ti	Cu
Atomic Number(Z)	13	22	29
Purity	88.30	98.37	98.57
Element Category	Alloy	Metal	Metal
Atomic Mass (u)	26.981539	47.867	63.5464
Phase at STP	Solid	Solid	Solid
Density at STP (g/cm^3)	2.7	4.54	8.96
Possible Oxidation State	+3	+4, +3, +2	+1 , +2
Melting Point(℃)	660	1668	1084.62
Boiling Point (℃)	2467	3287	2500
Thermal Conductivity (W/m.k)	239	19	392

2.3.4 Tungsten carbide nanoparticle (WC)

It has characteristics of the hard-facing particles offers a unique combination of high hardness, high toughness, good wear-resistance, good fracture resistance, high melting point and high temperature strength [121,122]. The chemical composition of tungsten carbide nanoparticles are shown in Table (2.6).

The tungsten carbide nanoparticle was utilizing in this work as an important auxiliary for the drilling process, it acts as a tool for drilling. This nanoparticle was of model (US2063, with CAS#: 12070-12-1), and from (US Research Nanomaterials, Houston, TX USA) Company.

Table (2.6): chemical composition of tungsten carbide nanoparticles

Total Carbon	Free Carbon	Average Crystalline size	Surface Area	Al	Ca	Cr	V	Fe	Mo	Si	O
6.61+0.1%	<0.08%	40-70 nm	1.3-2.0 m^2/g	50 ppm	50	200	280	200	50	50	0.3 %

The SEM test and X-Ray Diffraction of tungsten carbide nanoparticles (WC), as shown in Figures(2.7) and (2.8).

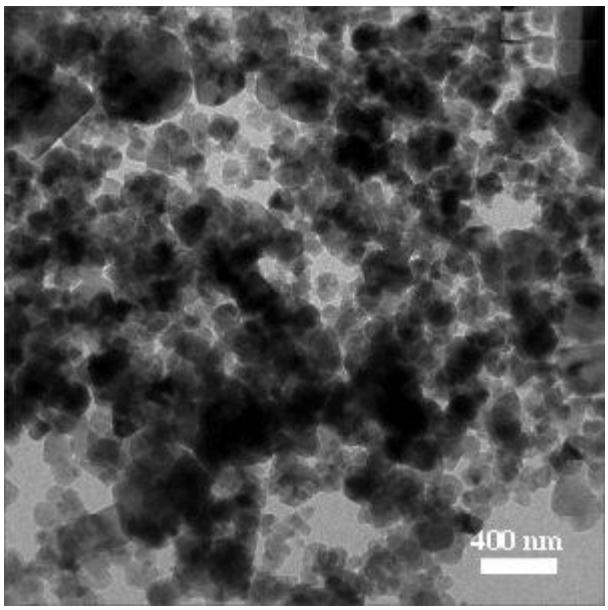

Figures(2.8): The SEM test of tungsten carbide nanoparticles

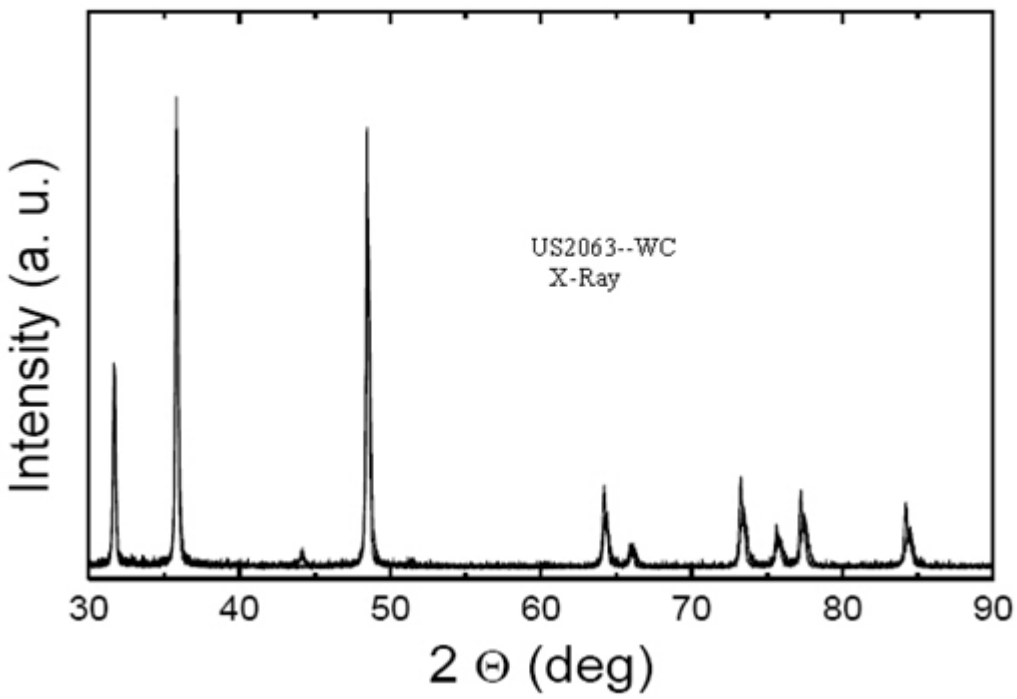

Figures(2.9): X-Ray diffraction of tungsten carbide nanoparticles

2.3.5 Silicon carbide nanoparticles

It has many superior characteristics, such as wide bandgap, excellent thermal conductivity and thermal shock resistance, good chemical, oxidation resistance and high electron mobility [123].

The silicon carbide nanoparticle is also employed in this work as an important assistant factor for the drilling process, it acts as a tool for drilling. This nanoparticle was of model (US2028), and from (US Research Nanomaterials, Houston, TX USA) Company. The SEM test and X-Ray Diffraction of silicon carbide nanoparticles (SiC), as shown in Figures(2.10) and (2.11).

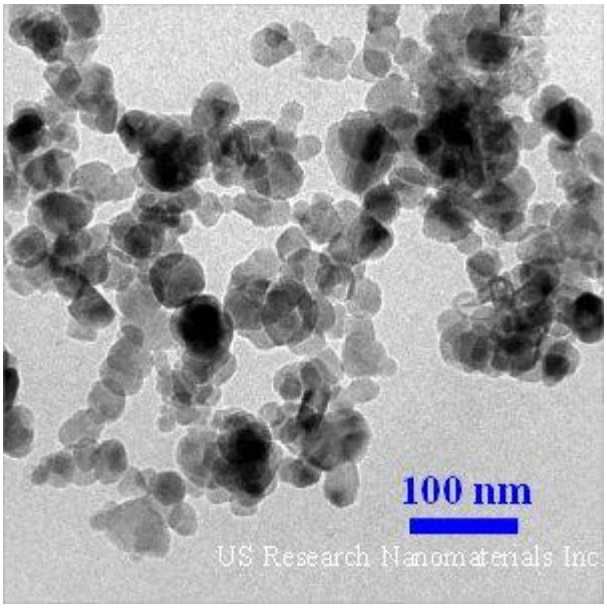

Figures(2.10): SEM test of silicon carbide nanoparticles(SiC)

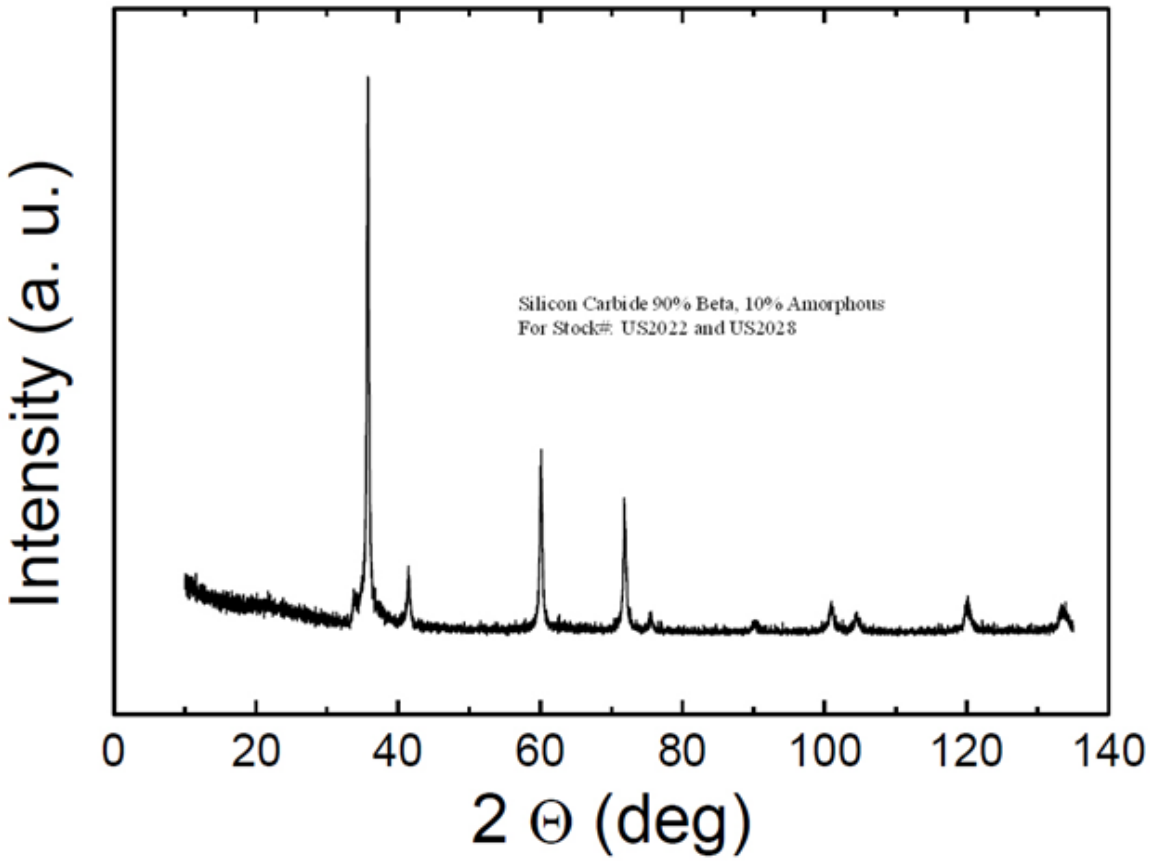

Figures(2.11): X-Ray Diffraction test of silicon carbide nanoparticles(SiC)

The characteristics of two kinds of nanoparticles, as shown in Table (2.7).

Table(2.7): The specification of nanoparticle

Nanoparicles	Tungsten carbide	Silicon carbide
Formula Molecule	WC	SIC
Crystal structure	Hexagonal	Cubic
Form	Powder	Powder
Purity	99.9 %	99%
Colour	Grey Black	Grayish white
Grain size	55 nm	50 nm
Average Particle Size (APS)	(150 – 200) nm	(45 – 65) nm
Melting point (m.p)	2870 ℃	2730 ℃
Solubility	Insoluble in water	Insoluble in water
Specific Surface Area (SSA)	(1.3 -2)m^2/g	(40 – 80) m^2/g
Density	15.63 g/cm^3	3.216 g/cm^3
Thermal conductivity	85	(120- 170)$W/m.K$
Free carbon	0.08 %	0.76 %

2.4 Preparation of Nanofluid

Nanofluids are a class of fluids with excellent heat transfer properties, which are designed and made by suspending metal and nonmetal nanoparticles in a base fluid such as water [124]. In this work, the distul water was used with nanoparticles to form nanofluids.

In a small container, tungsten carbide (WC) nanoparticles are mixed with water (base fluid) at room temperature using a magnetic stirrer bar (mixing capsule).

This nanofluid was placed on a magnetic stirrer device at a temperature of 50°C for (20-30) minute.

Depending on the ratio of nanoparticle powder to water, three degrees of concentration were obtained, high, medium and light concentration for each type of nanoparticles. Various materials are exposed to these nanofluid concentrations.

The same steps are applied again using the silicon carbide nanoparticles.

2.4.1 calculation of concentration ratio for nanofluid

-At 90% concentration ratio (high concentration of nanofluid)

In this case, it can be take 90g from silicon carbide nanoparticles (as a solute) mixing with 10g from distul water (D.W) (as a solvent) to obtain jel solution.

$$\text{Concentration ratio(g/g)} = \frac{mass\ of\ solut(SiC)}{mass\ of\ solution} * 100\%$$

$$X = \frac{mass\ of\ solute}{mass\ of\ solvent(water) + mass\ of\ solut} * 100\%$$

$$X = \frac{90g}{10g + 90g} * 100\%$$

$$X = \frac{90\ g}{10g + 90g} * 100\% = \frac{90\ g}{100g} * 100\% = 0.9 * 100\%$$

$$X = 90\%$$

-At 50% concentration ratio (medium concentration of nanofluid)

In this case, it can be take 50g from silicon carbide nanoparticles mixing with 50g from distul water (D.W) to obtain thick solution.

$$X = \frac{mass\ of\ solute}{mass\ of\ solvent(water) + mass\ of\ solut} * 100\%$$

$$X = \frac{50\ g}{50g+50g} * 100\% = \frac{50}{100} * 100\% = 50\%$$

-At 5% concentration ratio (light concentration of nanofluid)

In this case, it can be take 2.5g from silicon carbide nanoparticles (as solute) mixing with 47.5g of distul water (D.W) (as solvent) to obtain homegenius solution.

$$\text{Concentration ratio(g/g)} = \frac{mass\ of\ solut(SiC)}{mass\ of\ solution} * 100\%$$

$$X = \frac{mass\ of\ solute}{mass\ of\ solvent(water)+mass\ of\ solut} * 100\%$$

$$X = \frac{2.5g}{47.5g+2.5g} * 100\%$$

$$X = \frac{2.5\ g}{47.2g+2.5g} * 100\% = \frac{2.5\ g}{50g} * 100\% = 5\%$$

Chapter Three
Results and Discussion

3.1 Introduction

This chapter includes the experimental results that has been obtained in this work to get the micro and nano holes in the targets. These results were analysed using scanning electron microscopy (FESEM) test. Different results were obtained according to the various parametrs and different materials that have been used in this work. Different materials were used and examined in advance using X-ray fluorescence (XRF), and the experimental procedures were carried out using different laser pulse energies, various laser repetition rates and different nanoparticles. The use of different laser pulse energies with and without the nanofluid on different materials is compared. The materials that have been used in this work are aluminium alloy(AA8009), pure titanium and pure copper. The laser intensities used in this work with various laser energy, are listed in Table (3.1). The Beam Profile is Gaussian and the radius of spot size after focusing is 0.7516mm.

Table (3.1): listed the laser parameters with different laser energies

Repetition Rate(Hz)	Pulse Width (ns)	Pulse Energy (mJ)	Laser Intensity (W/cm^2)	Peak power (W)
5	10	600	6.6 x10^8	6.0 x10^7
10	10	700	7.7 x10^8	7.0 x10^7
10	10	800	8.8 x10^8	8.0 x10^7

3.2 Results

The first attempt to obtain nano and micro-holes, laser parameters applied on aluminum alloy that laser pulse energy of 400 mJ and repetition rate is 5Hz using silicon carbide nanoparticles and light concetration of nanfluid with exposure time is 5sec. The examination was conducted in the laboratories of the

University of Technology. The results of SEM test indicated that no penetrating holes and irregular surface were obtained, as shown in Figures(3.1). In this situation, a low laser energy was used with the same ideal parameters on the aluminum alloy, this lead to low absorption of laser energy, the nanoparticles could not reach the state of complete melting. In addition, aluminum has good thermal conductivity and good thermal expansion, which makes it difficult to obtain perfect holes under these conditions.

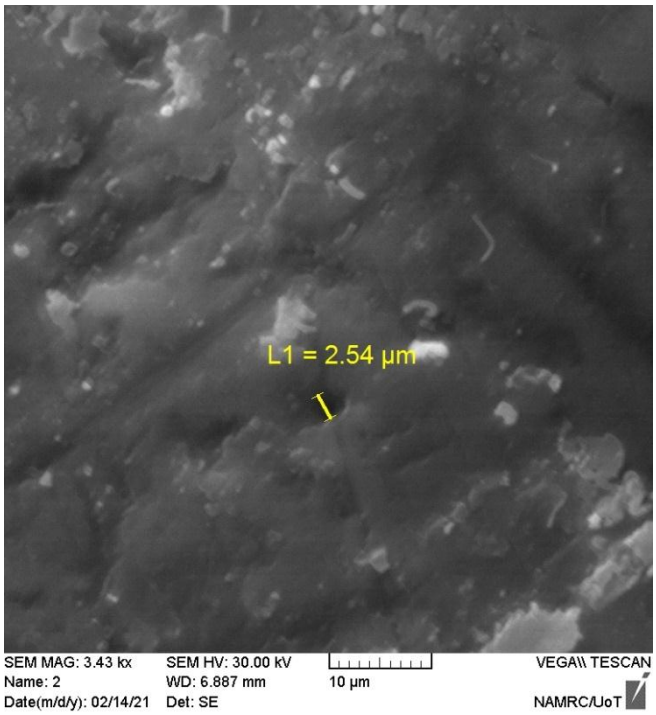

(a)

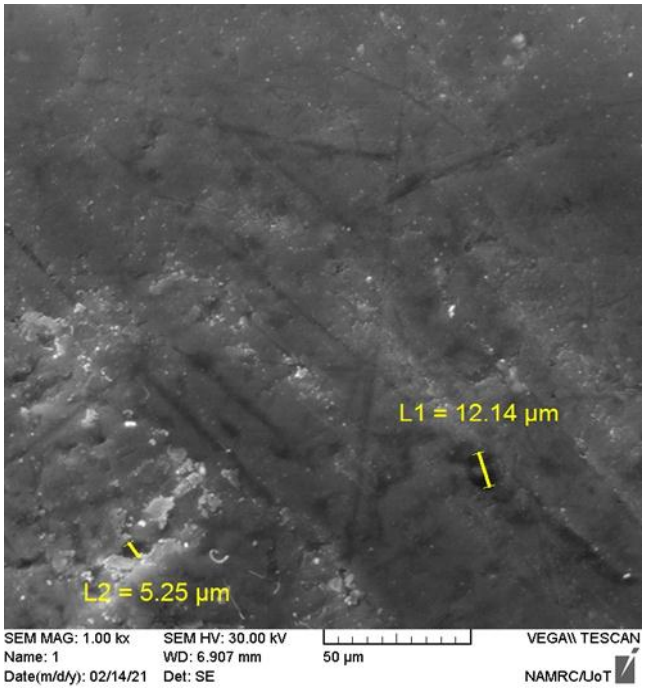

Fig.(3.1): The FESEM test for AA8009 alloy pulsed laser with 400mJ pulse energy, 5 Hz repetition using silicon carbide nanoparticles with exposure time is 10sec

The laser parameter had been used in this work, like different laser pulse energies of (600 mJ, 700 mJ and 800 mJ) with different repetition rates (5Hz, 10Hz) are focused on different nanoparticles and different materials to get the result of micro and nano drilling.

3.2.1 Q-switched Nd:YAG Laser interaction with aluminium alloy (AA8009)

3.2.1.1 Laser interaction with AA8009 without using nanoparticles

In this work, Q-switched Nd:YAG laser with energy of 800mJ, with 10Hz repetition rate subjected to AA8009 sheet for 40 sec. As a result there, no drilling holes clearly appeared as shown in Figure (3.2).

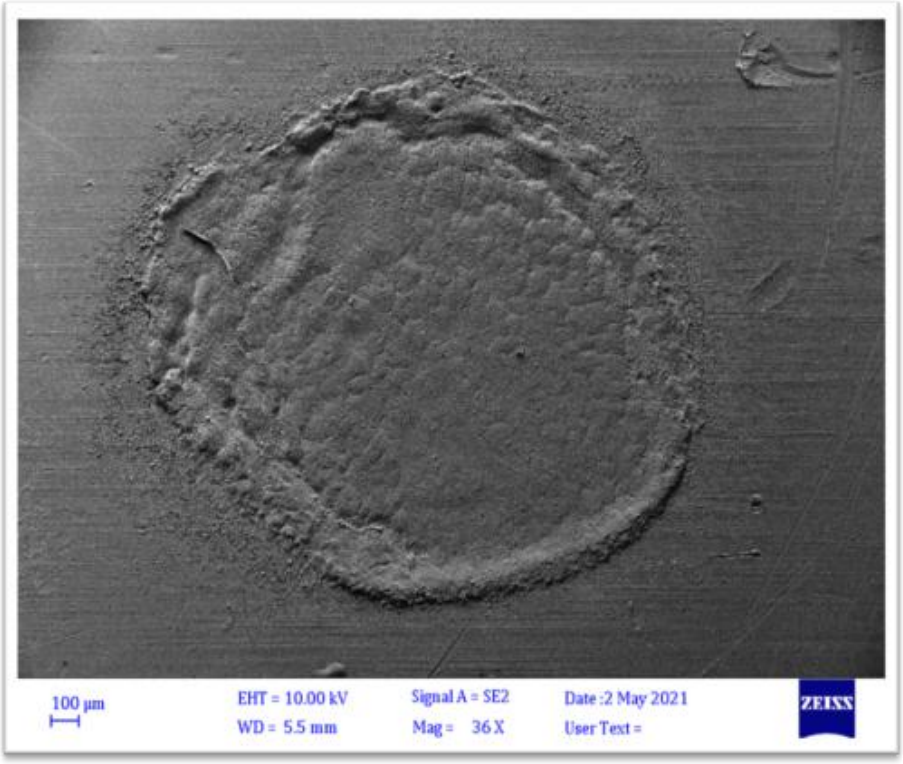

Figure(3.2): The FESEM test for AA8009 alloy using Nd: YAG pulsed laser with 800mJ pulse energy, 10 Hz repetition rate and 40 sec exposure time without using nanoparticles

This Figure shows the effect of the laser pulse on the target. There is only a thermal effect (without obtaining any holes on the target). This means that the laser with its maximum energy, with high repetition rate and with a long exposure time, couldn't make any hole in the target. There is only thermal effect(thermal expansion) on this material and aluiminum has high reflectance of the incident laser beam.

3.2.1.2 Laser interaction with AA8009 using SiC NPs fluid

In this work, the concentration ratio of nanofluid that has been used was 90% (of nanoparticles), the laser pulse energy is 800mJ, repetition rate is 10Hz and exposure time is 5sec. The (FESEM) test appears the aggregations of

nanoparticles and microcracks on the surface of the target, as shown in Figure (3.3).

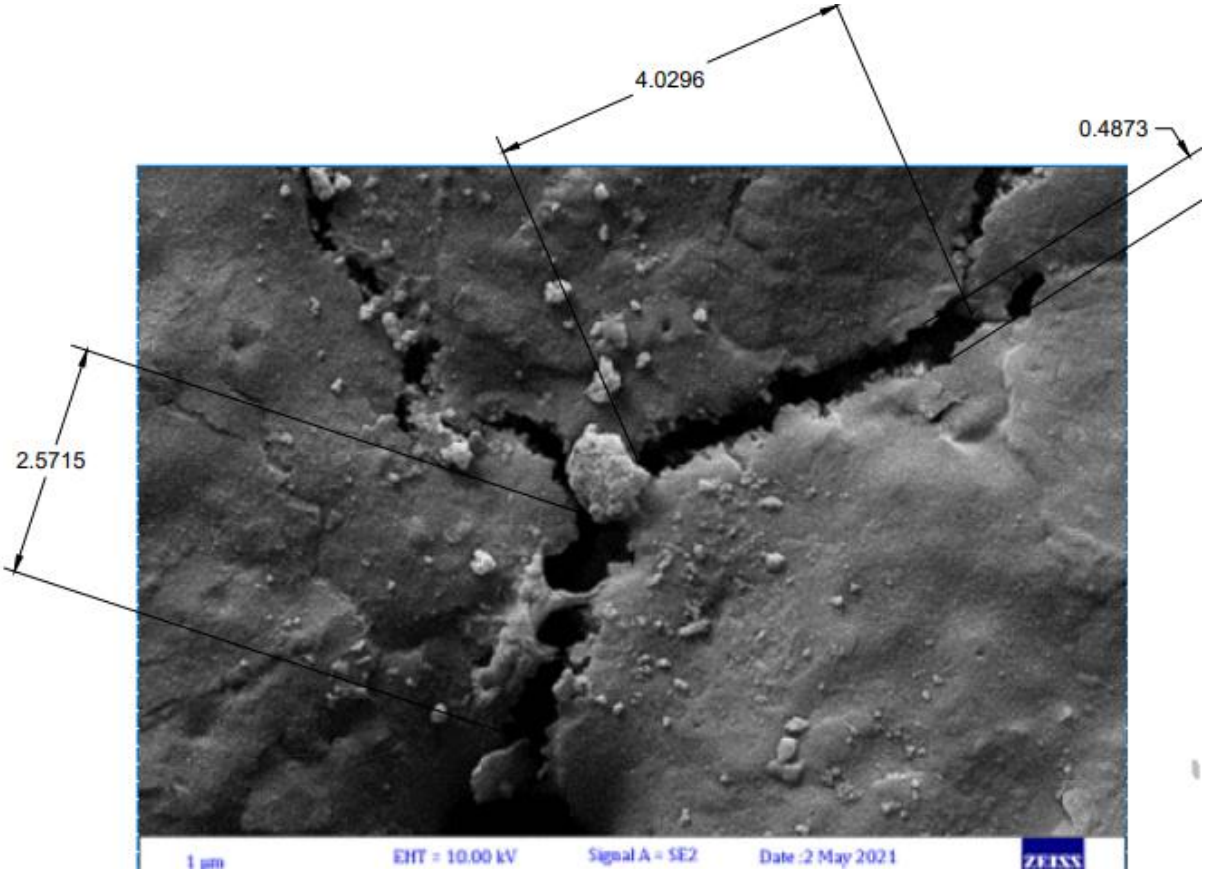

Figure(3.3): FESEM image for AA8009 alloy using Nd:YAG pulsed laser with 800mJ pulse energy, 10 Hz repetition rate, 5 sec exposure time and 90% concentration ratio of SiC nanofluid

This case can be attributed to the high concentration of nanoparticles and high laser energy . In the drilling process, the nanofluid continues to be pumped while the laser beam is focused on it. During this, a large group of nanoparticles reach the stage of melting, so the cracks are made, and the other reaches the heating stage only and descends as accumulations on the surface, according to the concentration of the nanofluid used in that case and the type of nanoparticles used. The cracks on this material as aresults of heat conduction and thermal stresses(mechanical stress).

If the concentration ratio of nanofluid is reduced to 50%, the laser pulse energy is 600mJ, repetition rate is 5Hz and exposure time 5sec, the microholes were obtained on the target, as shown in Figure (3.4).

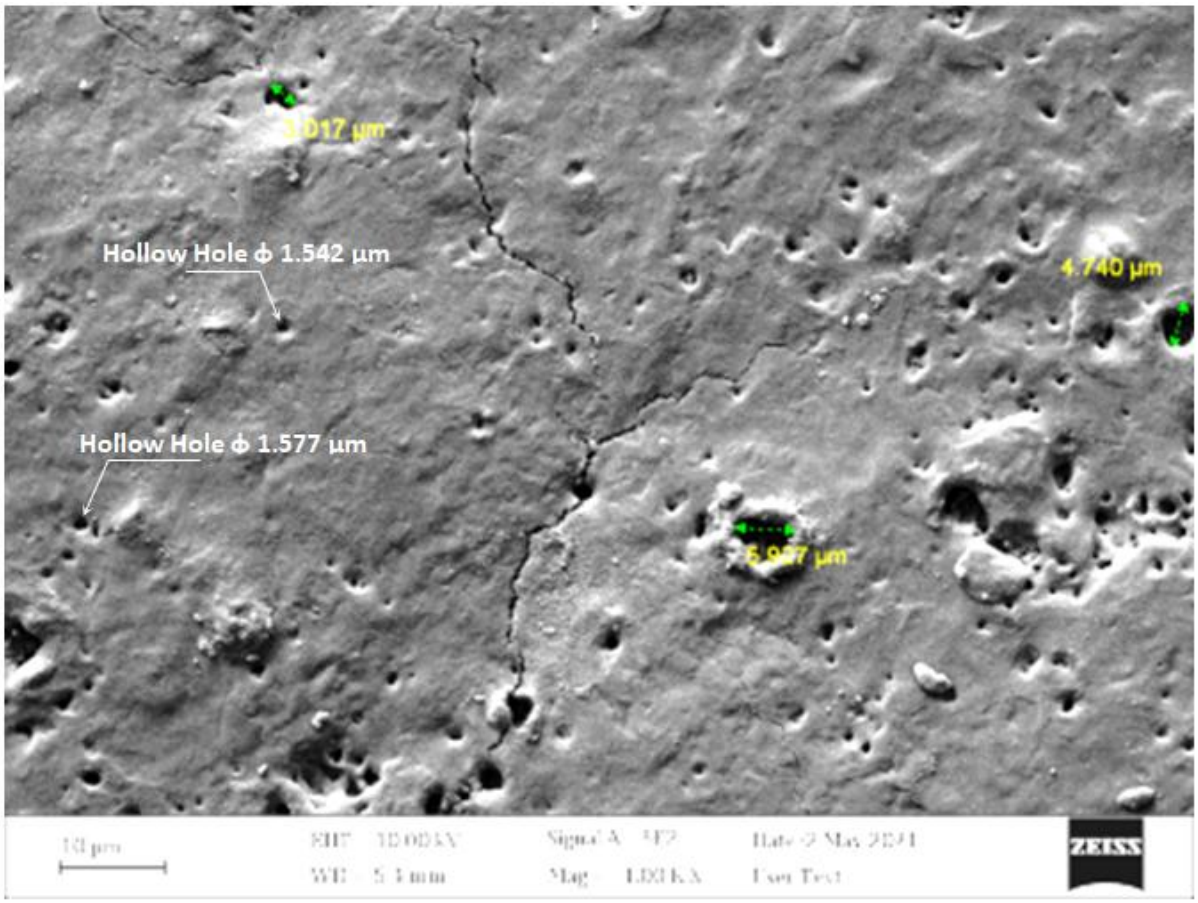

Fig.(3.4): The FESEM test for (AA8009) alloy using Nd:YAG pulsed laser with 600mJ pulse energy, 5 Hz repetition rate, 5sec exposure time and 50% concentration ratio of SiC nanofluid

The FESEM image of aluminium alloy(AA8009) Figure (3.4) shows some amount of (SiC) nanoparticles are melted and come down to the surface to drill micro holes and some of (SiC) nanoparticles accumulated sufficiently forming cracks on the target. The thermal elastic stress can lead to cracks because of different tempreture between aluminium alloy and (SiC) nanoparticles.

When the concentration ratio of the nanofluid is reduced to 5% (of the nanoparticles), the laser pulse energy is 600mJ, repetition rate is 5Hz and exposure time is 5sec, the microholes and nanoholes for aluminium alloy(AA8009) are obtained. Figure (3.5) indicate that, few numbers of fine nano holes appear on the target due to light concentration of nanoparticles. The number of nanoparticles in the fluid will be small. This will lead to make the number of these particles per unit volume is also small. These small sizes of nanoparticle groups will melted in a short time according to its size and density causing these holes.

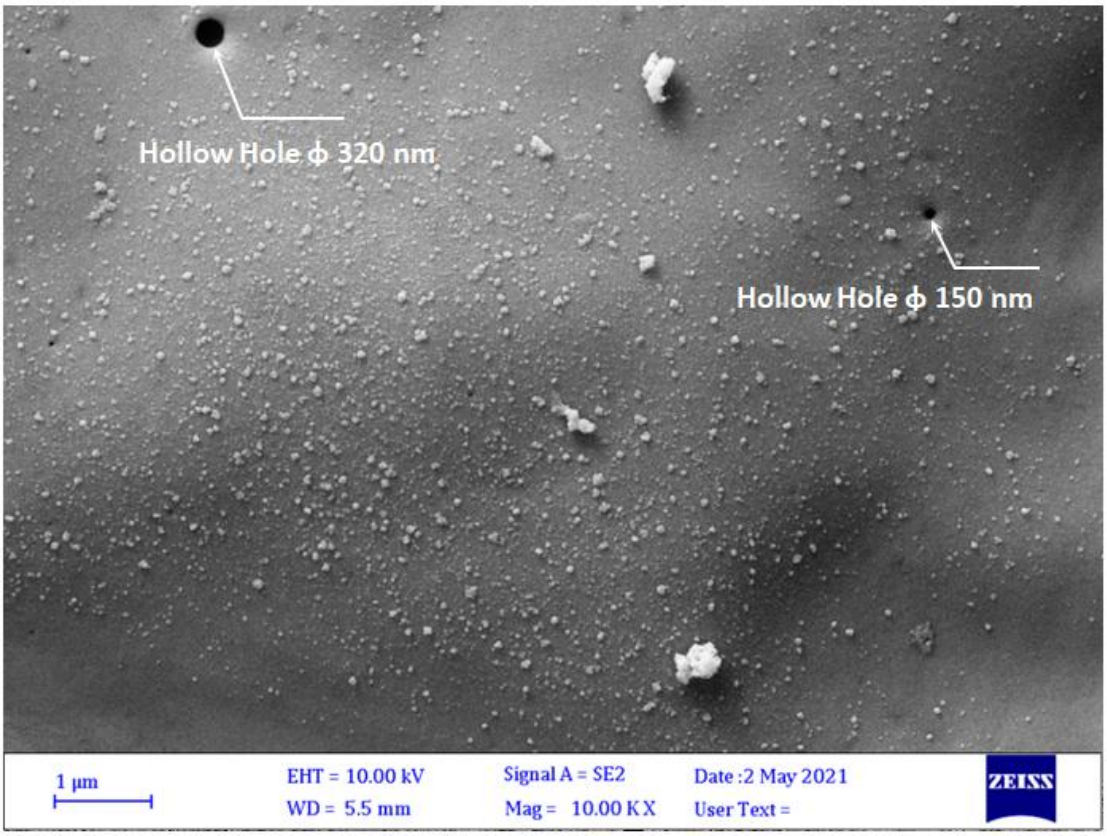

Fig.(3.5): The FESEM test for AA8009 alloy using Nd:YAG pulsed laser with 600mJ pulse energy, 5 Hz repetition rate, 5sec exposure time and 5% concentration ratio of SiC nanofluid

The result of Figure (3.6) indicates that, if the exposure time is increased to be 10 sec for the same laser parameters, a lot of fine nanoholes will appear on the target as shown in Figure (3.6). Figure (3.5) differs from Figure (3.6) in terms of the number of holes due to the difference in exposure time only for the same parameters. In addition to the physical properties of the material, especially with regard to the low melting point compared to the molten nanoparticles coming down, this makes it react easily and produce many nano and micro holes at a time of greater exposure.

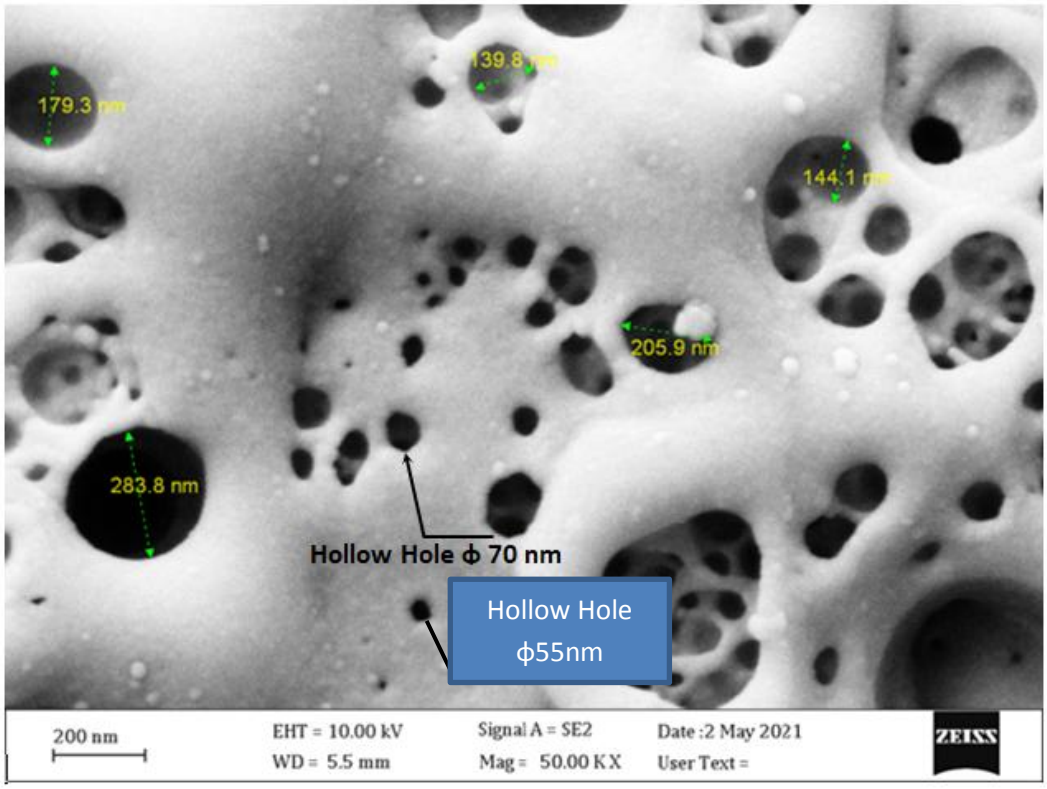

Fig.(3.6): The FESEM test for (AA8009) al alloy using a Yag pulsed laser with 600mJ pulse energy, 5 Hz repetition rate, 10sec exposure time and 5% concentration ratio of SiC nanofluid

3.2.1.3 Laser interaction with AA8009 using tungsten carbide(WCNPs) nanoparticles

When the concentration ratio of nanofluid is 90% (of the nanoparticles), the laser pulse energy is 800mJ, repetition rate is 10Hz and exposure time is (30sec), the aggregations of nanoparticles were obtained, as shown in Figure(3.7(a,b)). This belongs to the high laser energy, and high concentration of (WC) nanoparticles . These nanoparticles size, higher density and different physical properties as compared to SiC nanoparticles. Therefore, large numbers of nanoparticles need more time (30sec.) to melt and drill, they accumulated and fallen on the target with irregular holes and also aggregated on the surface and due to high energy, high absobtion by this material (aluminium has good thermal conductivity), this causes high temperature and high roughness on the target.

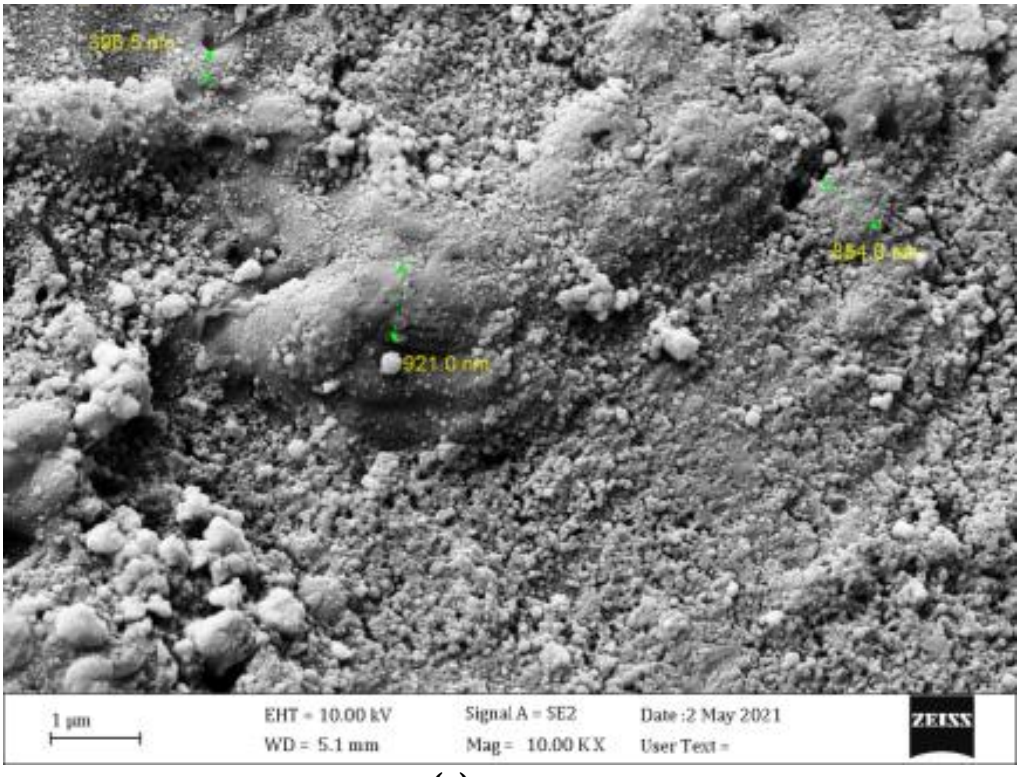

(a)

(a)

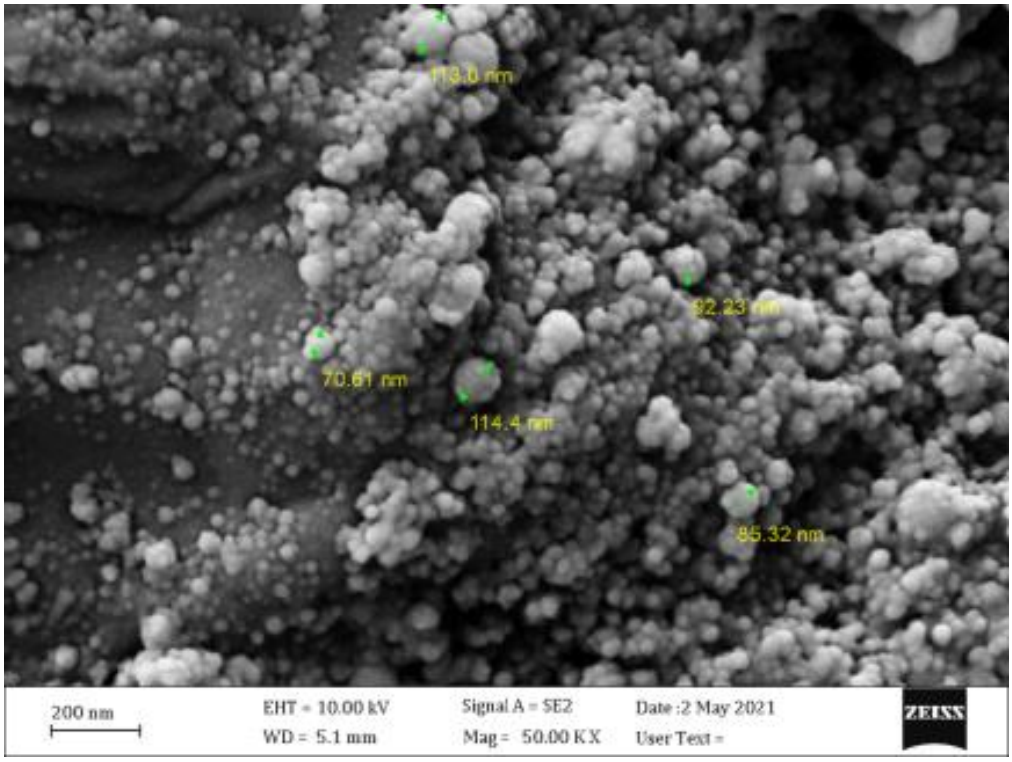

(b)

Fig.(3.7(a,b)): The FESEM test for AA8009 alloy using Nd:YAG pulsed laser with 800mJ pulse energy, 10 Hz repetition rate, 30sec exposure time and 90%concentration ratio of WC nanofluid

If the concentration ratio of nanofluid is reduced to 50% (of the nanoparticles), the laser pulse energy is 600mJ, repetition rate is 5Hz and exposure time (30)sec, the microholes were obtained on the target, as shown in Figure (3.8).

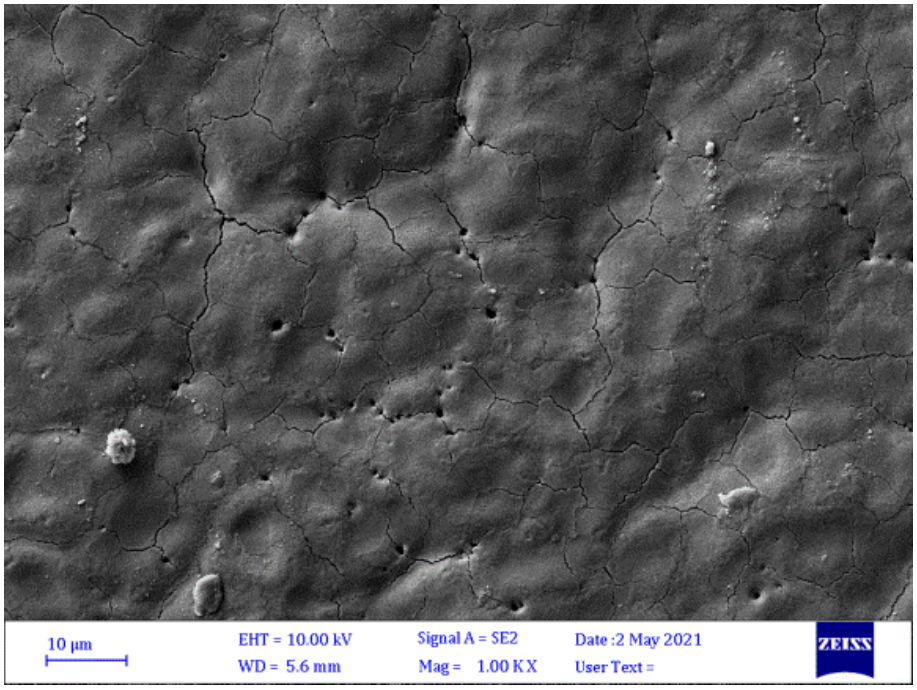
10 µm
EHT = 10.00 kV
WD = 5.6 mm
Signal A = SE2
Mag = 1.00 K X
Date :2 May 2021
User Text =
ZEISS

(a)

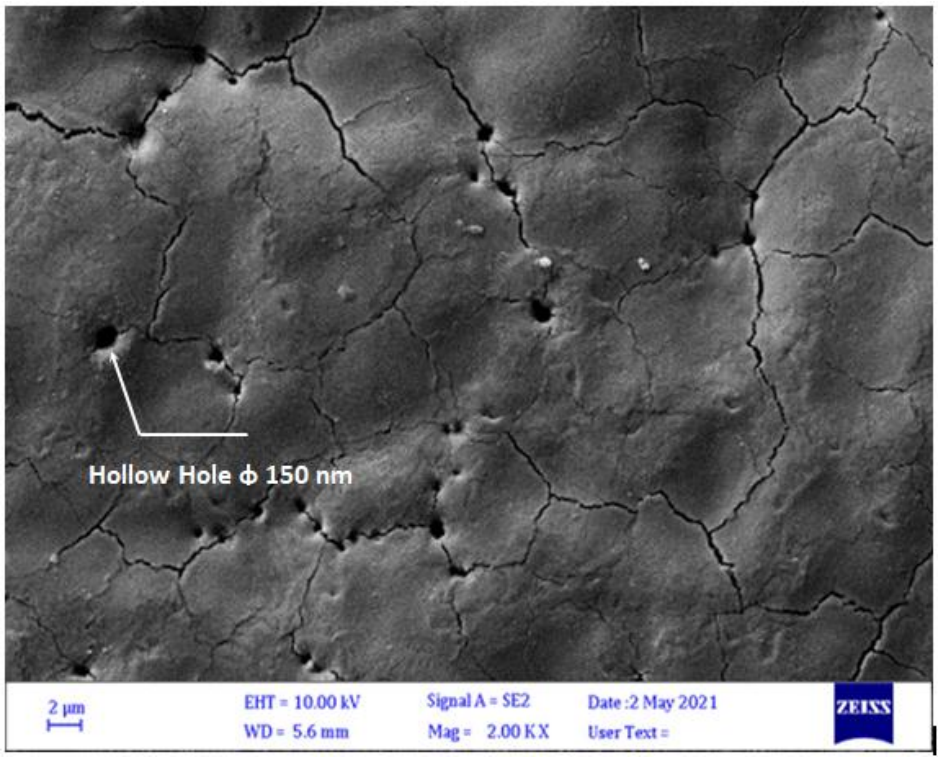
Hollow Hole ϕ 150 nm
2 µm
EHT = 10.00 kV
WD = 5.6 mm
Signal A = SE2
Mag = 2.00 K X
Date :2 May 2021
User Text =
ZEISS

(b)

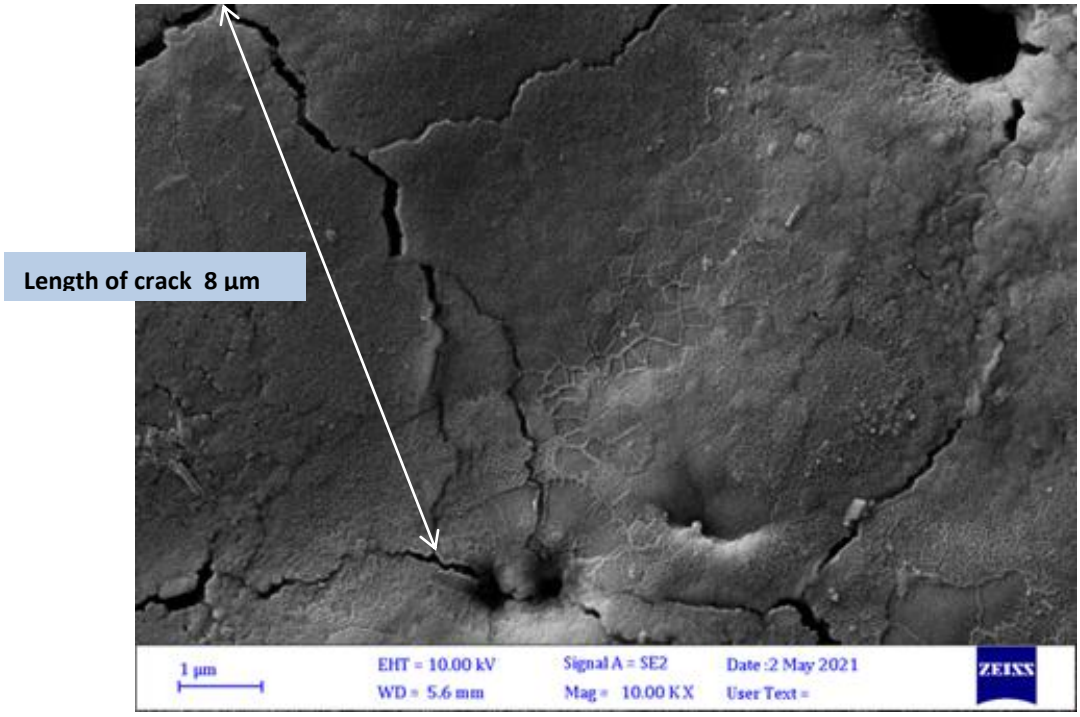

(c)

Fig.(3.8(a, b, c)): The FESEM test for AA8009 al alloy using Nd: YAG pulsed laser with 600mJ pulse energy, 5 Hz repetition rate, 30sec exposure time and 50% concentration ratio of WC nanofluid

These results indicate, the presence of micro holes and cracks in the material because of the concentration of the nanofluid is still high and the nanofluid continues pumping while the laser beam is focused on it. So, a large group of nanoparticles reach the stage of melting, forming large molten conglomerates that drop and drill for easy interaction between them so holes are made. The nanoparticle has an exposure time that varies according to its physical properties. As for some of the molten nanoparticles, they descend and cause a cracks due to the physical properties such as melting point and thermal properties of the target (good thermal conductivity).These cracks created by thermal elastic in this material due to variable of heating betweem aluminium alloy and melting nanoparticles.

The concentration ratio of the nanofluid is reduced to be as 5% and sprayed on the target. The laser pulse energy is 600mJ, repetition rate is 5Hz and exposure time is (30)sec, so the micro and nanoholes for the aluminium alloy (AA8009) are obtained, as shown in Fig.(3.9(a,b)). In this Figure, less regular holes were obtained as compared to holes achieved from SiC nanoparticles (Figure (3.5)). The reason for this is due to the difference in the melting point and physical properties between the two nanoparticle leads to different in exposure time. In this process, used light concentration of tungsten carbide nanoparticle will make small groups of nanoparticles melted and fell to drill in more time. Because of the continuous nanofluid spraying procedure used during the work, a portion of the tungsten carbide nanoparticle is heated but not melted. These heated nanoparticles will come down into the metal, causing irregularities in the diameter of the holes, but do not cause aggregations (or may cause a small aggregation) because the concentration here is little.

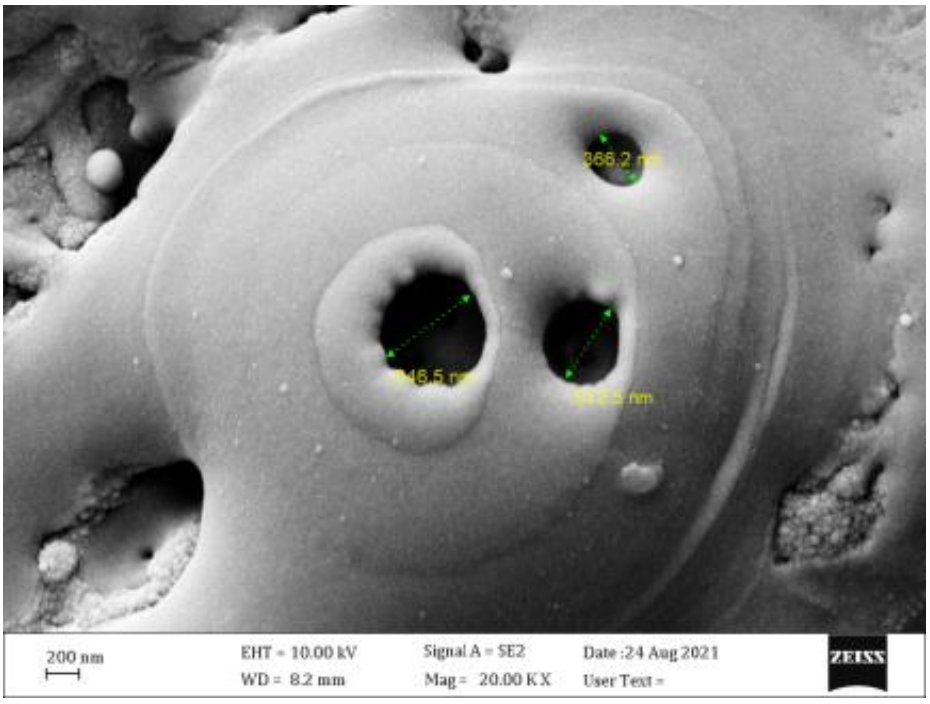

(a)

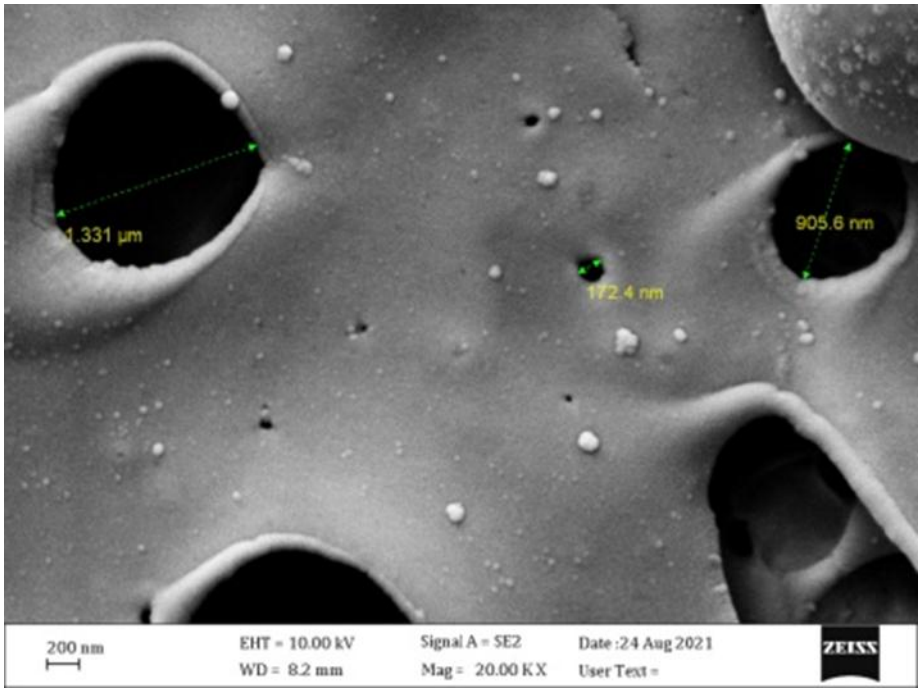

(b)

Fig.(3.9(a,b)): The FESEM test for AA8009 al alloy using Nd:YAG pulsed laser with 600mJ pulse energy, 5 Hz repetition rate, 30sec exposure time and 5% concentration ratio of WC nanofluid

3.2.2 Q-switched Nd:YAG laser interaction with Titanium

3.2.2.1 Laser interaction with titanium without using nanoparticles

In this state, the laser pulse energy of 800mJ was used, repetition rate was 10Hz and exposure time was (40sec). The drilling holes were not detected, as shown in Figure(3.10).

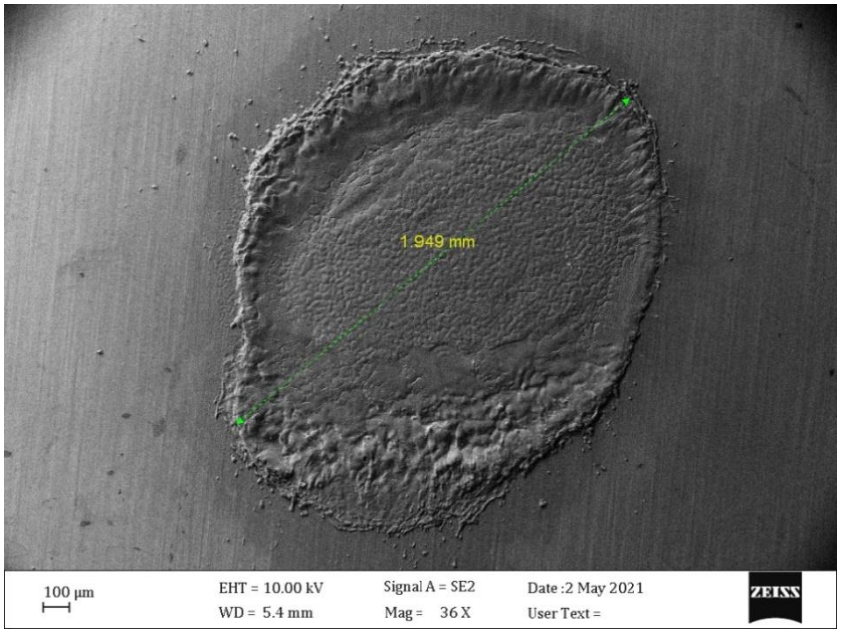

Fig.(3.10): The FESEM test for titanium using Nd:YAG pulsed laser with 800mJ pulse energy, 10 Hz repetition rate and 40sec exposure time without using nanoparticles

3.2.2.2 Laser interaction with titanium using SiC NPs

If the concentration ratio of nanofluid is 90% (of nanoparticles), the laser pulse energy is 800mJ, repetition rate is 10Hz and exposure time is 5sec, the cracks are formed, as shown in Figure(3.11a) and aggregations of nanoparticles are obtained on the target, as shown in Figure(3.11b). In this case the high concentration of nanoparticles causes drawback in titanium due to the pumping of nanofluid is continuous. So, amount of (SiC) nanoparticles are melted in this process and come down to deal with material caused cracks in short time. Some of nanoparticles are heated only and fallen on as agglomerations on the surface. Additionaly, because oh high energy of pule laser and the melted nanoparticles were falled, thermal elastic on the titanium.

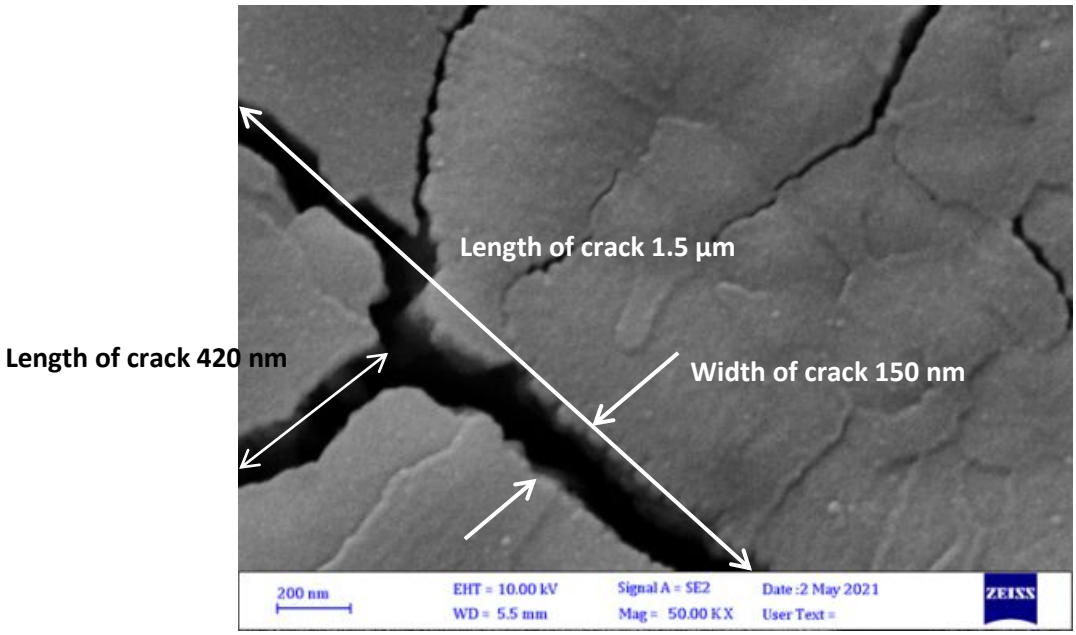

(a)

Fig.(3.11a): The FESEM test shows cracks in titanium using Nd: YAG pulsed laser with 800mJ pulse energy, 10 Hz repetition rate, 5sec exposure time and 90% concentration ratio of SiC

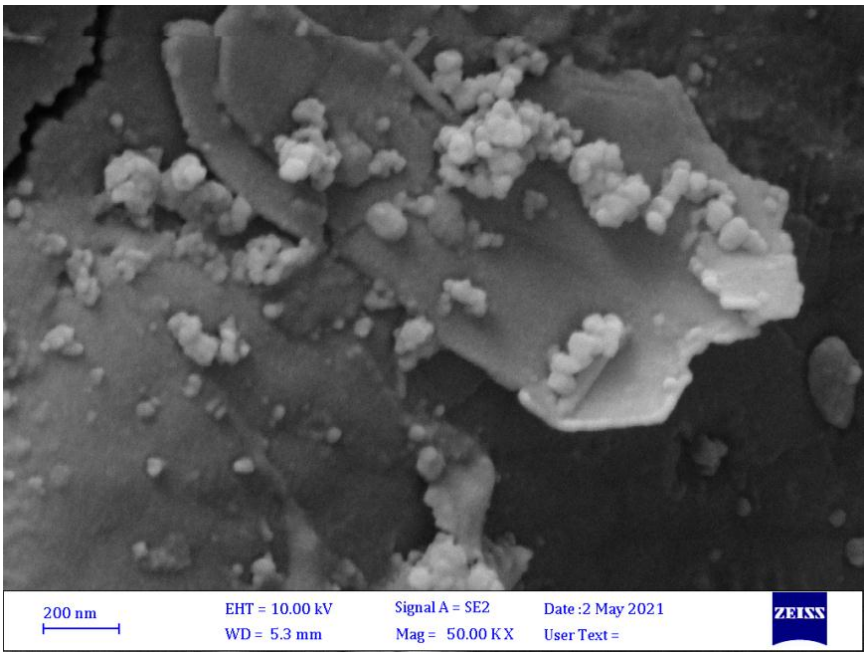

(b)

Fig.(3.11b): The FESEM test for titanium using a Yag pulsed laser with 800mJ pulse energy, 10 Hz repetition rate, 5sec exposure time and 90% concentration ratio of SiC nanofluid

When the nanofluid concentration ratio was reduced to 50% (of nanoparticles), the laser pulse energy is 600mJ, repetition rate is 5Hz and exposure time is (5, 10)sec, the micro holes on titanium are formed, as shown in Figure(3.12a). Irregular micro holes and aggregations of nanoparticles, can be shown in Figure(3.12b).

Figure (3.12a) indicates that, when the same parameters of laser were used, the same concentration of nanofluid and the same of nanoparticles but short exposure time (5sec), the large amount of nanoparticles are melted and become bulks caused micro and irregular holes on the surface in this short time.

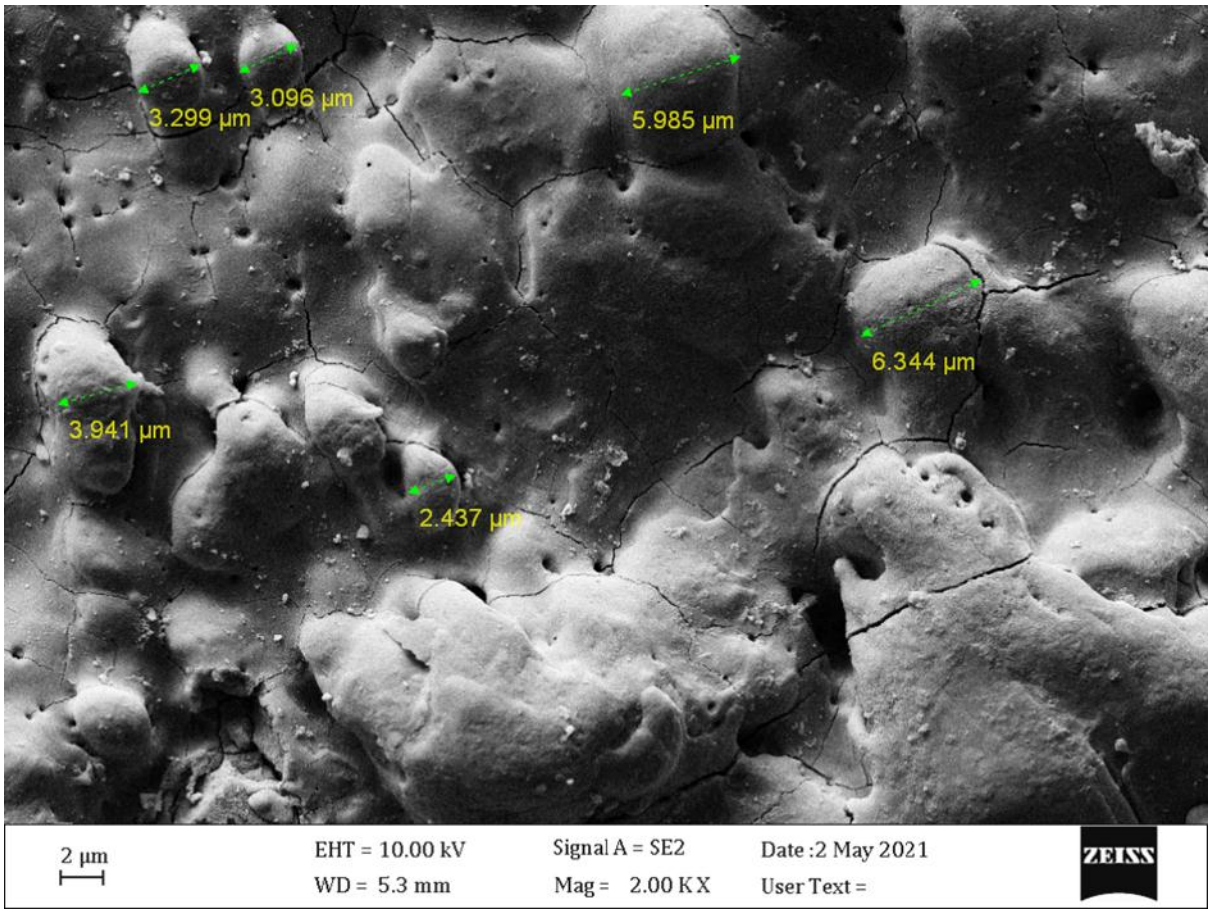

(a)

Fig(3.12a): The FESEM test of titanium using Nd: YAG pulsed laser with 600mJ pulse energy, 5 Hz repetition rate, 5sec exposure time and 50% concentration ratio of SiC nanofluid

When the exposure time of the process is increased to (10sec) for the same parameters on the same material, the large numbers of nanoparticles are melted and become bulks caused that irregular micro holes and large amount of agglomeration on surface, as shown in Figure (3.12b). The some other of nanoparticles are melted properly and drop down causing nano and micro holes.

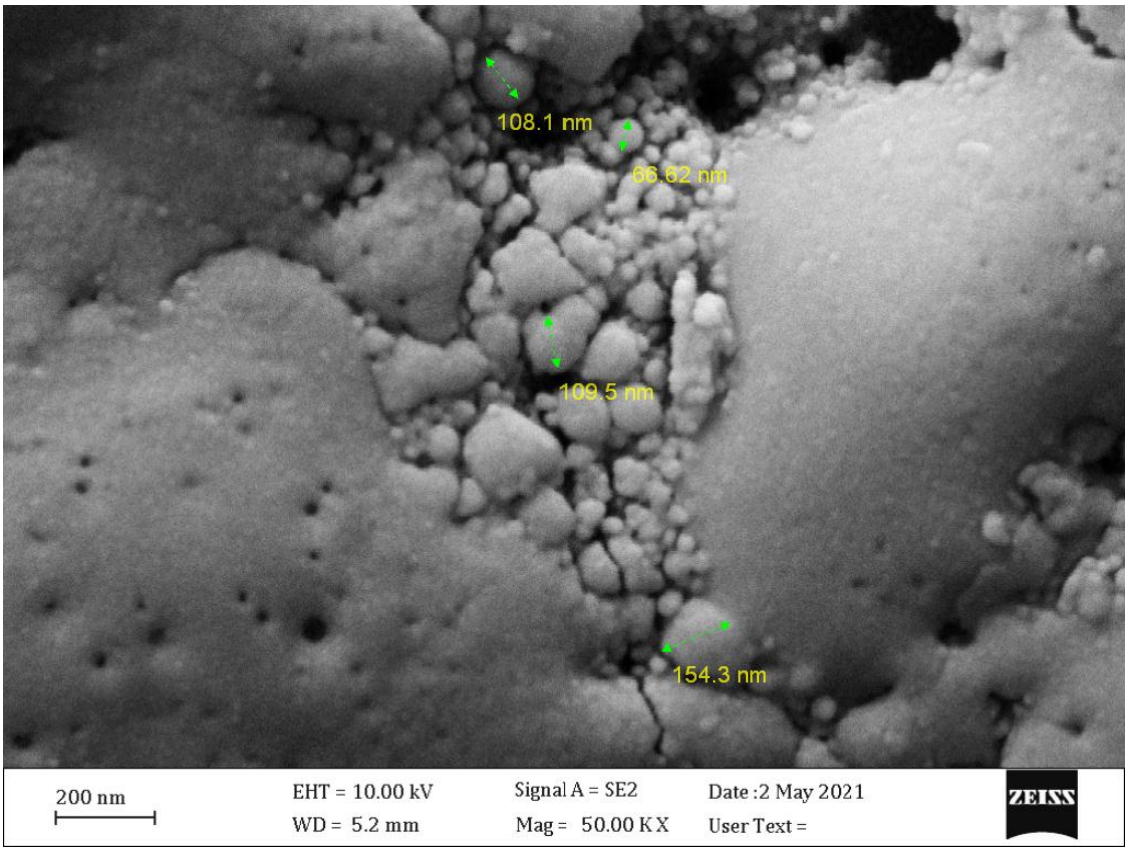

(b)

Fig.(3.12b): The FESEM test for titanium using Nd: YAG pulsed laser with 600mJ pulse energy, 5 Hz repetition rate, 10sec exposure time and 50% concentration ratio of SiC nanofluid

When the nanofluid concentration ratio is reduced to 5%, the laser pulse energy is 600mJ, repetition rate is 5Hz and exposure time is 5sec, the nano and the microholes in titanium are achieved, as shown in Figure (13(a,b)).

When the number of nanoparticles in the fluid will be small due to light concentration and the pumping of nanofluid is continuous, these nanoparticles will melted in a short time 5sec according to its size and density causing these fine holes.

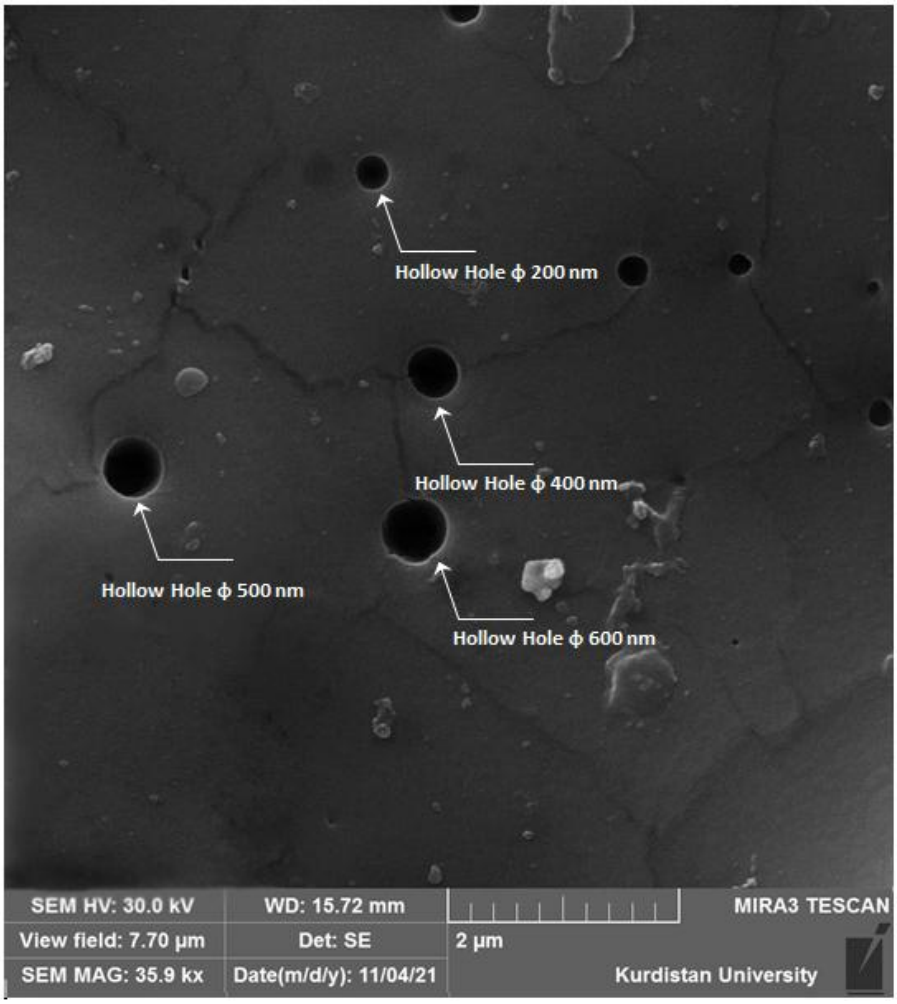

(a)

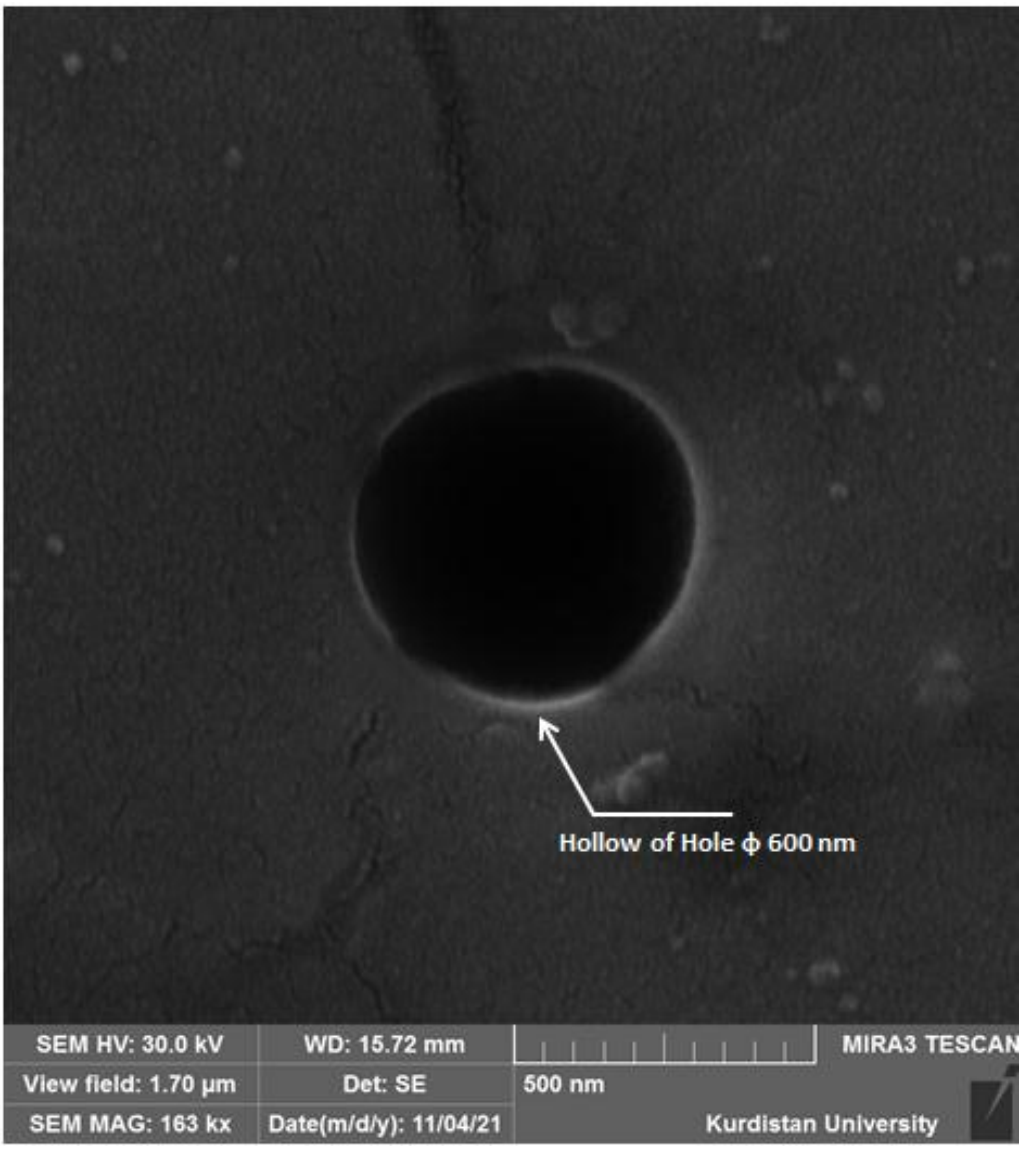

(b)

Fig.(3.13)(a,b): The FESEM test for titanium using Nd: YAG pulsed laser with 600mJ pulse energy, 5 Hz repetition rate, 5sec exposure time and 5% concentration ratio of SiC nanofluid

The FESEM test was conducted in this case at the University of Kurdistan and it shows the accuracy and regularity of the resulting holes due to the physical and mechanical properties of titanium, where titanium has the lowest thermal conductivity (19W/m.k) compared to aluminum and copper in additional it has high moduls and ductile.

3.2.2.3 Laser interaction with titanium using tungsten carbide(WC) nanoparticles

If the nanofluid concentration ratio is 90% (of nanoparticles), the laser pulse energy is 800mJ, repetition rate is 10Hz and exposure time is (30)sec, the irregular holes will appear on surface, as shown in Figure (3.14a) and aggregations of nanoparticles are obtained in the target, as shown in Figure (3.14b).

This result indicates that a high roughness on titanium when compared with Figure (3.7a), high roughness for the same laser parameters, the same nanoparticles and the same concentration of nanofluid due to the different thermal properties, as aluminum has the highest thermal conductivity compared to titanium material.

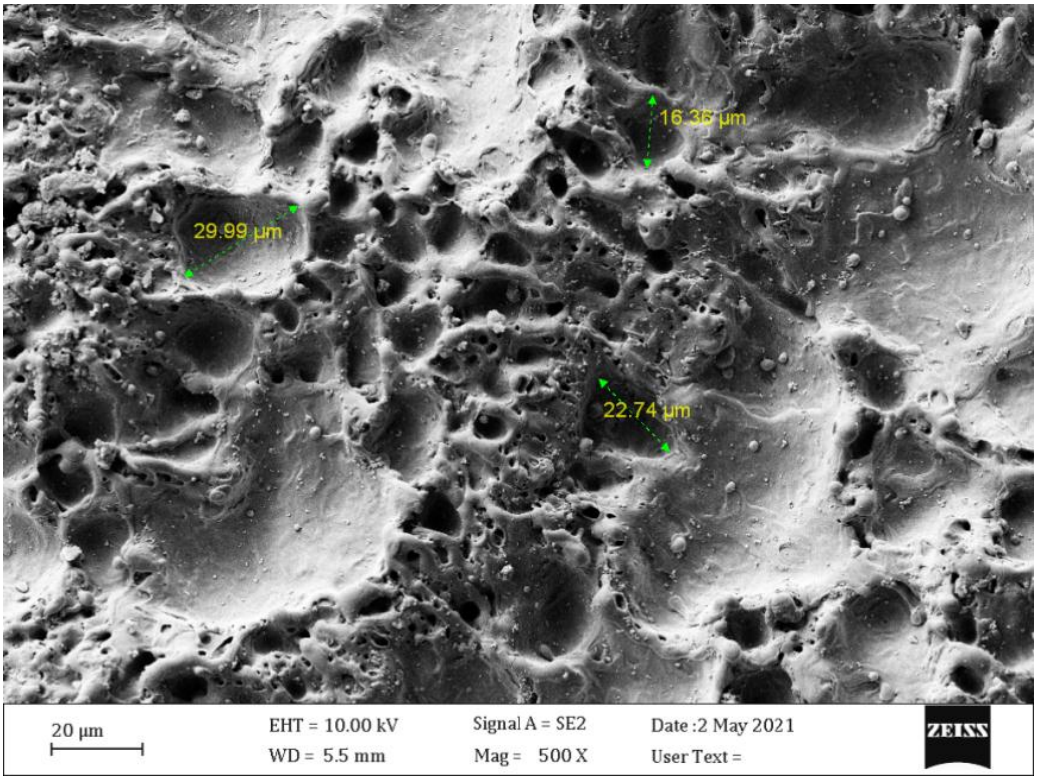

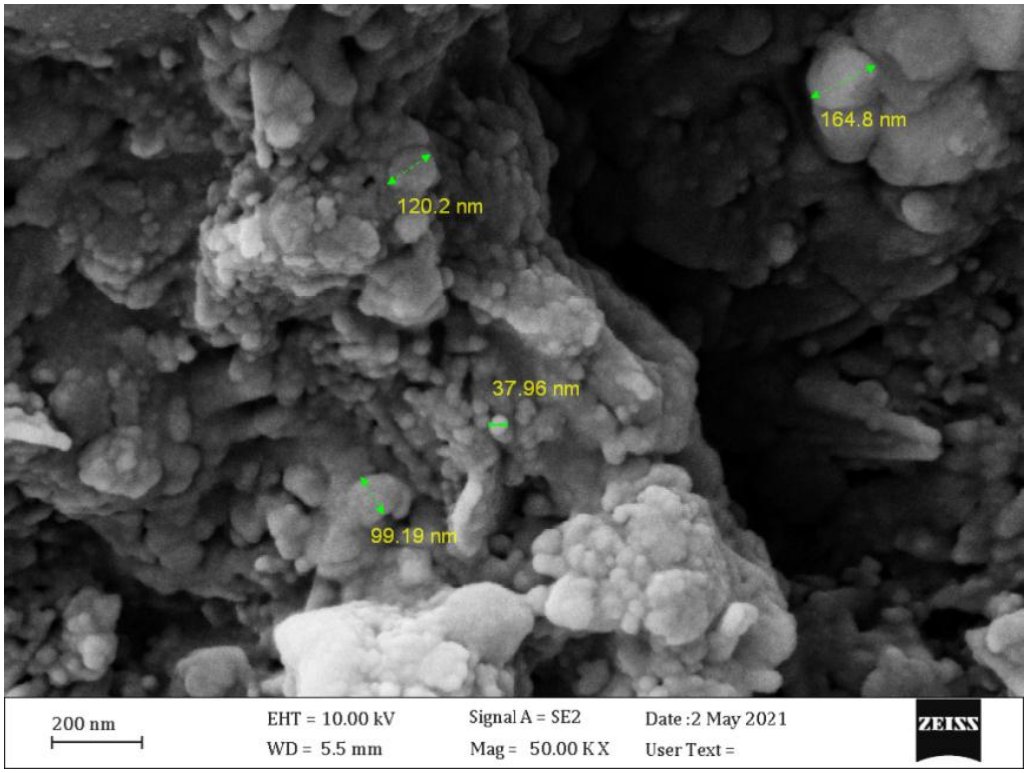

(b)

Fig.(3.14)(a,b): The FESEM test for titanium using Nd: YAG pulsed laser with 800mJ pulse energy, 10 Hz repetition rate, 30sec exposure time and 90% concentration ratio of WC nanofluid

When the nanofluid concentration ratio was lowered to 50% (of nanoparticles), the laser pulse energy is 600mJ, repetition rate is 5Hz and exposure time is (30)sec, the micro holes were obtained on the target, as shown in Figure (3.15a) and cracks are formed, as shown in Figure (3.15b).

These results indicate that reducing the laser parameters while reducing the nanoparticles concentrations by half, not achieving perfect holes and even making cracks as defects in the sample. Because the non-light concentrations which lead to the large number of nanoparticles are melted for a long exposure time, a part of them is collected and come down causing a crack on the surface, and the other part fall on in the form of irregular holes.

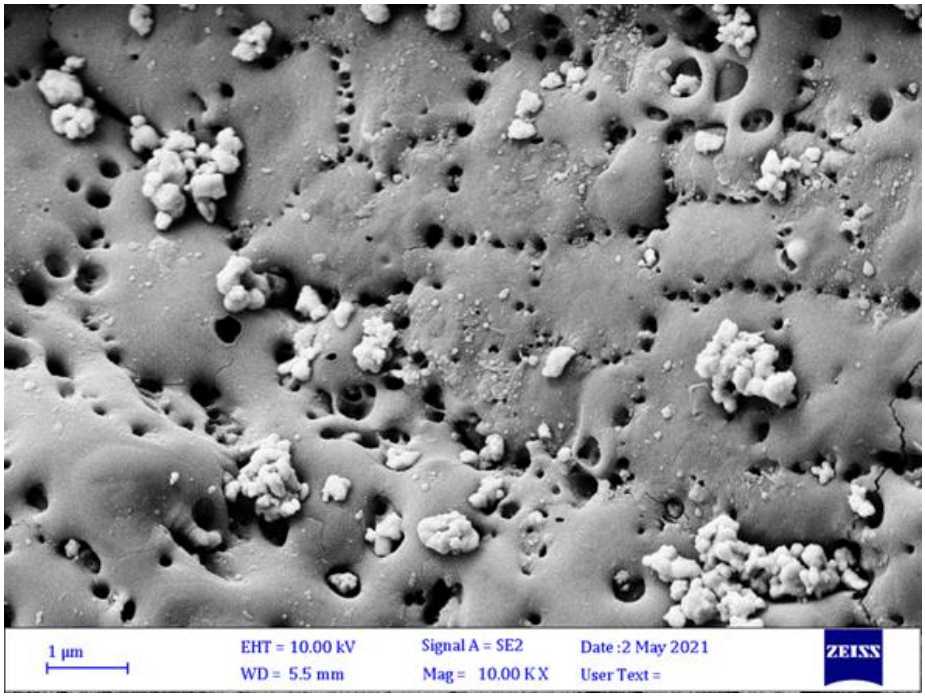

(a)

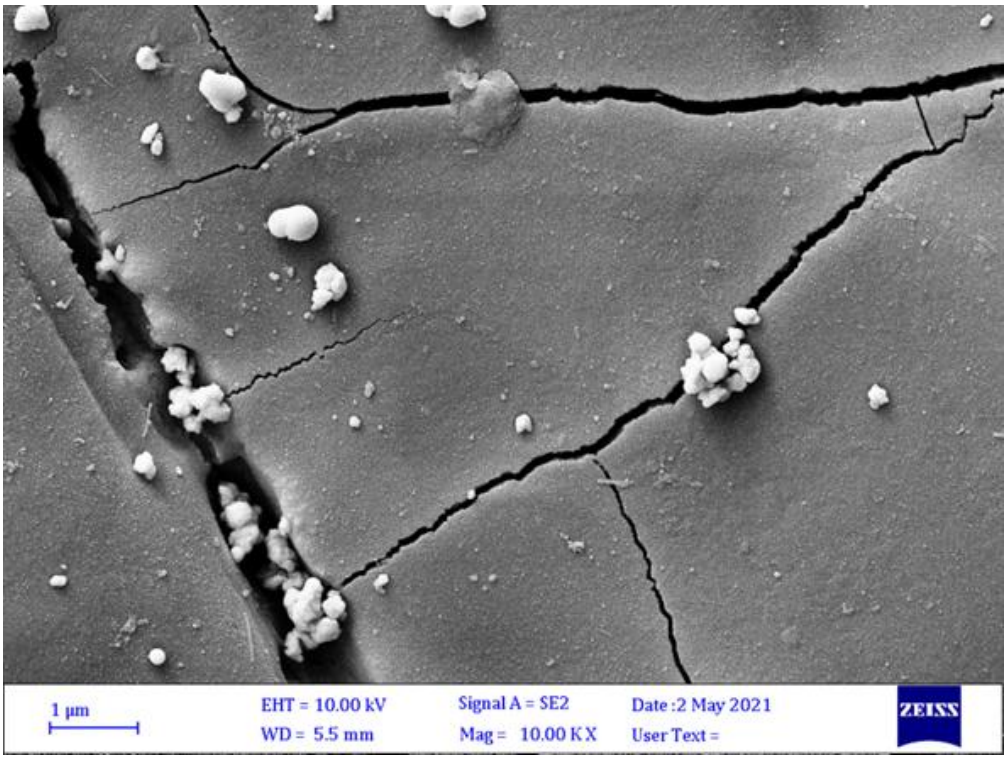

(b)

Fig.(3.15)(a,b): The FESEM test for titanium using a Yag pulsed laser with 600mJ pulse energy, 5 Hz repetition rate, 30sec exposure time and 50% concentration ratio of WC nanofluid

If the nanofluid concentration ratio is reduced to be as 5% and sprayed it on the target, the laser pulse energy is 600mJ, repetition rate is 5Hz and exposure time is (30)sec, the microholes and nanoholes for the titanium are achieved with the minimum heat affected zone (HAZ) and least amount of nanoparticles' aggregations, as shown in Figure (3.16).

This result indicates the effected of light concentration on target, so a few of number of tungsten carbide nanoparticle is melt completely. They have higher melting point (2870℃0)compared with silica carbide nanoparticles. When the nanoparticles reach the melting stage, they drop and drill the nano and micro holes perfectly and easily because of dealing with titanium metal, whose melting point is less than the tungsten carbide. Due to the continues nano fluid pumping process during the work, part of tungsten carbide nanoparticle do not melt, they reach the heating stage. They descend into the metal, causing micro and nano holes on the surface, but cause a very little aggregations because the concentration here is minimum.

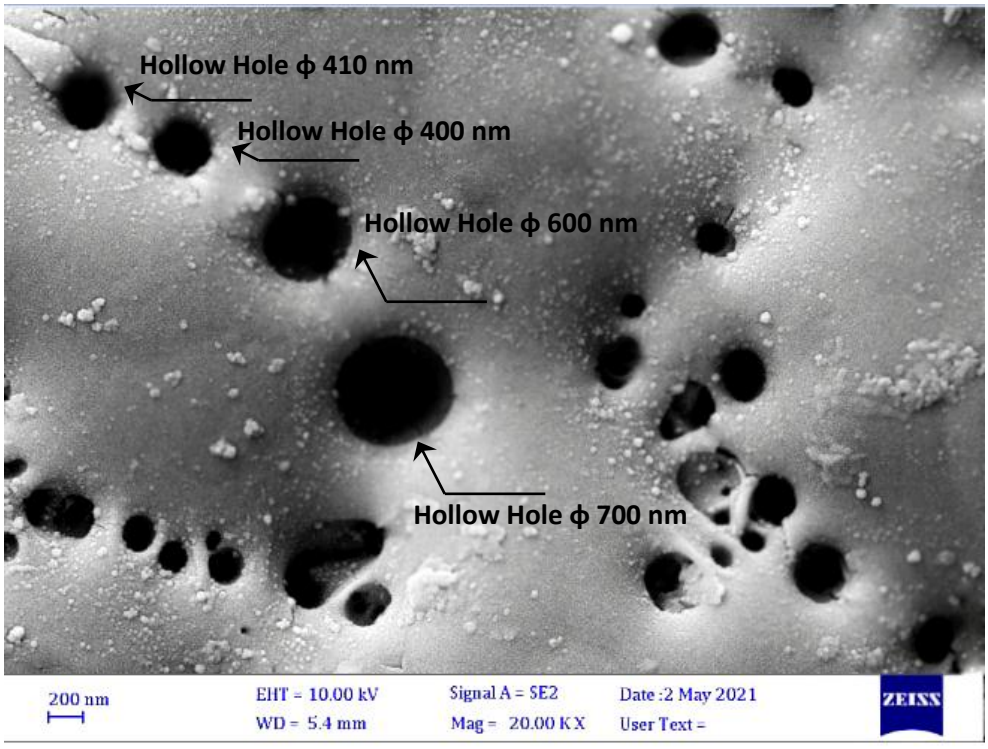

Fig. (3.16): The FESEM test for titanium using Nd: YAG pulsed laser with 600mJ pulse energy, 5 Hz repetition rate, 30sec exposure time and 5% concentration ratio of WC nanofluid

3.2.3 Q-switched Nd:YAG laser interaction with Copper

3.2.3.1 Laser interaction with copper without using nanoparticles

The laser parameters that were used in this work are the laser pulse energy of 600mJ, and increased to (700-800)mJ, repetition rate was 10Hz and exposure time was (40sec), the drilling holes were not investigated, as shown in Figure(3.17).

This result shows the effect of the laser parameters on the copper. There is only a thermal effect (without obtaining any holes on the target). This shows that using of the maximum laser parameters (energy, repetition rate and exposure time) didnt make any drilling effect on the copper target.

When comparing the results(3.1), (3.10) and (3.17) for different metals, there is a difference in the area of the thermal effect due to the various optical and thermal properties of each of them. The low reflectivity of conduvtion metal made it the most effective because it had a higher absorption of laser energy and thus a higher thermal effect, and the high reflectivity of copper made it the least affected, because the absorption of laser energy was low and therefore less thermal effect and so on for aluminum.

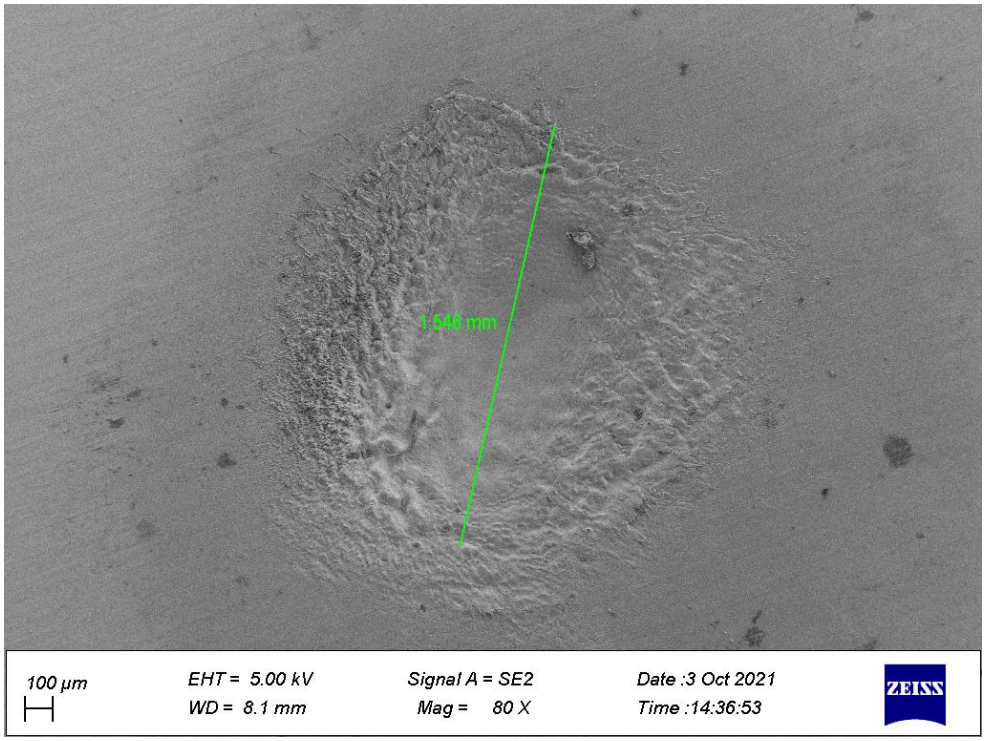

Fig.(3.17): The FESEM test for copper using Nd:YAG pulsed laser with 800mJ pulse energy, 10 Hz repetition rate, 40sec exposure time and without nanoparticles

3.2.3.2 Laser interaction with copper using silicon carbide(SiC) nanoparticles

The large diameter hole sizes and amount of aggregations of nanoparticles on surface of cooper are obtained from the high concentration ratio of nanofluid of 90%, the laser pulse energy is 800mJ, repetition rate is 10Hz and exposure time is 40sec, as shown in Figure (3.18(a,b)).

The results of this figure explain the effect of high concentration with laser parameters on drilling process which causes size of holes to be in large diameter and cracks due to the thermal stress in this material which created by changing in temperature between material and melted nanoparticles. During this, a large group of nanoparticles reach the stage of melting, so holes are made in exposure time of (5sec), as shown in Figure(3.18a). During this process with exposure time is (10ses), the part of nanoparticles reached only heating stage at this high concentration, and accumulate to form very large amount of agglomerates, as shown in Figure(3.18b).

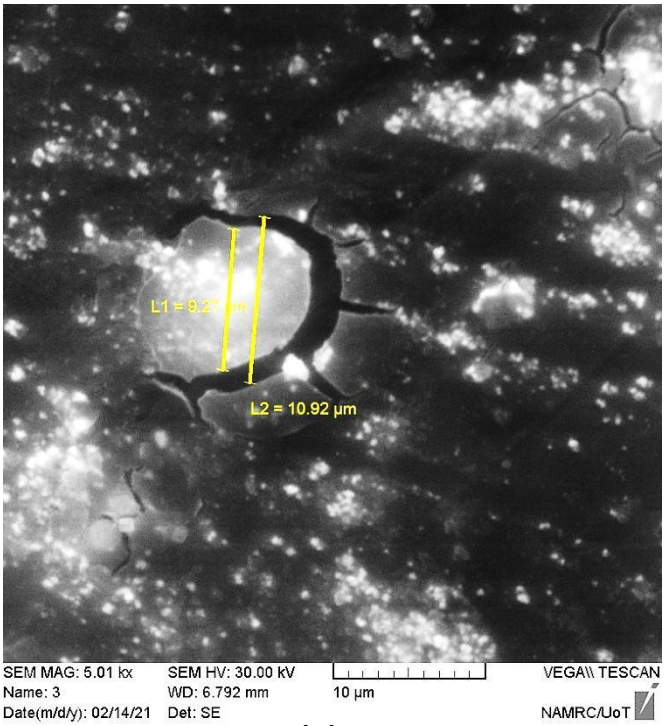

(a)

Fig.(3.18a): The FESEM test copper drilled by Yag pulsed laser and high concentration of silicon carbide nanoparticles (laser energy is 800mJ, frequency is 10Hz, exposure time is 5sec and 90%concentration ratio).

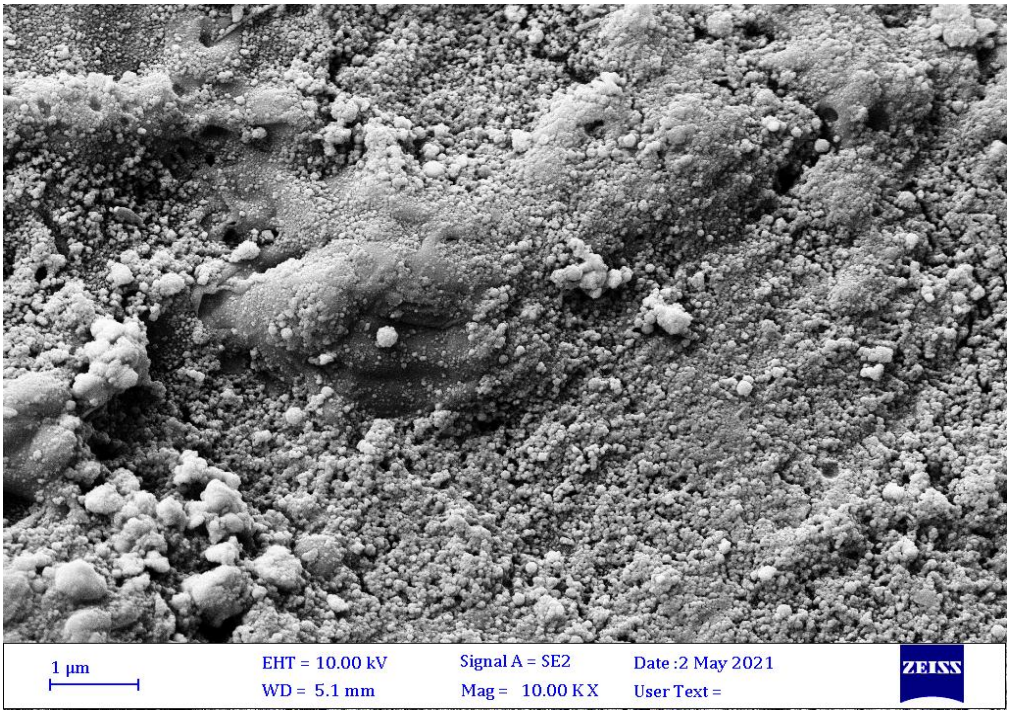

(b)

Fig.(3.18b): The FESEM test for copper using Nd: YAG pulsed laser with 800mJ pulse energy, 10 Hz repetition rate, 10sec exposure time and 90% concentration ratio of SiC nanofluid

If the nanofluid concentration ratio was reduced to 50%, the laser pulse energy is 600mJ, repetition rate is 5Hz and exposure time is 5sec, the aggregation of nanoparticles on copper are formed, as shown in Figure(3.19). This result indicates that decreasing the laser pulse energy and the concentration of nanfluid to half, some of the nanoparticles can melt and fall on to form irregular holes, and the other part of the nanoparticles do not melt, but come down as aggregations. By changing of temperature between them, the thermal stresses or plastic deformation created on this material.

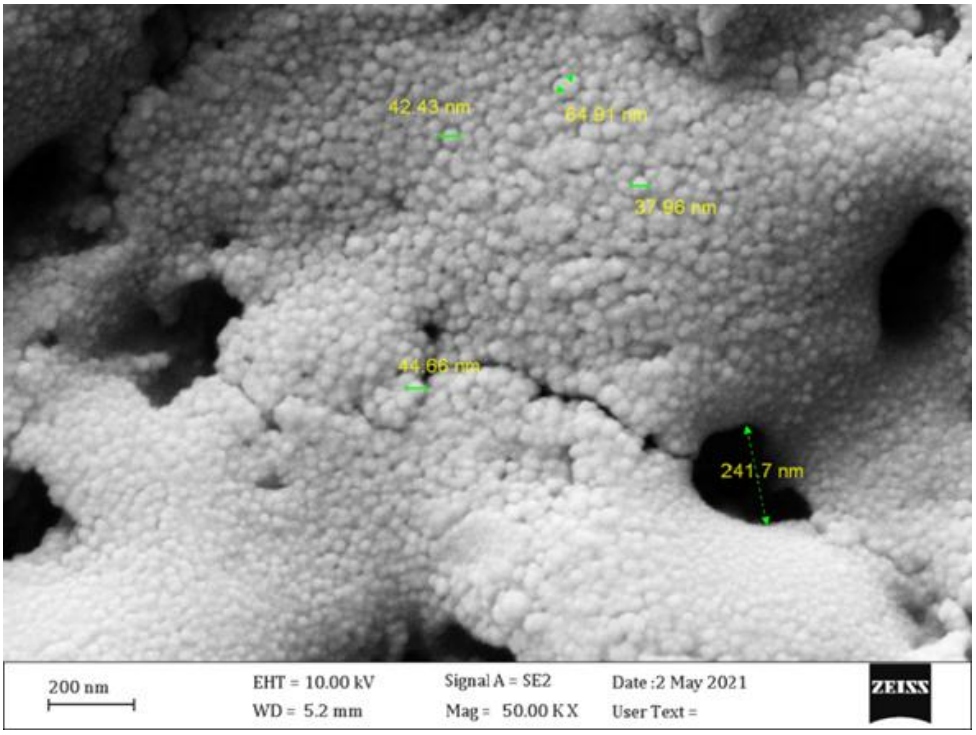

Fig.(3.19): The FESEM test for copper using Nd: YAG pulsed laser with 600mJ pulse energy, 5 Hz repetition rate, 5sec exposure time and 50% concentration ratio of SiC nanofluid

When the nanofluid concentration ratio is reduced to 5%, the laser pulse energy is 600mJ, repetition rate is 5Hz and exposure time is 5sec, the nanoholes in copper are achieved with the minimum heat affected zone(HAZ) width, as shown in Figure (3.20(a, b)). This result shows and explains the effect of light concentration nanofluid on the accuracy and regularity of drilling holes on the surface, due to small numbers of silica carbide nanoparticles according to them physical properties reach to melt completely to go down. These nanoparticles react with the copper which has less melting point to get perfect holes.

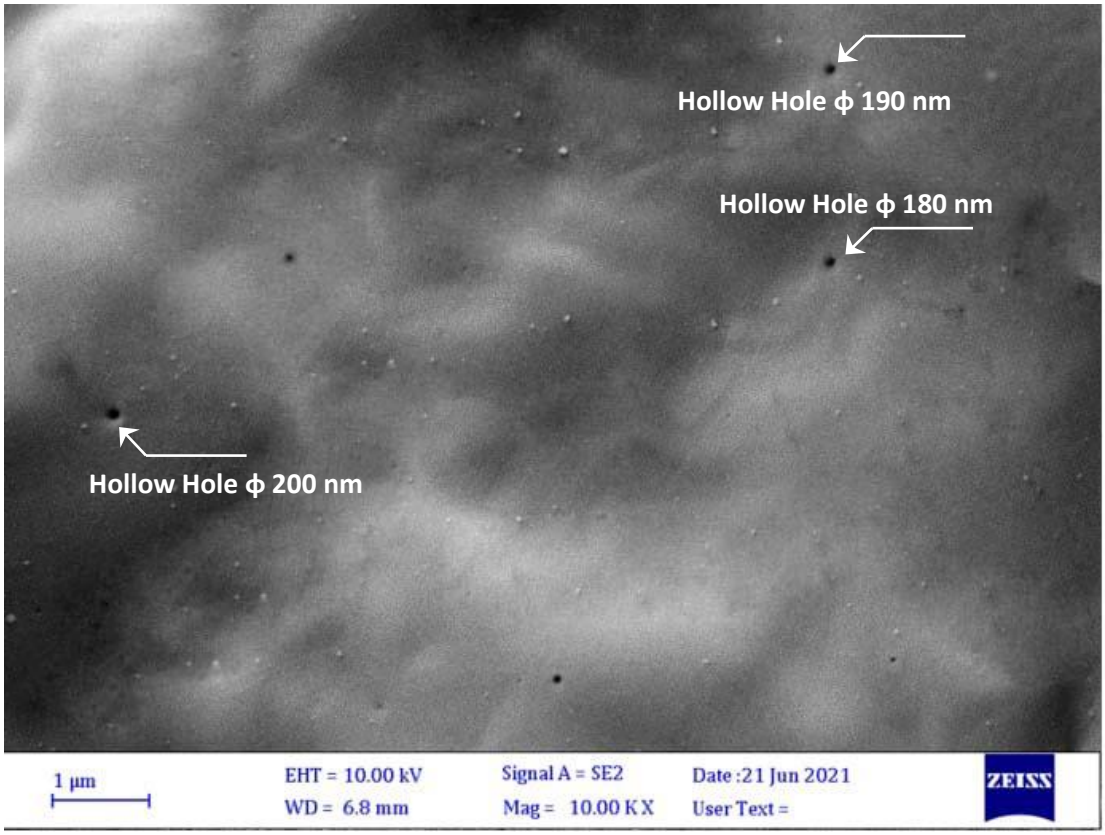

(a)

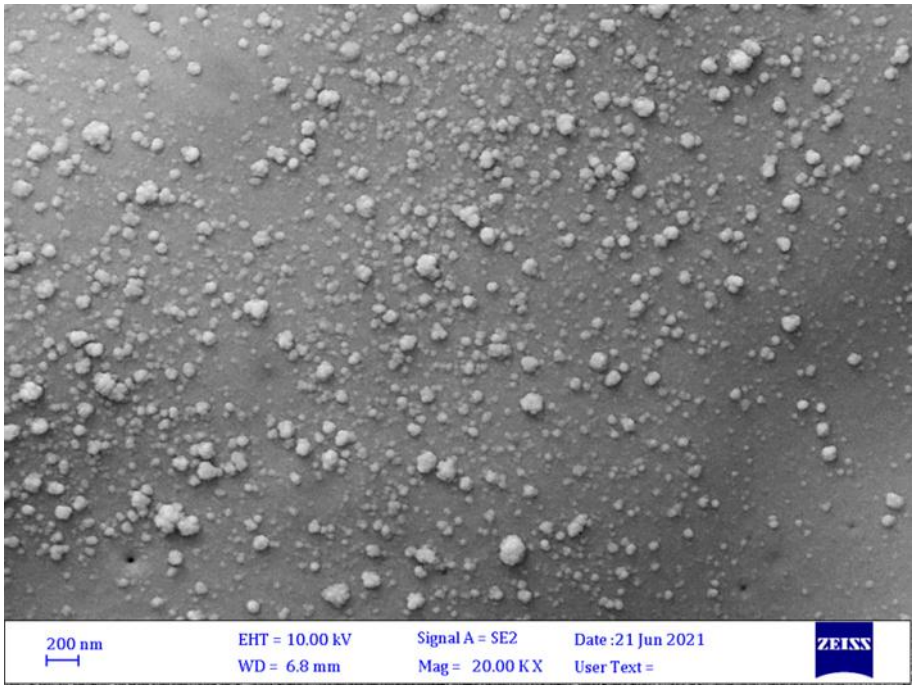

(b)

Fig. (3.20(a, b)): The FESEM test for copper using a Yag pulsed laser with 600mJ pulse energy, 5 Hz repetition rate, 5sec exposure time and 5% concentration ratio of SiC nanofluid

3.2.3.3 Laser interaction with copper using tungsten carbide(WC) nanoparticles

In this work, the high concentration ratio of nanofluid of 90% has been used with the laser pulse energy of 800mJ, repetition rate is 10Hz and exposure time is (30)sec, the aggregations of nanoparticles are obtained in the target, as shown in Figure(3.21(a,b)). This results due to high energy of laser applied on copper and high absorbtion because it has good thermal conductivity.

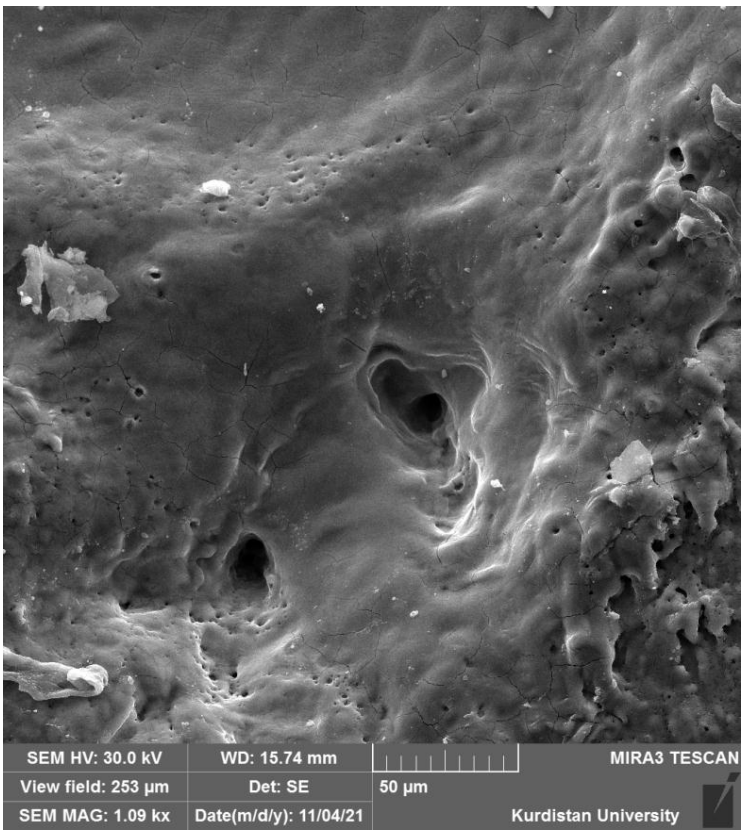

(a)

Fig.(3.21a): The FESEM test for copper using Nd: YAG pulsed laser with 800mJ pulse energy, 10 Hz repetition rate, 30sec exposure time and 90% concentration ratio of WC nanofluid

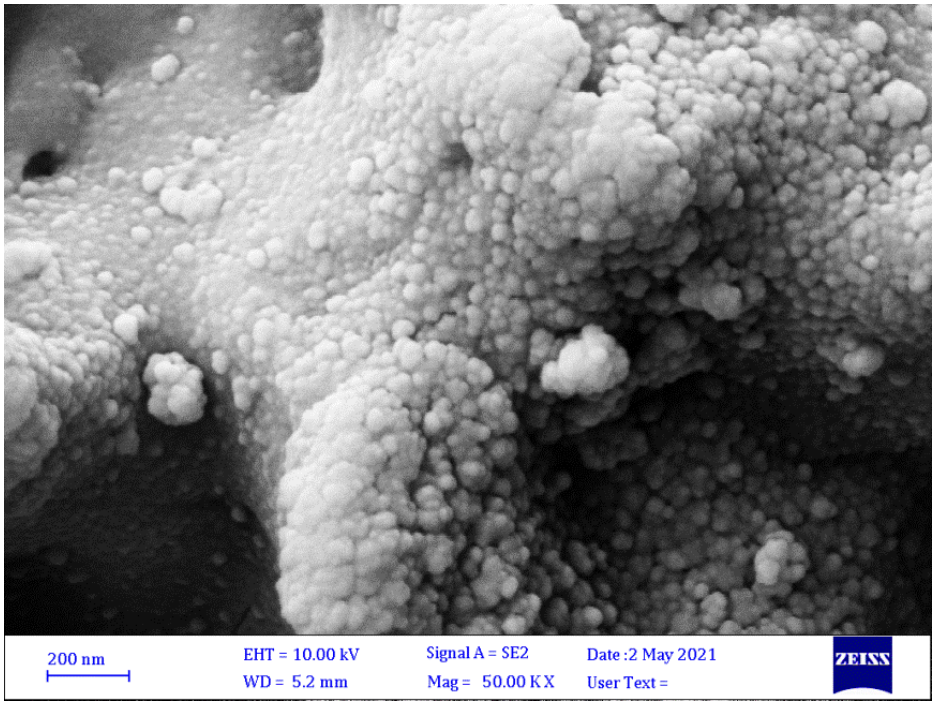

(b)

Fig.(3.21b): The FESEM test for copper using a Yag pulsed laser with 800mJ pulse energy, 10Hz repetition rate, 30sec exposure time and 90% concentration ratio of WC nanofluid

When the nanofluid concentration ratio was reduced to 50% (of nanoparticles), the laser pulse energy is 600mJ, repetition rate is 5Hz and exposure time is (30)sec, the irregular micro holes on copper are formed, as shown in Figure(3.22) due to the continuous pumping of the high concentrated nanofluid while the laser beam is focused on it, leads to large amount of tungsten carbide nanoparticles are melted in a long time, forming larger melted bulks, which comes down the surface, forming irregular holes.

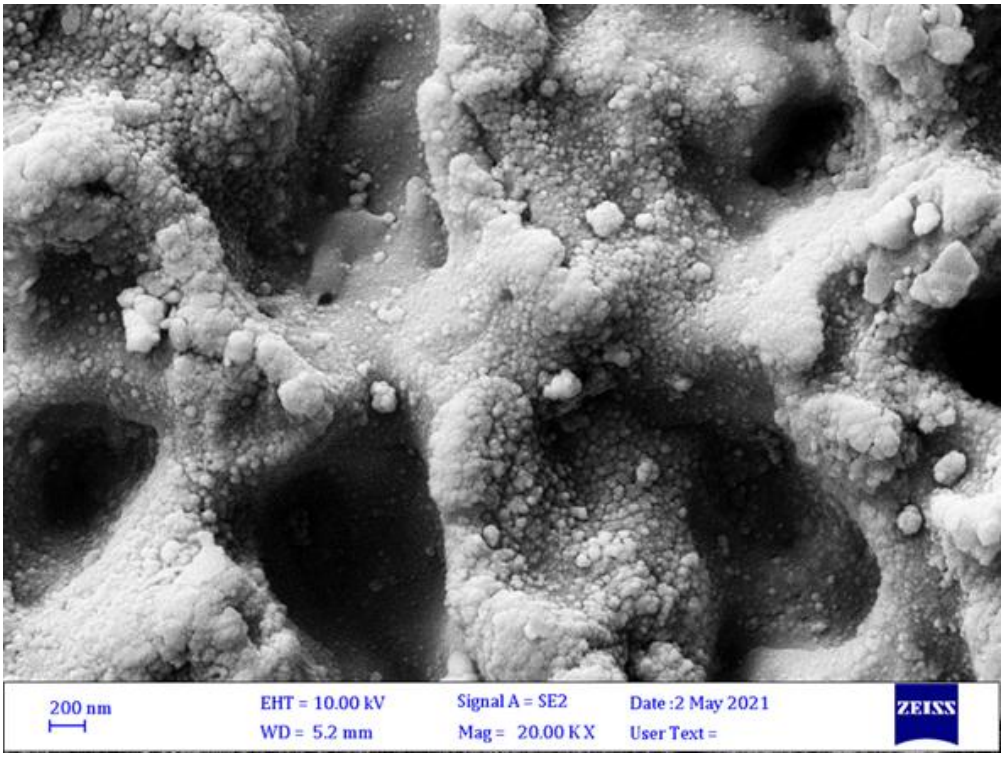

Figure (3.22): The FESEM test for copper using a Yag pulsed laser with 600mJ pulse energy, 5 Hz repetition rate, 30sec exposure time and 50% concentration ratio of WC nanofluid

When the nanofluid concentration ratio is reduced to 5% (of nanoparticles), the laser pulse energy is 600mJ, repetition rate is 5Hz and exposure time is 30sec, the nano and the microholes in copper are achieved, as shown in Figure (3.23). This result shows that light concentration with appropriate parameters of laser produce amount of nano and micro holes due to a small number of nanoparticles that are melted and fall on the surface. The physical property of melting point and good thermal conductively for the copper, made it difficult to obtain holes in this conditions with minimum heat affected zone.

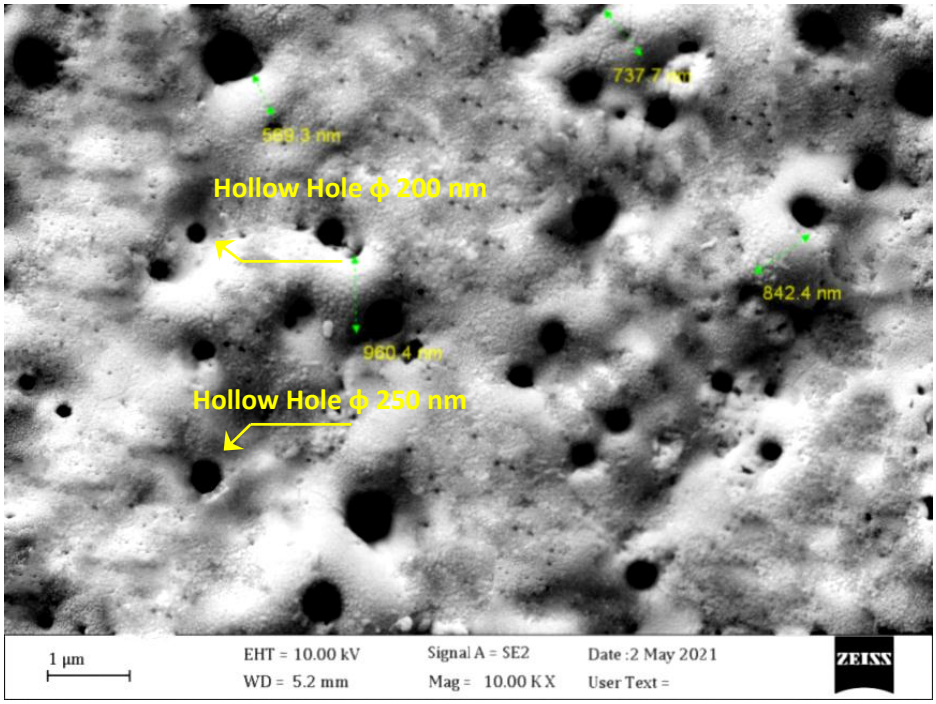

Fig.(3.23): The FESEM test for copper using Nd: YAG pulsed laser with 600mJ pulse energy, 5 Hz repetition rate, 30sec exposure time and 5% concentration ratio of WC nanofluid

3.3 The Summary

The results of perfect micro and nanoholes on materials are listed in Table(3.2), uasing laser energy of 600mJ, repetition rates of 5Hz and exposure time is (5,30)sec for silicon carbide and tungsten carbide nanoparticles respectively. The best holes had been obtained on titanium because of the physical and thermal properties in order of poor thermal conductivity (19W/mk), then appared on aluminium alloy best thermal conductivity (239W/mk). As for copper, it is difficult to obtain nano and micro holes because of the excellent thermal conductivity of the metal (392W/mk).

Table(3.2): showing the uniform holes from the pulsed laser with the metal

Material	Type of nanoparticles	Concentration of nanofluid	Energy density(W/cm^2)	Hole diameter (Hollow diameter)
Aluminum Alloy	Silicon carbide	5%	6.6×10^8	320nm 150nm 70nm 55nm
	Tungsten carbide	5%	6.6×10^8	322nm 445nm
Titanium	Silicon carbide	5%	6.6×10^8	200nm 400nm 500nm 600nm
	Tungsten carbide	5%	6.6×10^8	700nm 600nm 400nm 410nm
Copper	Silicon carbide	5%	6.6×10^8	200nm 190nm 180nm
	Tungsten carbide	5%	6.6×10^8	200nm 250nm

3.4 Conclusion

From the previous expremantial work for the investigated nano and micro holes, the following important conclusions must be mentioned.

1- The nano and micro holes were produced in different materials at laser energy is 600mJ, repetition rate is 5Hz and exposure time is (5, 30)sec for light concentration of silica carbide nanoparticles and tungsten carbide nanoparticles respectively.

2- The high concentration of nanoparticles in nanofluid shows cracks, aggregation of nanoparticles, irregular holes on the target material.

3- For (AA8009) Al alloy, the best holes has been obtianed with the laser energy of 600mJ, repition rate is 5Hz exposure time is 5sec with using of light concentration of silica carbide nanoparticles only according to the properties of materials and caracteristics of nanopaticles.

4- From the same laser parameters that laser energy of 600mJ, repition rate is 5Hz exposure time is 5sec and light concentration fluid of silica carbide nanoparticles 5%, the accurate nano and micro holes on titanium material are achieved and also appeared in titanium material at the same parameters. With using of light concentration of tungsten carbide nanoparticles and exposure time is 30sec.

5- The holes had been obtained on copper using a pulsed laser with 600mJ laser energy, 5Hz repition rate, 5sec exposure time and light concentration fluid 5% of silica carbide nanoparticles.

3.5 Future work

For the future work, the following points may be taken in consideration:

1- Examining the effect of adding various nanoparticles to the nanofluid according to the target materials used and their applications.

2-Utilizing different materials to study the effect of using this method to form micro and nano holes.

3- Using different kinds of lasers to see the effect of each laser with its parameters on micro and nano drilling process.

4- Trying to use automatic or computerized systems to control the nanofluid spraying method, increase its orientation to the target to ensure the arrangement and accuracy of the holes and prevent its scattering for safety and security.

5- Using different laser parameters to study the effect on the material in vacuum and compared the result with using the same parameters to make these holes in air.

References

[1] **Kansal, H., Jain, A., & Grover, V. (2017).** *"Micro Drilling and Drilling with Nano Materials: A Review".* 4th National Conference on Advancements in Simulation and Experimental Techniques in Mechanical Engineering.

[2]١ **.Singh, P., Pramanik, A., Basak, A. K., et al**. "*Developments of non-conventional drilling methods—a review*," The International Journal of Advanced Manufacturing Technology, V. 106, Nos. 5–6, 2019, pp. 2133–66.

[3] **Tu, J., Paleocrassas, A. G., Reeves, N., & Rajule, N. (2014).** ‟ *Experimental characterization of a micro-hole drilling process with short micro-second pulses by a CW single-mode fiber laser* ". Optics and Lasers in Engineering, 55, 275-283.

[4] **Casalino, G., Losacco, A. M., Arnesano, A., Facchini, F., Pierangeli, M., & Bonserio, C. (2017).** "*Statistical analysis and modelling of an Yb: KGW femtosecond laser micro-drilling process". Procedia CIRP*, *62*, 275-280.

[5] **Huang, H., Yang, L. M., & Liu, J. (2014)."** *Micro-hole drilling and cutting using femtosecond fiber laser."* Optical engineering, 53(5), 051513.

[6] **1.Zhao, W., and Wang, L.** *"Microdrilling of Through-Holes in Flexible Printed Circuits using Picosecond Ultrashort Pulse Laser,"* Polymers, V. 10, No. 12, 2018, p. 1390.

[7] **Cheng, M. Y. (2017).** "*An experimental investigation into tool wear in micro-drilling of aluminium, aluminium/copper metal alloys and carbon fibre reinforced composites "*(Doctoral dissertation, Brunel University London).

[8] **Roy, N., Kuar, A. S., Mitra, S., & Acherjee, B. (2015).** *"Nd:YAG Laser Microdrilling of SiC-30BN Nanocomposite: Experimental Study and Process Optimization"*. In Lasers Based Manufacturing (pp. 317–341). Springer India.

[9] **Ranjan, J., Patra, K., Szalay, T., Mia, M., Gupta, M. K., Song, Q., ... & Pimenov, D. Y. (2020).”** *Artificial intelligence-based hole quality prediction in micro-drilling using multiple sensors”.* Sensors, 20(3), 885.

[10] **Zhu, X., Naumov, A. Y., Villeneuve, D. M., & Corkum, P. B. (1999).** *"Influence of laser parameters and material properties on micro drilling with femtosecond laser pulses* ". Applied Physics A, 69(1), S367-S371.

[11] **Nandi, S., & Kuar, A. S. (2015***).”Parametric optimisation of Nd: YAG laser micro-drilling of alumina using NSGA II”*. International Journal of Machining and Machinability of Materials, 17(1), 1-21.

[12] **Singh, T., & Dvivedi, A. (2016).** *"Developments in electrochemical discharge machining: a review on electrochemical discharge machining, process variants and their hybrid methods* ". International Journal of Machine Tools and Manufacture, 105, 1-13.

[13] **Brown, M. S., & Arnold, C. B. (2010).** " *Fundamentals of laser-material interaction and application to multiscale surface modification* ". In Laser precision microfabrication (pp. 91-120). Springer, Berlin, Heidelberg.

[14] **Kajita, S., Takamura, S., Ohno, N., Nishijima, D., Iwakiri, H., & Yoshida, N. (2007).**" *Sub-ms laser pulse irradiation on tungsten target damaged by exposure to helium plasma"*. Nuclear Fusion, 47(9), 1358.

[15] **Amendola, V., & Meneghetti, M. (2009).** *"Laser ablation synthesis in solution and size manipulation of noble metal nanoparticles* ". Physical chemistry chemical physics, 11(20), 3805-3821.

[16] **Han, J., & Li, Y. (2011).** “*Interaction between pulsed laser and materials”.* Lasers applications in Science and Industry.

[17] **Chichkov, B. N., Momma, C., Nolte, S., Von Alvensleben, F., & Tünnermann, A. (1996)**. " *Femtosecond, picosecond and nanosecond laser ablation of solids".* Applied physics A, 63(2), 109-115.

[18] **1.Sugioka, K., Meunier, M., and Piqué, A., eds.** ,(2010). "*Laser Precision Microfabrication,"* Springer Berlin Heidelberg

[19] **Geszti, T." (1967).** *On the Theory of Thermally Activated Processes*". physica status solidi (b), 20(1), 165-177.

[20] **Mazaev, A. V., Ajeneza, O., & Shitikova, M. V. (2020).** *" Auxetics materials: classification, mechanical properties and applications "*. In IOP Conference Series: Materials Science and Engineering (Vol. 747, No. 1, p. 012008). IOP Publishing.

[21] **Hashimoto, S., Werner, D., & Uwada, T. (2012).** *" Studies on the interaction of pulsed lasers with plasmonic gold nanoparticles toward light manipulation, heat management, and nanofabrication".* Journal of Photochemistry and Photobiology C: Photochemistry Reviews, 13(1), 28-54.

[22] **Jawalkar, C. S., & Kant, S. (2015).″** *A review on use of aluminium alloys in aircraft components "*. i-Manager's Journal on Material Science, 3(3), 33.

[23**] Stojanovic, B., & Epler, I. (2018).** *" Application of aluminum and aluminum alloys in engineering".* Applied Engineering Letters.

[24]**Chen, P., Fan, X., Yang, Q., Zhang, Z., Jia, Z., & Liu, Q. (2021).** *" Creep behavior and microstructural evolution of 8030 aluminum alloys compressed at intermediate temperature".* Journal of Materials Research and Technology, 12, 1755-1761.

[25] **Barbaux, Y., & Pons, G. (1993).** *"New rapidly solidified aluminium alloys for elevated temperature applications on aerospace structures "*. Le Journal de Physique IV, 3(C7), C7-191.

[26] **Gospodinov, D., Ferdinandov, N., & Dimitrov, S. (2016).** *"Classification, properties and application of titanium and its alloys "*. Proceedings of university of ruse, 55(2), 27-32.

[27] **Ahmed, Y. M., Sahari, K. S. M., Ishak, M., & Khidhir, B. A. (2014).** *" Titanium and its Alloy".* International Journal of Science and Research, 3(10), 1351-1361.

[28] **Avvari, M., Manjaiah, M., Able, M., Laubscher, R. F., & Raghavendra, K. (2017)**. *"Optimization of hole characteristics during pulse Nd: YAG laser drilling of commercially pure titanium alloy".* Lasers in Manufacturing and Materials Processing, 4(2), 76-91.

[29] **Li, M., & Zinkle, S. J. (2012).** 4.20-"physical and mechanical properties of copper and copper alloys". Comprehensive nuclear materials, 667-690.

[30] **Al-Motasem, A. T., Posselt, M., Bergner, F., & Birkenheuer, U. (2011).** *Structure, energetics and thermodynamics of copper–vacancy clusters in bcc-Fe: An atomistic study".* Journal of nuclear materials, 414(2), 161-168.

[31] **Chau, M. Q. (2019).** *An overview study on the laser technology and applications in the mechanical and machine manufacturing industry* . J. Mech. Eng. Res. Dev.(JMERD), 42(5), 16-20.

[32] **Santos, E. C., Shiomi, M., Osakada, K., & Laoui, T. (2006).** *Rapid manufacturing of metal components by laser forming".* International Journal of Machine Tools and Manufacture, 46(12-13), 1459-1468.

[33] **Krstulović, N., Shannon, S., Stefanuik, R., & Fanara, C. (2013).** *"Underwater-laser drilling of aluminum* . The International Journal of Advanced Manufacturing Technology, 69(5), 1765-1773.

[34] **Majumdar, J. D., Galun, R., Mordike, B. L., & Manna, I**. **(2003).** "*Effect of laser surface melting on corrosion and wear resistance of a commercial magnesium alloy*". Materials Science and Engineering: A, 361(1-2), 119-129

[35] **Steen, W. M. (2003).** *Laser material processing—an overview".* Journal of Optics A: Pure and Applied Optics, 5(4), S3.

[36] **1.Kusinski, J., Kac, S., Kopia, A., et al**. (2012). "*Laser modification of the materials surface layer – a review paper,"* Bulletin of the Polish Academy of Sciences: Technical Sciences, V. 60, No. 4, pp. 711–28.

[37] **Kwok, C. T., Cheng, F. T., & Man, H. C**. (2000).*" Laser surface modification of UNS S31603 stainless steel. Part I: microstructures and corrosion characteristics"*. Materials Science and Engineering: A, 290(1-2), 55-73.

[38] **d Oliveira, A. S. C. M., Paredes, R. S. C., Weber, F. P., & Vilar, R**. **(2001).** *"Microstructural changes due to laser surface melting of an AISI 304 stainless steel*". Materials Research, 4(2), 93-96.

[39] **Mustafa, F. F. (2008).***" Heating and Melting Model Induced by Laser Beam in Solid Material* ". Al-Khwarizmi Engineering Journal, 4(3), 98-107.

[40] **1.Colombo, P., Demir, A. G., Norgia, M., et al**. (2017). "*Self-mixing interferometry as a diagnostics tool for plasma characteristics in laser microdrilling,*" Optics and Lasers in Engineering, V. 92, pp. 17–28.

[41] **Crivellaro, S., Guadagnini, A., Arboleda, D. M., Schinca, D., & Amendola, V. (2019).** *"A system for the synthesis of nanoparticles by laser ablation in liquid that is remotely controlled with PC or smartphone"*. Review of Scientific Instruments, 90(3), 033902.

[42] **Russo, R. E., Mao, X., Gonzalez, J. J., Zorba, V., & Yoo, J. (2013).** "Laser ablation in analytical chemistry".

[43] **Aragón, C., & Aguilera, J. A. (2008)**." *Characterization of laser induced plasmas by optical emission spectroscopy: A review of experiments and methods"*. Spectrochimica Acta Part B: Atomic Spectroscopy, 63(9), 893-916.

[44] **Zhang, Y., Zhang, D., Wu, J., He, Z., & Zhang, H. (2016).** *〞A novel laser ablation plasma thruster with electromagnetic acceleration"*. Acta Astronautica, 127, 438-447.

[45] **Wu, J., Zhang, Y., Cheng, Y., Huang, Q., Li, J., & Zhu, X. (2018). ”***Plasma Generation and Application in a Laser Ablation Pulsed Plasma Thruster”.* In Plasma Science and Technology-Basic Fundamentals and Modern Applications. IntechOpen.

[46] **Chaudhary, K., Rizvi, S. Z. H., & Ali, J. (2016).** *"Laser-induced plasma and its applications〞*. Plasma Science and Technology-Progress in Physical States and Chemical Reactions, 259-291.

[47] **Le Harzic, R., Breitling, D., Weikert, M., Sommer, S., Föhl, C., Valette, S., ... & Dausinger, F. (2005)**. *〞Pulse width and energy influence on laser micromachining of metals in a range of 100 fs to 5 ps〞*. applied surface science, 249(1-4), 322-331.

[48] **Harilal, S. S., Freeman, J. R., Diwakar, P. K., & Hassanein, A. (2014).** *〞Femtosecond laser ablation: Fundamentals and applications".* In Laser-Induced Breakdown Spectroscopy (pp. 143-166). Springer, Berlin, Heidelberg.

[49] **Abdelmalek, A., Bedrane, Z., & Amara, E. H. (2018, March).** *〞Thermal and non-thermal explosion in metals ablation by femtosecond laser pulse: classical approach of the two temperature model"*. In Journal of Physics: Conference Series (Vol. 987, No. 1, p. 012012). IOP Publishing.

[50] **Zhang, Y., Zhang, D., Wu, J., He, Z., & Deng, X. (2017).〞** *A thermal model for nanosecond pulsed laser ablation of aluminum"*. AIP Advances, 7(7), 075010.

[51] **Selvan, C. P., Rammohan, N., & Hk, S. (2015).** *“Laser Beam Machining: A Literature Review on Heat affected Zones, Cut Quality and Comparative*

Study". European Journal of Advances in Engineering and Technology, 2(10), 70-76.

[52] **Dutta Majumdar, J., & Manna, I. (2011).*"*** *Laser material processing*‟ . In International Materials Reviews (Vol. 56, Issues 5–6, pp. 341–388). Informa UK Limited.

[53] **Meijer, J. (2004)**. *"Laser beam machining (LBM), state of the art and new opportunities* ‟. Journal of materials processing technology, 149(1-3), 2-17.

[54] **Latif, A., Rafiq, M. S., Bhatti, K. A., & Perveen, A. (2016).** *"Crater geometry and morphological changes on gold sheet during laser microdrilling* ‟. The International Journal of Advanced Manufacturing Technology, 85(9), 2847-2855.

[55] **Davim, J. P. (2013).** ‟ *Nontraditional machining processes"*. Manufacturing process selection handbook, 205-226.

[56] **Pattanayak, S., & Panda, S. (2018)**." *Laser Beam Micro Drilling – a Review".* In Lasers in Manufacturing and Materials Processing (Vol. 5, Issue 4, pp. 366–394). Springer Science and Business Media LLC.

[57] **Corcoran, A., Sexton, L., Seaman, B., Ryan, P., & Byrne, G. (2002).** ‟ *The laser drilling of multi-layer aerospace material systems. Journal of materials processing technology"*, 123(1), 100-106.

[58] **Fornaroli, C., Holtkamp, J., & Gillner, A. (2013).** *"Laser-beam helical drilling of high quality micro holes* ‟. Physics Procedia, 41, 661-669.

[59] **Dubey, A. K., & Yadava, V. (2008).** *"Laser beam machining—A review".* In International Journal of Machine Tools and Manufacture (Vol. 48, Issue 6, pp. 609–628). Elsevier BV.

[60] **Lazare, S., & Tokarev, V. (2004, October).** *Recent experimental and theoretical advances in microdrilling of polymers with ultraviolet laser beams*. In Fifth International Symposium on Laser Precision Microfabrication (Vol. 5662, pp. 221-231). International Society for Optics and Photonics.

[61] **Majumdar, J. D., & Manna, I. (2003)**. *Laser processing of materials*. Sadhana, 28(3), 495-562.

[62] **Colombo, P., Demir, A. G., Norgia, M., & Previtali, B. (2017).** *Self-mixing interferometry as a diagnostics tool for plasma characteristics in laser microdrilling* . Optics and Lasers in Engineering, 92, 17-28.

[63]**SADEGH, A. M. (2017).** *Expert System Approach for Manufacturability Evaluation of Nd: YAG Laser Beam Machining Process*. INTERNATIONAL JOURNAL OF ADVANCED DESIGN AND MANUFACTURING TECHNOLOGY, Vol. 10 , Number 2, 15- 24.

[64] **Mishra, S., & Yadava, V. (2015).** *Laser beam micromachining (LBMM)–a review*. Optics and lasers in engineering, 73, 89-122.

[65] **Hasan, M., Zhao, J., & Jiang, Z. (2017).** *A review of modern advancements in micro drilling techniques*. Journal of Manufacturing Processes, 29, 343-375.

[66] **Gautam, G. D., & Pandey, A. K. (2018).** *"Pulsed Nd: YAG laser beam drilling: A review* . Optics & Laser Technology, 100, 183-215.

[67] **Biswas, R., Kuar, A. S., Biswas, S. K., & Mitra, S. (2010).** *Effects of process parameters on hole circularity and taper in pulsed Nd: YAG laser microdrilling of Tin-Al2O3 composites*. Materials and Manufacturing Processes, 25(6), 503-514.

[68] **Hedberg, J., Ekvall, M. T., Hansson, L.-A., Cedervall, T., & Odnevall Wallinder, I. (2017)**. *"Tungsten carbide nanoparticles in simulated surface*

water with natural organic matter: dissolution, agglomeration, sedimentation and interaction with Daphnia magna". In Environmental Science: Nano (Vol. 4, Issue 4, pp. 886–894). Royal Society of Chemistry (RSC).

[69] **Parandoush, P., & Hossain, A. (2014)**. *"A review of modeling and simulation of laser beam machining"*. International journal of machine tools and manufacture, 85, 135-145.

[70] **Nayak, S. S., Puhan, P., & Mishra, D. (2017).** *"Influence of Process Parameters of Nd-YAG laser Microdrilling on CNT-NiAl Composites"* .

[71] **Ravisubramanian, S., & Shunmugam, M. S. (2015).** *"On reliable measurement of micro drilling forces and identification of different phases"*. Measurement, 73, 335-340.

[72] **Shen, N., Bude, J. D., Ly, S., Keller, W. J., Rubenchik, A. M., Negres, R., & Guss, G. (2019)**. *"Enhancement of laser material drilling using high-impulse multi-laser melt ejection"* . Optics express, 27(14), 19864-19886.

[73] **Barthels, T., Reininghaus, M., & Westergeling, H. (2019, September**). *"High-precision ultrashort pulsed laser drilling of micro and nano holes using multibeam processing".* In Laser Beam Shaping XIX (Vol. 11107, p. 111070K). International Society for Optics and Photonics.

[74] **Lin, Z., & Hong, M. (2021).** *"Femtosecond Laser Precision Engineering: From Micron, Submicron, to Nanoscale"*. Ultrafast Science, 2021. Volume 2021, Article ID 9783514, 22 pages.

[75] **Tokarev, V. N., Cheshev, E. A., Bezotosnyi, V. V., Khomich, V. Y., Mikolutskiy, S. I., & Vasil'yeva, N. V. (2015).** *"Optimization of plasma effect in laser drilling of high aspect ratio microvias".* In Laser Physics (Vol. 25, Issue 5, p. 056003). IOP Publishing.

[76] **Gerhard, C., Viöl, W., & Wieneke, S. (2016)**. *"Plasma-Enhanced Laser Materials Processing".* In Plasma Science and Technology - Progress in Physical States and Chemical Reactions.

[77] **Hamad, A. H. (2016)."** *Effects of Different Laser Pulse Regimes (Nanosecond, Picosecond and Femtosecond) on the Ablation of Materials for Production of Nanoparticles in Liquid Solution"*. In High Energy and Short Pulse Lasers.

[78] **Ravi- Kumar, S., Lies, B., Zhang, X., Lyu, H., & Qin, H. (2019).** *"Laser ablation of polymers: A review"*. Polymer International, 68(8), 1391-1401.

[79**] Li, L., & Achara, C. (2004).** *"Chemical assisted laser machining for the minimisation of recast and heat affected zone"*. CIRP annals, 53(1), 175-178.

[80] **Gerhard, C., Gimpel, T., Tasche, D., née Hoffmeister, J. K., Brückner, S., Flachenecker, G., ... & Viöl, W. (2018)**. *"Atmospheric pressure plasma-assisted femtosecond laser engraving of aluminium"*. Journal of Physics D: Applied Physics, 51(17), 175201.

[81] **Chaudhary, K., Rizvi, S. Z. H., & Ali, J. (2016).** *"Laser-induced plasma and its applications"* . Plasma Science and Technology-Progress in Physical States and Chemical Reactions, 259-291.

[82] **Guzmán, M. G., Dille, J., & Godet, S. (2009).** *"Synthesis of silver nanoparticles by chemical reduction method and their antibacterial activity"*. Int J Chem Biomol Eng, 2(3), 104-111.

[83] **Jeevanandam, J., Barhoum, A., Chan, Y. S., Dufresne, A., & Danquah, M. K. (2018).** *"Review on nanoparticles and nanostructured materials: history, sources, toxicity and regulations"*. Beilstein journal of nanotechnology, 9(1), 1050-1074.

[84] **1.Khan, I., Saeed, K., and Khan, I**. (2019). *"Nanoparticles: Properties, applications and toxicities,"* Arabian Journal of Chemistry, V. 12, No. 7, pp. 908–31.

[85] **1.Sajid, M., and Płotka-Wasylka, J**. **(2020).** *"Nanoparticles: Synthesis, characteristics, and applications in analytical and other sciences,"* Microchemical Journal, V. 154, p. 104623.

[86] **1.Yang, L., Wei, J., Ma, Z., et al**. (2019). *"The Fabrication of Micro/Nano Structures by Laser Machining,"* Nanomaterials, V. 9, No. 12, p. 1789.

[87] **Ealia, S. A. M., & Saravanakumar, M. P. (2017, November).″** *A review on the classification, characterisation, synthesis of nanoparticles and their application*〞. In IOP Conference Series: Materials Science and Engineering (Vol. 263, No. 3, p. 032019). IOP Publishing.

[88] **Das, S., Bhardwaj, A., & Pandey, L. M. (2021).** 〝*Functionalized biogenic nanoparticles for use in emerging biomedical applications: a review".* Current Nanomaterials, 6(2), 119-139.

[89]**Samyn, P., Barhoum, A., Öhlund, T., & Dufresne, A. (2018).** 〝*Nanoparticles and nanostructured materials in papermaking".* Journal of Materials Science, 53(1), 146-184.

[90]**Hoyle, R. (2008).** *"Developments in micro and nano engineering and manufacturing*〞. Plastics, rubber and composites, 37(2-4), 50-56.

[91] **Tunna, L., O'Neill, W., Khan, A., & Sutcliffe, C. (2005)**. "*Analysis of laser micro drilled holes through aluminium for micro-manufacturing applications ".* In Optics and Lasers in Engineering (Vol. 43, Issue 9, pp. 937–950).

[92] **Kumar, A., Singh, K., & Pandey, O. P. (2011).** *"Sintering behavior of nanostructured WC–Co composite* ". Ceramics International, 37(4), 1415-1422.

[93] **1.Baig, U., Gondal, M. A., Dastageer, M. A., et al**. **(2018).** *"Photo-catalytic deactivation of hazardous sulfate reducing bacteria using palladium nanoparticles decorated silicon carbide: A comparative study with pure silicon carbide nanoparticles,"* Journal of Photochemistry and Photobiology B: Biology, V. 187, pp. 113–9.

[94] **Andrievski, R. A**. **(2009).** "*Synthesis, structure and properties of nanosized silicon carbide".* Rev. Adv. Mater. Sci, 22, 1-20.

[95] **1.Sahu, T., Ghosh, B., Pradhan, S. K., et al. (2012).** "*Diverse Role of Silicon Carbide in the Domain of Nanomaterials,"* International Journal of Electrochemistry, V. 2012, pp. 1–7.

[96] **Ekimov, E. A., Krivobok, V. S., Kondrin, M. V., Litvinov, D. A., Grigoreva, L. N., Koroleva, A. V., ... & Nikolaev, S. N. (2021).** *"Structural and Optical Properties of Silicon Carbide Powders Synthesized from Organosilane Using High-Temperature High-Pressure Method"*. Nanomaterials, 11(11), 3111.

[97] **Paszkiewicz, S., Taraghi, I., Szymczyk, A., Huczko, A., Kurcz, M., Przybyszewski, B., ... & Rosłaniec, Z. (2017)**. *Electrically and thermally conductive thin elastic polymer foils containing SiC nanofibers*. Composites Science and Technology, 146, 20-25.

[98] **1.Mahyari, A. A., Karimipour, A., and Afrand, M**. (2019). *"Effects of dispersed added Graphene Oxide-Silicon Carbide nanoparticles to present a statistical formulation for the mixture thermal properties,"* Physica A: Statistical Mechanics and its Applications, V. 521, pp. 98–112.

[99] **Rafati, R., Smith, S. R., Haddad, A. S., Novara, R., & Hamidi, H. (2018).** *"Effect of nanoparticles on the modifications of drilling fluids properties: A review of recent advances"*. Journal of Petroleum Science and Engineering, 161, 61-76.

[100] **Salim, M. S., Sabri, N., Ibrahim, T. K., Noaman, N. M., Akram, I. N., & Latif, I. H. (2019).** *" Effect of laser processing parameters on the efficiency of material: a review in industrial application field".*

[101] **1.Pyatenko, A., Wang, H., Koshizaki, N., et al. (2013).** *"Mechanism of pulse laser interaction with colloidal nanoparticles,"* Laser & Photonics Reviews, V. 7, No. 4, pp. 596–604.

[102] **Habiba, K., Makarov, V. I., Weiner, B. R., & Morell, G. (2014).** *"Fabrication of nanomaterials by pulsed laser synthesis*." Manufacturing Nanostructures, 10, 263-292.

[103] **Li, L., Diver, C., Atkinson, J., Giedl-Wagner, R., & Helml, H. J. (2006).** *"laser and EDM micro-drilling for next generation fuel injection nozzle manufacture "*. CIRP annals, 55(1), 179-182.

[104] **Biffi, C. A., Lecis, N., Previtali, B., Vedani, M., & Vimercati, G. M. (2011).** *"Fiber laser microdrilling of titanium and its effect on material microstructure "*. The International Journal of Advanced Manufacturing Technology, 54(1), 149-160.

[105] **Mahmood, I. J. (2015).** *" Theoretical study of drilling process materials by laser pulses (Micro, Nano and Picoseconds)".* IJSR, 4(1), 1447-1452.

[106] **Meng, L. N., Wang, A. H., Wu, Y., Wang, X., Xia, H. B., & Wang, Y. N. (2015).** *"Blind micro-hole array Ti6Al4V templates for carrying biomaterials fabricated by fiber laser drilling "*. Journal of Materials Processing Technology, 222, 335-343.

[107] **Tu, J., Lehman, T., & Reeves, N. (2016).** *" Rapid and High Aspect Ratio Micro-hole Drilling With Multiple Micro-Second Pulses Using a CW Single-Mode Fiber Laser".* High Speed Machining–Modern Manufacturing Technologies, 10.

[108] **Courvoisier, F., Stoian, R., & Couairon, A. (2016).** *" Ultrafast laser micro-and nano-processing with nondiffracting and curved beams: invited*

paper for the section: hot topics in ultrafast lasers". Optics & Laser Technology, 80, 125-137.

[109] **Dhaker, K. L., Pandey, A. K., & Upadhayay, B. N. (2017).** *"Experimental investigation of hole diameter in laser trepan drilling of Inconel718 sheet* ". Materials Today: Proceedings, 4(8), 7599-7608.

[110] **Gautam, G. D., & Pandey, A. K. (2018).** " *Pulsed Nd: YAG laser beam drilling: A review"*. Optics & Laser Technology, 100, 183-215.

[111**] Stephen, A., Ocana, R., Esmoris, J., Thomy, C., Soriano, C., Vollertsen, F., & Sanchez, R. (2018).**" *Laser micro drilling methods for perforation of aircraft suction surfaces"***.** Procedia CIRP, 74, 403-406**.**

[112] Dongre, G. G., Rajurkar, A., Gondil, R., & Philip, J. (2019). " *High aspects ratio micro-drilling of super-alloys using ultra short pulsed laser".* International Journal of Precision Technology, 8(2-4), 124-141.

[113] **Pramanik, D., Roy, N., Kuar, A. S., Sarkar, S., Mitra, S., & Bose, D. (2021)**. *"Laser Trepan Drilling of Monel k-500 Superalloy in Low Power Laser Beam Machining* ". In Machine Learning Applications in Non-Conventional Machining Processes (pp. 137-159). IGI Global.

[113] **Reddy, V. C., Thota, K., Niskala, T., & Yadav, G. M. P. (2021).** *"Analysis and optimization of laser drilling process during machining of AISI 303 material using Grey relational analysis approach* ". SN Appl. Sci., 3(3), 335.

[115] **Chatterjee, S., Mahapatra, S. S., Bharadwaj, V., Upadhyay, B. N., & Bindra, K. S. (2021).**" *Prediction of quality characteristics of laser drilled holes using artificial intelligence techniques".* Engineering with Computers, 37(2), 1181-1204.

[116] **Jia, X., Chen, Y., Liu, L., Wang, C., & Duan, J. A. (2022).**" *Advances in Laser Drilling of Structural Ceramics* ". Nanomaterials, 12(2), 230.

[116] **Guidote Jr, A. M., Pacot, G. M. M., & Cabacungan, P. M. (2015).** "*Low-cost magnetic stirrer from recycled computer parts with optional hot plate"*. Journal of Chemical Education, 92(1), 102-105.

[117] **Liu, H. B., Su, H. G., Fu, D. F., Jiang, F. L., & Zhang, H. (2020).** *〞Phase evolution in AlSi20/8009 aluminum alloy during high temperature heating near melting point and cooling processes"*. Transactions of Nonferrous Metals Society of China, 30(5), 1157-1168.

[118] **Kuchariková, L., Liptáková, T., Tillová, E., Kajánek, D., & Schmidová, E. (2018).″** *Role of chemical composition in corrosion of aluminum alloys* 〞. Metals, 8(8), 581.

[119] **Avvari, M., Manjaiah, M., Able, M., Laubscher, R. F., & Raghavendra, K. (2017)**.〞 *Optimization of hole characteristics during pulse Nd: YAG laser drilling of commercially pure titanium alloy"*. Lasers in Manufacturing and Materials Processing, 4(2), 76-91.

[120] **Talati, M., Posselt, M., Bonny, G., Al-Motasem, A., & Bergner, F. (2012).** *"Vibrational contribution to the thermodynamics of nanosized precipitates: vacancy–copper clusters in bcc-Fe* 〞. Journal of Physics: Condensed Matter, 24(22), 225402.

[121] **1.Yan, Z., Cai, M., and Shen, P. K. (2013).** *"Nanosized tungsten carbide synthesized by a novel route at low temperature for high performance electrocatalysis,"* Scientific Reports, V. 3, No. 1.

[122] **Farahmand, P., Liu, S., Zhang, Z., & Kovacevic, R. (2014).** 〞 *Laser cladding assisted by induction heating of Ni–WC composite enhanced by nano-WC and La2O3* 〞. Ceramics International, 40(10), 15421-15438.

[123] **1.Voon, C. H., Lim, B. Y., and Ho, L. N. (2018).** *"Silicon Carbide Nanomaterials,"* Synthesis of Inorganic Nanomaterials, pp. 213–53.

[124]Yu, W., France, D. M., Choi, S. U., & Routbort, J. L. (2007). 〞 *Review and assessment of nanofluid technology for transportation and other*

applications (No. ANL/ESD/07-9). Argonne National Lab.(ANL), Argonne, IL (United States).

وزارة التعليم العالي و البحث العلمي
جامعة بغداد
معهد الليزر للدراسات العليا

التثقيب المايكروي / النانوي للمعادن بواسطة الليزر واعتمادا على الجسيمات النانوية

رسالة مقدمة الى

معهد الليزر للدراسات العليا /جامعة بغداد/لأستكمال متطلبات نيل شهادة

ماجستير علوم في الليزر/ الهندسة الميكانيكية

من قبل

نبراس حامد عبد

بكالوريوس هندسة ميكانيكية

بأشراف

المدرس الدكتور محمود شاكر محمود

١٤٤٣هـ **٢٠٢٢م**

الخلاصة

في هذا العمل تم الحصول على الثقوب المايكروية والنانوية بتفاعل ليزر Q-switched Nd: YAG 1064) نانومتر) مع المعادن المختلفة باستخدام الجسيمات النانوية. تم استخدام نبضات ليزرية بطاقات مختلفة (٦٠٠ ، ٧٠٠ ، ٨٠٠) مللي جول، ومعدلات تكرار مختلفة (٥ هرتز و ١٠ هرتز) وتراكيزمختلفة من الدقائق النانوية (٩٠٪، ٥٠٪ و ٥٪).

تم استخدام ثلاثة أنواع من المعادن في هذا العمل. هذه المعادن هي سبيكة الألومنيوم(AA8009) والتيتانيوم والنحاس. أيضا ، تم استخدام نوعين من الجسيمات النانوية ، هذه الجسيمات النانوية هي كربيد السيليكا(SiC) وكربيد التنجستن (WC).

تم تحليل تأثيرات طاقة نبضة الليزر ومعدل تكرار نبض الليزر ونسبة تركيز الجسيمات النانوية ووقت التعرض على شكل وحجم الثقوب.

تمت دراسة نسب التراكيز المختلفة لكل من الدقائق النانوية على معادن مختلفة. تسببت التراكيز العالية من المائع النانوي (٥٠٪ و ٩٠٪) في إعاقة عملية الحفر في المعادن مثل توليد الشقوق وتراكمات نانوية على سطح المعدن.

تم الكشف عن الثقوب المايكروية و النانوية لكل معدن من خلال استخدام تركيز(٥٪) من الدقائق النانوية. بالنسبة لسبائك الألومنيوم (AA8009) ، ظهرت الثقوب المثالية عندما تكون طاقة نبضة الليزر ٦٠٠ مللي جول ، ومعدل تكرار نبض الليزر ٥ هرتز ، تراكيز الدقائق النانوية من كربيدات السيليكا النانوية (٥٪) ووقت التعرض ٥ ثوانٍ. في معدن التيتانيوم، تم فحص الثقوب المنتظمة أيضًا في نفس معاملات الليزر ونفس التراكيز لنوعين من الدقائق النانوية مع وقت التعرض ٥ ثوانٍ لدقائق كربيد السيليكا النانوية ، و ٣٠ ثانية لدقائق كربيد التنجستن النانوية. في معدن النحاس، ظهرت الثقوب الدقيقة بنفس معايير الليزر بتركيز (٥٪) من دقائق كربيد السيليكا النانوية ووقت التعرض ٥ ثوانٍ.